

**UTILIZING UNACTIVATED ALKYL AMINE DERIVATIVES IN
REDUCTIVE CROSS-ELECTROPHILE COUPLING REACTIONS**

by

Bria Garcia

A dissertation submitted to the Faculty of the University of Delaware in partial fulfillment of the requirements for the degree of Doctor of Philosophy in Chemistry and Biochemistry

Winter 2025

© 2025 Bria Garcia
All Rights Reserved

**UTILIZING UNACTIVATED ALKYL AMINES DERIVATIVES IN
REDUCTIVE CROSS-ELECTROPHILE COUPLING REACTIONS**

by

Bria Garcia

Approved: _____

Joel Rosenthal, Ph.D.
Chair of the Department of Chemistry and Biochemistry

Approved: _____

Debra Hess Norris
Interim Dean of the College of Arts and Sciences

Approved: _____

Louis F. Rossi, Ph.D.
Vice Provost for Graduate and Professional Education and
Dean of the Graduate College

I certify that I have read this dissertation and that in my opinion it meets the academic and professional standard required by the University as a dissertation for the degree of Doctor of Philosophy.

Signed:

Mary P. Watson, Ph.D.
Professor in charge of dissertation

I certify that I have read this dissertation and that in my opinion it meets the academic and professional standard required by the University as a dissertation for the degree of Doctor of Philosophy.

Signed:

Joseph M. Fox, PhD.
Member of dissertation committee

I certify that I have read this dissertation and that in my opinion it meets the academic and professional standard required by the University as a dissertation for the degree of Doctor of Philosophy.

Signed:

Sharon L. Neal, Ph.D.
Member of dissertation committee

I certify that I have read this dissertation and that in my opinion it meets the academic and professional standard required by the University as a dissertation for the degree of Doctor of Philosophy.

Signed:

Sarah E. Wengryniuk, Ph.D.
Member of dissertation committee

ACKNOWLEDGMENTS

“You may write me down in history
With your bitter, twisted lies,
You may trod me in the very dirt
But still like dust, I’ll rise.

Does my sassiness upset you?
Why are you beset with gloom?
‘Cause I walk like I’ve got oil wells
Pumping in my living room.

Just like moons and like suns
With the certainty of tides,
Just like hopes springing high,
Still I’ll rise.

Did you want to see me broken?
Bowed head and lowered eyes?
Shoulders falling down like teardrops,
Weakened by my soulful cries?

Does my sassiness upset you?
Don't take it too hard
'Cause I laugh like I have gold mines
Diggin' in my own backyard.

You can shoot me with your words,
You can cut me with your lies,
You can kill me with your hatefulness
But just like life, I'll rise.

Does my sexiness offend you?
Does it come as a surprise
That I dance like I've got diamonds
At the meeting of my thighs?

Out of the huts of history's shame
I rise
Up from a past rooted in pain
I rise
A black ocean, leaping and wide,
Welling and swelling and bearing in the tide

Leaving behind nights of terror and fear
I rise

Into a daybreak miraculously clear
I rise
Bringing the gifts my ancestors gave,
I am the hope and the dream of the slave
And so, I rise
I rise
I rise
There I go.”

Maya Angelou

“Still I Rise” from *And Still I Rise: A Book of Poems*. Copyright © 1978 by Maya Angelou and “Still I Rise” 1987 Live Performance by Maya Angelou.

TABLE OF CONTENTS

LIST OF TABLES	x
LIST OF FIGURES	xii
LIST OF SCHEMES	xiii
ABSTRACT	xv

Chapter

1	PRIMARY VS. SECONDARY ALKYLPIRIDINIUM SALTS: A COMPARISON UNDER ELECTROCHEMICAL AND CHEMICAL REDUCTION CONDITIONS.....	1
1.1	Introduction	1
1.2	Results and Discussion	6
1.2.1	Investigations with 24 Diverse Aryl Bromides	6
1.2.2	Investigations with Informer Halides	10
1.3	Conclusions	13
1.4	Experimental.....	14
1.4.1	General Information	14
1.4.2	High-Throughput Electrochemical (HTE-Chem) Procedures	16
1.4.2.1	Constant Voltage Procedure with Primary Alkylpyridinium Salt	16
1.4.2.2	Constant Current Procedure with Secondary Alkylpyridinium Salt	17
1.4.3	High-Throughput Experimentation (HTE) Procedures with Chemical Reductants	19
1.4.3.1	General Procedure A for Primary Alkylpyridinium Salt 1	19
1.4.3.2	General Procedure B using Mn ⁰ with Secondary Alkylpyridinium Salt 2	20
1.4.4	Reproducibility Data for Aryl Bromide Scope.....	21

1.4.4.1	Primary Alkylpyridinium Salt (Scheme 1.2A).....	21
1.4.4.2	Secondary Alkylpyridinium Salt (Scheme 1.2B).....	21
1.4.5	Reproducibility Data for Informer Halide Scope	22
1.4.5.1	Primary Alkylpyridinium Salt (Scheme 1.3A).....	22
1.4.5.2	Secondary Alkylpyridinium Salt (Scheme 1.3B).....	23
1.4.6	Evaluation of Alternative Conditions with Mn ⁰ and TDAE for Secondary Katritzky Pyridinium Salt 2.....	23
1.4.7	Comparison of Electrochemical vs. Chemical Conditions for Aryl Bromide Scope	25
1.4.8	Comparison of Electrochemical vs. Chemical Conditions for Informer Halide Scope	26
1.4.9	Comparison of ArBr Scope for 1° vs. 2° Alkylpyridinium Salts under Electrochemical Conditions	27
1.4.10	Preparation and Characterization of Katritzky Alkylpyridinium Salts	28
1.4.10.1	Synthesis of Primary Alkylpyridinium Salt 1	28
1.4.10.2	Synthesis of Secondary Alkylpyridinium Salt 2	29
REFERENCES		31
2	CROSS-ELECTROPHILE COUPLING OF PRIMARY ALKYLPYRIDINIUM SALTS AND ARYL CHLORIDES VIA NICKEL- CATALYZED ELECTROCHEMICAL REDUCTION	35
2.1	Introduction	35
2.2	Results and Discussion.....	40
2.2.1	Reaction Development with Primary Alkylpyridinium Salt	40
2.2.2	Aryl Chloride and Alkylpyridinium Salt Scope	44
2.2.3	Investigations with Secondary Alkylpyridinium Salt.....	49
2.3	Conclusions	50
2.4	Experimental.....	50
2.4.1	General Information	50
2.4.2	General Procedures.....	52
2.4.2.1	General Procedure A: High-Throughput Electrochemical (HTe ⁻ Chem) Investigation	52

2.4.2.2	General Procedure B: Optimization Studies Using Electrochemical Reduction.....	53
2.4.2.3	General Procedure C: Investigations Using Mn ⁰	54
2.4.2.4	General Procedure D: Optimization and Investigation at 0.3 mmol Scale	54
2.4.3	Characterization of Isolated Products.....	55
2.4.4	Preparation of Alkylpyridinium Salt Substrates.....	61
2.4.4.1	Synthesis of Alkylpyridinium Salt 7	62
REFERENCES		64
3	NICKEL-CATALYZED CASCADE CYCLIZATION OF ALKENE-TETHERED ALKYLPIRIDINIUM SALTS AND ARYL HALIDES	68
3.1	Introduction	68
3.2	Results and Discussion	72
3.2.1	Initial Optimization Investigations	72
3.2.2	Mechanistic Experiments	76
3.2.3	Additional Optimization and Effect of the Tether.....	80
3.2.4	Scope in Aryl Halide	84
3.2.5	Conclusions	86
3.2.6	Experimental.....	86
3.2.6.1	General Information	86
3.2.6.2	General Optimization Procedure	87
3.2.6.3	Synthesis and Purification of N,N-Diisopropylacetamide.....	88
3.2.6.4	General Procedure for Cross-Coupling of Alkene-Tethered Alkylpyridinium Salts and Aryl Halides.....	89
3.2.6.5	Synthesis and Characterization of Alkene-Tethered Alkylpyridinium Salt Substrates.....	90
REFERENCES		94
Appendix		
A	PERMISSIONS	97
B	FUNDAMENTAL OBSERVATIONS	98
C	SPECTRAL DATA FOR CHAPTER 1	100
D	SPECTRAL DATA FOR CHAPTER 2	107
E	SPECTRAL DATA FOR CHAPTER 3	131

LIST OF TABLES

4	Table 1.1 Primary ArBr Reproducibility Data for Electrochemical Conditions (A)	21
5	Table 1.2 Primary ArBr Reproducibility Data for Mn ⁰ Conditions (B).....	21
6	Table 1.3 Primary ArBr Reproducibility Data for TDAE Conditions (C).....	21
7	Table 1.4 Secondary ArBr Reproducibility Data for Electrochemical Conditions (A)	21
8	Table 1.5 Secondary ArBr Reproducibility Data for Mn ⁰ Conditions (B).....	22
9	Table 1.6 Primary Informer Reproducibility Data for Electrochemical Conditions (A)	22
10	Table 1.7 Primary Informer Reproducibility Data for Mn ⁰ Conditions (B).....	22
11	Table 1.8 Primary Informer Reproducibility Data for TDAE Conditions (C).....	22
12	Table 1.9 Primary Informer Reproducibility Data for Electrochemical Conditions (A)	23
13	Table 1.10 Primary Informer Reproducibility Data for Mn ⁰ Conditions (B).....	23
14	Table 2.1 Optimization of Reaction Conditions ^a	43
15	Table 3.1 Investigation of Reductant ^a	73
16	Table 3.2 Investigation of Ligands ^a	74
17	Table 3.3 Investigation of Nickel Sources ^a	75
18	Table 3.4 Investigation of Solvent with TDAE as Reductant ^a	76
19	Table 3.5 Investigation of Aryl Bromide Equivalents ^a	81
20	Table 3.6 Investigation of Alkylpyridinium Salt Equivalents ^a	82

21	Table 3.7 Optimization of NTs Substrate ^a	83
----	--	----

LIST OF FIGURES

22	Figure 1.1 Structure of 24 Aryl Bromides Used for Scope Studies	7
23	Figure 1.2 Structure of Informer Halides	11

LIST OF SCHEMES

24	Scheme 1.1 Recently Developed Electroreductive Cross-Coupling Methods ...	2
25	Scheme 1.2 Proposed Mechanisms ^a	4
26	Scheme 1.3 Comparative Strategy for Primary and Secondary Alkylpyridinium Salts	6
27	Scheme 1.4 Primary and Secondary Aryl Bromide Scope Results	8
28	Scheme 1.5 Primary and Secondary Informer Halide Scope Results	12
29	Scheme 1.6 Evaluation of Mn ⁰ Conditions Optimal for 1° Alkylpyridinium Salt	23
30	Scheme 1.7 Evaluation of TDAE Conditions Optimal for 1° Alkylpyridinium	24
31	Scheme 1.8 Evaluation of TDAE Conditions at 45°C	24
32	Scheme 1.9 Evaluation of TDAE Conditions with Ligand L1	24
33	Scheme 1.10 ArBr Condition Comparison for Primary Alkylpyridinium Salt (Scheme 1.2A)	25
34	Scheme 1.11 ArBr Condition Comparison for Secondary Alkylpyridinium Salt (Scheme 1.2B)	25
35	Scheme 1.12 Informer Condition Comparison for Primary Alkylpyridinium Salt (Scheme 1.A)	26
36	Scheme 1.13 Informer Condition Comparison for Secondary Alkylpyridinium Salt (Scheme 1.3B)	26
37	Scheme 1.14 Comparison of ArBr and Informer Halide Scope for 1° vs 2° Alkylpyridinium Salts under Electrochemical Conditions	27
38	Scheme 2.1 Increased Functional Group Tolerance of Reductive Deaminative Cross-Couplings	36

39	Scheme 2.2 Prior Activation Methods of Aryl Chlorides	37
40	Scheme 2.3 Investigations of Aryl Chlorides in Deaminative Cross-Coupling Reactions with Chemical Reductant.....	38
41	Scheme 2.4 Previous Electrochemical Method and This Work	39
42	Scheme 2.5 Electrochemical Coupling of Secondary Substrate by the Stahl Group	39
43	Scheme 2.6 HTe-Chem Investigation of Ligand-Mediator Pairings ^a	41
44	Scheme 2.7 Scope and Limitations ^a	46
45	Scheme 2.8 Ligand-Mediator Pairing Investigation with 4-Chloroanisole ^a	48
46	Scheme 2.9 Electrochemical Investigations for Secondary Alkylpyridinium Salt ^a	49
47	Scheme 3.1 Heterocyclic Natural Products	69
48	Scheme 3.2 Dicarbofunctionalization of Alkenes	70
49	Scheme 3.3 Prior Art Utilizing Dicarbofunctionalization of Alkenes	71
50	Scheme 3.4 Cascade Cyclization of Alkene-Tethered Alkylpyridinium Salts.	72
51	Scheme 3.5 Proposed Mechanisms	77
52	Scheme 3.6 Nickel Concentration Experiments ^a	79
53	Scheme 3.7 Possible Side Products of Cascade Cyclization	80
54	Scheme 3.8 Aryl Halide Scope ^a	85

ABSTRACT

This dissertation focuses on the utilization of unactivated alkyl amines, a diverse and abundant substrate class, in cross-electrophile coupling reactions. Alkyl amines can be activated through a condensation reaction to form the corresponding Katritzky alkylpyridinium salts. Under reductive conditions, the alkylpyridinium salts fragment, resulting in the formation of an alkyl radical that can react with an aryl partner through a nickel-catalyzed mechanism. Compared to redox neutral cross-coupling techniques, reductive deamination has become an attractive approach to the formation of carbon-carbon (C-C) bonds for valuable, bioactive molecules and precursors.

Chapter 1 details a systematic examination of the scope of aryl bromide (ArBr) reactivity in nickel-catalyzed, reductive cross-electrophile couplings of primary vs. secondary alkylpyridinium salts using both electrochemical and chemical reductants. Facilitated using high-throughput experimentation (HTE) techniques, 37 aryl bromides, including 13 complex, drug-like examples, were investigated. By using primary and secondary substrates differing only by one methylene, we observed that the trends in ArBr reactivity are similar for the primary and secondary alkylpyridinium salts investigated, although distinctions were observed in isolated cases. In addition, the effectiveness of electrochemical conditions compared favorably to that of chemical reductants, especially for the more complex, drug-like aryl halides.

Chapter 2 focuses on the development of a nickel-catalyzed electrochemical method for the cross-electrophile coupling of primary alkylpyridinium salts and aryl

chlorides (ArCl_s). A cobalt anode and stainless-steel cathode were utilized in an undivided cell to yield various arylated products. During the reaction optimization process it was observed that high concentrations of electrolyte and aryl chloride coupling partner promote reaction efficiency. When reactions were done on large scale (1.0 mmol), larger surface area of anodes and cathodes are required to maintain sufficient electrolysis. This work demonstrates that the challenging coupling of alkylpyridinium salts is possible, but that several key limitations remain.

Chapter 3 describes a cascade cyclization of alkene-tethered alkylpyridinium salts. Alkyl amine starting materials can be functionalized with alkene tethers and activated as Katritzky pyridinium salts. When subjected to reductive nickel-catalyzed conditions, deamination of the alkene-tethered substrate occurred to give an alkyl radical, which then cyclized on the pendant alkene. Subsequent coupling with an aryl halide then allowed the formation of two new C–C bonds in one step. This chemistry provides an efficient method to access saturated (hetero)cyclic molecules.

Chapter 1

PRIMARY VS. SECONDARY ALKYL PYRIDINIUM SALTS: A COMPARISON UNDER ELECTROCHEMICAL AND CHEMICAL REDUCTION CONDITIONS

Work described here has been published (Garcia, B.; Sampson, J.; Watson, M. P.; Kalyani, D. *Faraday Discuss.* **2023**, *247*, 324-332). It is reprinted in this chapter with permission from the *Royal Society of Chemistry*. This work was a collaboration between myself in the M. Watson group at the University of Delaware, Dr. Jessica Sampson who is the director of the UD High-Throughput Experimentation Core Facility, and Dr. Dipannita Kalyani who is a principal scientist in discovery chemistry at Merck & Co Inc.

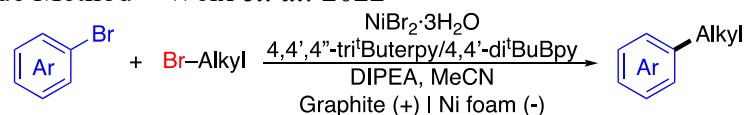
1.1 Introduction

Reductive cross-electrophile couplings are a powerful synthetic approach for the formation of C(sp³)-C(sp²) bonds, often offering broader functional group tolerance than their redox-neutral counterparts.¹⁻⁴ Other advantages include access to more diverse aryl halide feedstock classes and the ability to avoid extra synthetic steps to convert aryl halides into aryl nucleophiles. These types of methods were originally developed with manganese (Mn⁰) or tetrakis(dimethylamino)ethylene (TDAE) reductants.⁵⁻²¹ More recently, electrochemical conditions have been investigated to replace chemical reductants with an inherently more tunable approach.²²⁻²⁷ Electroreductive couplings have been developed for alkyl halides (Scheme 1.1A), NHPI esters (Scheme 1.1B),²⁸ and very recently Katritzky pyridinium salts (Scheme

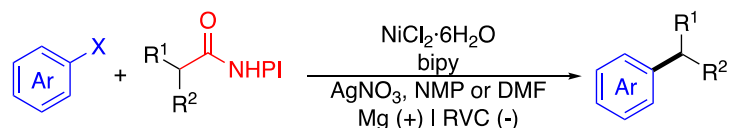
1.1C).²⁹⁻³¹ In these investigations, the reaction outcomes using electrochemical conditions are often compared to those using chemical reductants, with electrochemistry often providing complementary or improved results. However, a “mix and match” approach is often applied in scope studies, making systematic comparisons of the differences (or similarities) between scope for primary (1°) vs. secondary (2°) vs. tertiary (3°) alkyl substrates difficult. Importantly, the rates of oxidative addition of the aryl bromide and the alkyl electrophile activation must be matched for productive catalysis. Hence it is difficult to predict *a priori* whether the trends in ArBr scope would be the same for various alkyl classes.

Scheme 1.1 Recently Developed Electroreductive Cross-Coupling Methods

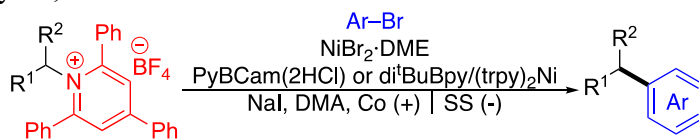
A. Alkyl Halide Method – Weix *et. al.* 2022



B. For NHPI Esters – Baran *et. al.* 2022



C. Watson, Kalyani, & Sevov *et. al.* 2023

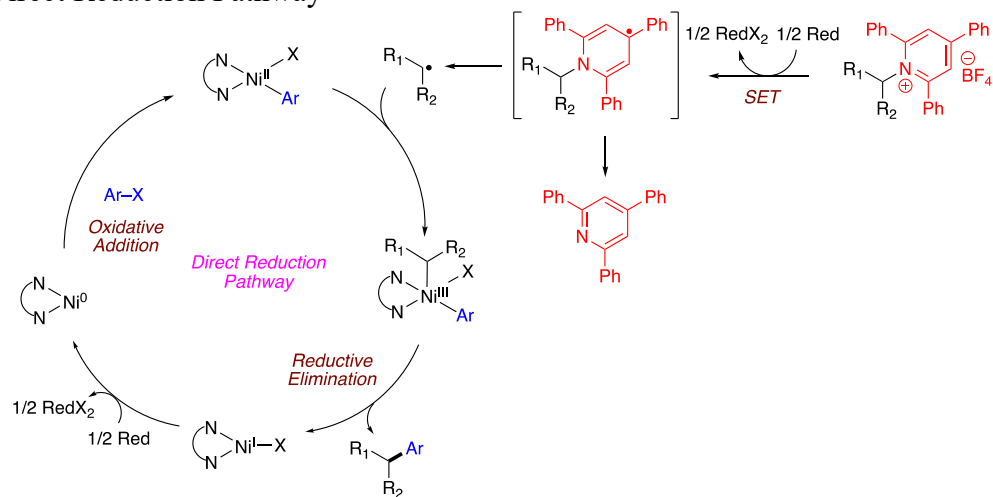


The ubiquity and diversity of alkyl amines in the inventories of pharmaceutical companies and the ease of activating them as Katritzky pyridinium salts makes deaminative couplings particularly useful in the context of medicinal chemistry

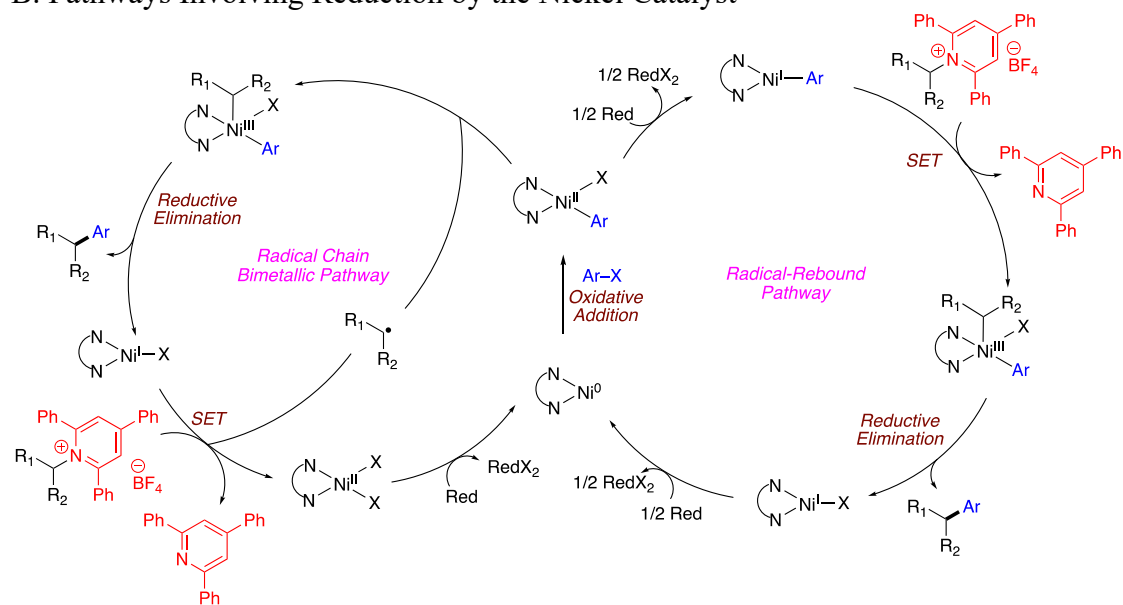
applications. Our previous report demonstrated dramatic differences in the optimal reaction conditions for 1° vs. 2° alkylpyridinium salts. This result is consistent with previous reactions of alkylpyridinium salts (Scheme 1.3A).^{16-20, 29} The difference in stability of 1° vs. 2° alkyl radicals impacts both the rate and reversibility of C–N bond cleavage,³² and different conditions are often required to achieve adequate yields using these two classes of substrates across a wide range of reaction types. In reductive couplings, this difference is exacerbated because the alkylpyridinium salts may be directly reduced by the reductant (Scheme 1.2A), instead of by single electron transfer (SET) with the Ni catalyst (Scheme 1.2B), leading to an imbalance in the rate of alkyl radical formation and the rate of ArBr oxidative addition. Because of these differences in the reactivity between 1° and 2° alkylpyridinium salts, it was unclear if they would have complementary or distinct trends in their ArBr scope, making it challenging to extrapolate ArBr scope studies from one alkylpyridinium class to another.

Scheme 1.2 Proposed Mechanisms^a

A. Direct Reduction Pathway



B. Pathways Involving Reduction by the Nickel Catalyst

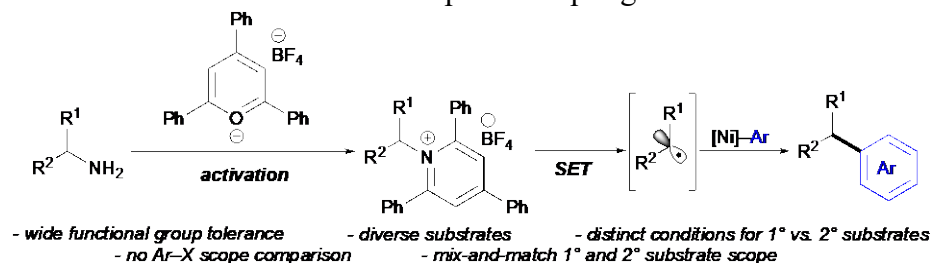


^aRed = reductant

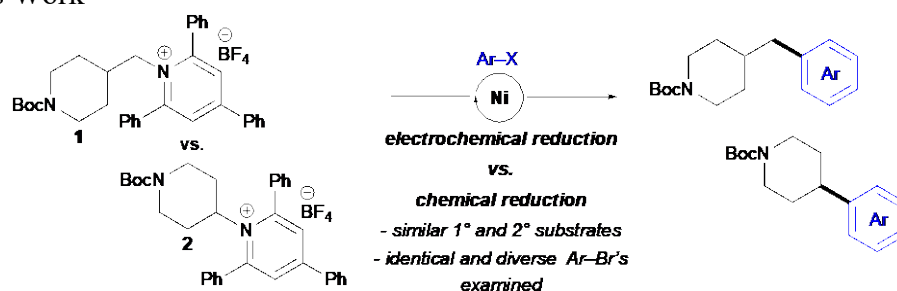
Herein, we report a systematic comparison of nickel-catalyzed reductive cross-electrophile couplings of primary and secondary alkylpyridinium salts with a diverse set of aryl bromides (Scheme 1.3B). This study builds upon our previous report on electrochemical reductive coupling of alkyl pyridiniums with aryl halides.²⁹ We now uncover relative reactivity trends between primary and secondary alkyl pyridinium substrates, where the primary and secondary substrates differ only by one methylene, making systematic comparison appropriate (Scheme 1.3B). Investigations were done using three distinct reaction conditions: (1) electrochemical reduction, (2) Mn^0 as a heterogeneous reductant and (3) TDAE as a homogeneous reductant. Facilitated by the use of high-throughput experimentation (HTE) techniques, including use of the recently developed HTE-Chem reactor,³³ 24 aryl bromides were investigated, along with 13 informer halides, which are complex, drug-like aryl halides from the chemistry informer library pioneered by researchers at Merck & Co., Inc., Rahway, NJ, USA.³⁴ We found that the trends in ArBr scope are fairly consistent between the primary and secondary alkylpyridinium salts, although distinctions were observed in isolated cases. In addition, the electrochemical conditions compared favorably to those using chemical reductants, especially among the more complex informer halides. The translatability of ArBr scope between 1° and 2° alkyl pyridiniums will be particularly useful in the context of medicinal chemistry where predictability of the reaction scope is crucial to provide confidence for applications of cross-couplings using precious drug-discovery program intermediates.

Scheme 1.3 Comparative Strategy for Primary and Secondary Alkylpyridinium Salts

A. Reductive Deaminative Cross-Electrophile Coupling Reactions



B. This Work



1.2 Results and Discussion

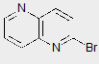
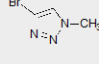
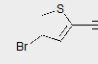
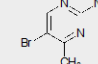
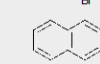
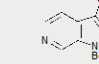
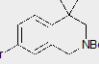
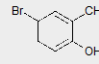
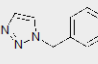
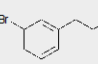
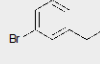
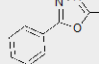
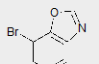
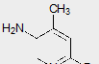
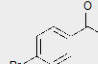
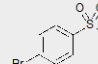
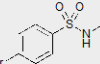
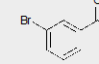
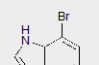

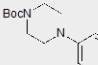
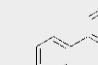
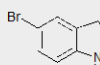
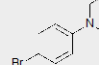
All experiments discussed below were performed at the University of Delaware as a close collaboration between myself and Dr. Jessica Sampson.

1.2.1 Investigations with 24 Diverse Aryl Bromides

We selected primary alkylpyridinium **1** and secondary alkylpyridinium **2** as our model substrates (Scheme 1.3B). Importantly, these substrates differ only by one methylene, making their results comparable. In addition, they provide mass-active products to facilitate LC-MS analysis of the crude reaction mixtures from the HTE experiments. Aryl bromides **ArBr-1–ArBr-24** were chosen as coupling partners, because they resulted in a wide range of product LC area percents (LCAPs) when used in our previously reported electroreductive coupling of a primary alkylpyridinium salt (Figure 1.1).²⁹ It should be noted that LCAPs were used to facilitate analysis of how

efficiently 24 different products formed without the need to independently prepare each product to obtain correction factors for yield determination from LC data. LCAPs show a general correlation to yields, but they are not yields. Caution should be used in extrapolating trends from differences in LCAPs between different substrates.

Figure 1.1 Structure of 24 Aryl Bromides Used for Scope Studies

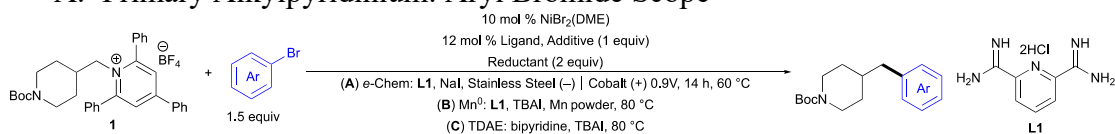
ArBr-1 	ArBr-2 	ArBr-3 	ArBr-4 	ArBr-5 	ArBr-6 
ArBr-7 	ArBr-8 	ArBr-9 	ArBr-10 	ArBr-11 	ArBr-12 
ArBr-13 	ArBr-14 	ArBr-15 	ArBr-16 	ArBr-17 	ArBr-18 
ArBr-19 	ArBr-20 	ArBr-21 	ArBr-22 	ArBr-23 	ArBr-24 

To determine suitable conditions for primary alkylpyridinium salt **1**, we initially evaluated conditions from the literature (Scheme 1.4A). Our previously published electrochemical conditions [NiBr₂(DME), pyridine-2,6-bis(carboximidamide) dihydrochloride (**L1**) as ligand, NaI as electrolyte, with a cobalt sacrificial anode and stainless-steel cathode at 60 °C]²⁹ provided satisfactory product LCAPs. Conditions using Mn⁰ and TDAE were chosen based on our previous report of reductive couplings of lysine-derived pyridinium salts.²¹

The results of these HTE campaigns using 1° alkylpyridinium substrate **1** are depicted in Scheme 1.4A. The electrochemical conditions compared favorably to the reactions using both chemical reductants (Mn and TDAE), with all three sets of conditions providing approximately the same average product LCAP across the 24 ArBr's. The scope of ArBr's for all three sets of conditions roughly follows similar trends. However, consistent with our previous reports, the TDAE conditions are often low-yielding for substrates with protic functional groups, such as **ArBr-8**, **ArBr-11**, and **ArBr-23**. However, there are also examples that fail with TDAE conditions for as yet unknown reasons, including **ArBr-1**, **ArBr-2**, and **ArBr-7**. Interestingly, the use of Mn⁰ conditions with **ArBr-11** also gave low LCAP, yet these conditions generally tolerate other protic functional groups.

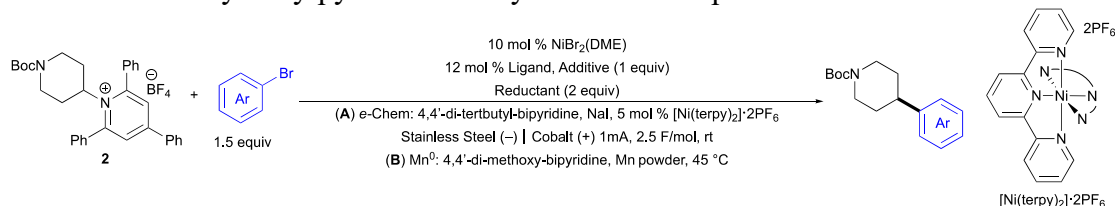
Scheme 1.4 Primary and Secondary Aryl Bromide Scope Results

A. Primary Alkylpyridinium: Aryl Bromide Scope



ArBr	Lowest LCAP																								Highest LCAP																								Average
	1	2	3	4	5	6	7	8	9	10	11	12	13	14	15	16	17	18	19	20	21	22	23	24	1	2	3	4	5	6	7	8	9	10	11	12	13	14	15	16	17	18	19	20	21	22	23	24	
e-Chem Condition A	0	2	2	4	9	11	8	19	17	21	22	21	19	18	29	22	25	32	36	31	36	47	38	41	21	19	18	29	22	25	32	36	31	36	47	38	41	21											
Mn Condition B	16	4	3	14	9	27	6	24	16	17	4	18	16	27	29	16	22	20	45	22	31	34	37	36	21	19	18	29	22	25	32	36	31	36	47	38	41	21											
TDAE Condition C	2	3	20	24	47	15	8	10	26	14	1	37	22	33	44	37	44	45	23	36	19	61	13	16	21	19	18	29	22	25	32	36	31	36	47	38	41	21											

B. Secondary Alkylpyridinium: Aryl Bromide Scope



ArBr	Lowest LCAP																								Highest LCAP																								Average					
	1	2	3	4	5	6	7	8	9	10	11	12	13	14	15	16	17	18	19	20	21	22	23	24	1	2	3	4	5	6	7	8	9	10	11	12	13	14	15	16	17	18	19	20	21	22	23	24						
e-Chem Condition A	3	0	20	5	25	9	19	10	4	9	5	10	20	5	25	17	21	30	3	19	16	13	27	21	14	13	12	11	10	9	8	7	6	5	4	3	2	1	0	1	2	3	4	5	6	7	8	9	10	11	12	13	14	14
Mn Condition B	3	0	13	3	15	8	3	2	1	2	1	12	4	3	24	17	23	16	13	27	4	1	1	7	14	13	12	11	10	9	8	7	6	5	4	3	2	1	0	1	2	3	4	5	6	7	8	9	10	11	12	13	14	14

Percentages reflect product LCAPs that are the average of multiple runs (see Experimental). Formation of triphenylpyridine was not considered for LCAP determinations. **(A)** Primary substrate coupling conditions: (a) **e-Chem** = **1** (35 μmol , 1 equiv), ArBr (52.5 μmol , 1.5 equiv), NiBr₂(DME) (10 mol %), pyridine-2,6-bis(carboximidamide) dihydrochloride (12 mol %), NaI (1 equiv), DMA [0.1 M], 0.9V, 60 °C, 14 h. (b) **Mn** = **1** (10 μmol , 1 equiv), ArBr (15 μmol , 1.5 equiv), NiBr₂(DME) (10 mol %), pyridine-2,6-bis(carboximidamide) dihydrochloride (12 mol %), Mn⁰ (2 equiv), TBAI (1 equiv), DMA [0.1 M], 80 °C, 24 h. (c) **TDAE** = **1** (10 μmol , 1 equiv), ArBr (15 μmol , 1.5 equiv), NiBr₂(DME) (10 mol %), bipyridine (12 mol %), TDAE (2 equiv), TBAI (1 equiv), DMA [0.1 M], 80 °C, 24 h. **(B)** Secondary substrate coupling conditions: (a) **e-Chem** = **2** (35 μmol , 1 equiv), ArBr (52.5 μmol , 1.5 equiv), NiBr₂(DME) (10 mol %), 4,4'-di-*tert*-butyl-bipyridine (12 mol %), [Ni(terpy)₂] \cdot 2PF₆ (5 mol%), NaI (1 equiv), DMA [0.1 M], 1mA constant current, 30V maximum 2.5 F/mol, rt. (b) **Mn** = **2** (10 μmol , 1 equiv), ArBr (15 μmol , 1.5 equiv), NiBr₂(DME) (10 mol %), 4,4'-di-methoxy-bipyridine (14 mol %), Mn⁰ (2 equiv), NMP [0.1 M], 45 °C, 24 h.

For the secondary alkylpyridinium salt **2**, we used electrochemical conditions that were optimal in our previous work (Scheme 1.4B).²⁹ The use of electrochemical mediator [Ni(terpy)₂] \cdot 2PF₆ was shown to be beneficial for the cross-coupling of secondary alkylpyridinium salts and alkyl halides. The anode (Co) and the cathode (stainless steel) were the same as those used for the primary alkylpyridinium salt couplings. The Mn⁰ conditions were inspired by work done by Martin and co-workers, where secondary alkylpyridinium salts were the prime focus.¹⁶ Because no

conditions using TDAE as a reductant have been previously reported for secondary pyridiniums, we evaluated several possible conditions (see Experimental); however, average LCAP was generally poor (<3%). Because optimal reaction conditions have not yet been developed with this substrate class, comparison of the results using TDAE was deprioritized for this study.

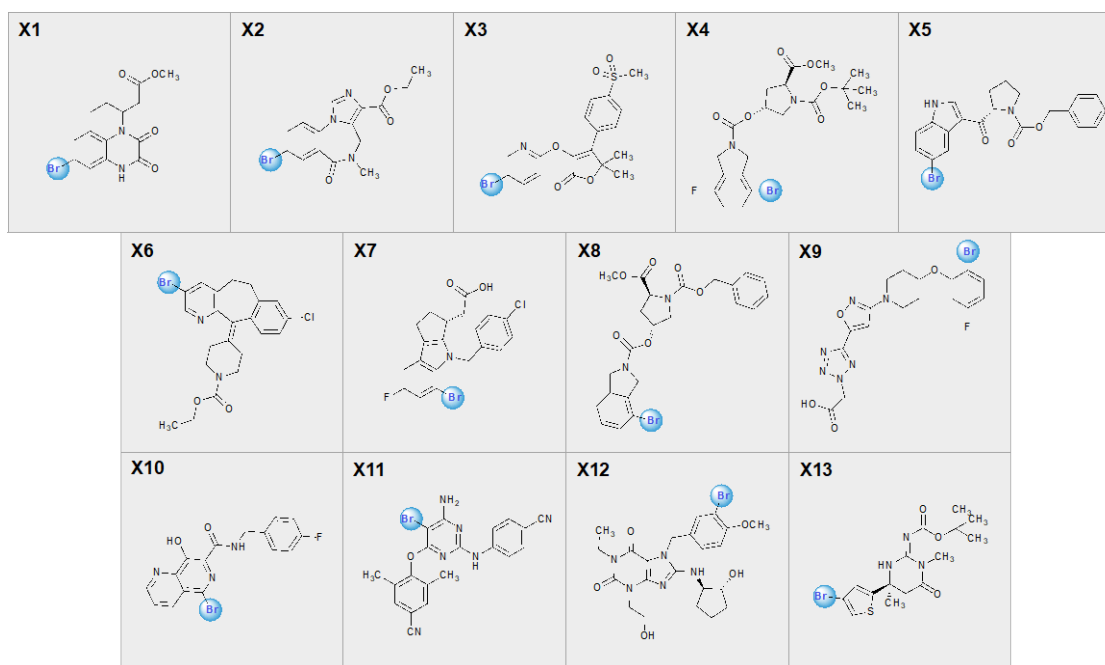
Analogous to the results with primary alkyl pyridiniums (Scheme 1.4A), the electrochemical conditions compare favorably with the chemical reductant for reactions with the 2° pyridinium **2**, with an average LCAP of 12% vs. 9% for Mn⁰. As a benchmark for how LCAP compares to yield, the coupling of pyridinium **2** and **ArBr-15** resulted in a 24% LCAP in this study, and 67% yield under the Mn conditions, as reported by the Martin group.¹⁶ Unlike the 1° pyridiniums, aryl bromides bearing protic functional groups afford low product LCAPs under both conditions (**ArBr-8**, **ArBr-10**, and **ArBr-11**). Interestingly, however, **ArBr-3** and **ArBr-5** afford higher product LCAPs than analogous reactions with 1° alkylpyridinium **1** using both the electrochemical and Mn⁰ conditions. We speculate that this change in scope between 1° and 2° alkylpyridinium salts may be due to the faster and more irreversible formation of the 2° alkyl radical, which requires in turn a faster oxidative addition of the ArBr. Thus, electron-rich aryl bromides (e.g., **ArBr-8**, **ArBr-10**, and **ArBr-11**) are less effective with alkylpyridinium **2**.

1.2.2 Investigations with Informer Halides

Encouraged by the scope with the 24 ArBr's detailed above, we also investigated the coupling of both 1° and 2° alkylpyridinium salts with informer halides to assess the efficacy of these methods in the context of complex, drug-like substrates (Fig. 1.2).³⁴ This informer halide library was defined by Merck researchers in an effort

to encourage the community to validate the generality of new methods against a standardized set of substrates with pharmaceutically relevant motifs. Because we focused this study on ArBr scope, the informer aryl iodides (**X14** and **X15**) and chlorides (**X16**, **X17**, and **X18**) were left out of this study. We investigated the scope across the remaining 13 informer halides with alkylpyridinium substrate **1** under the three sets of conditions (electrochemical, Mn^0 , and TDAE) and **2** under electrochemical and Mn^0 conditions.

Figure 1.2 Structure of Informer Halides



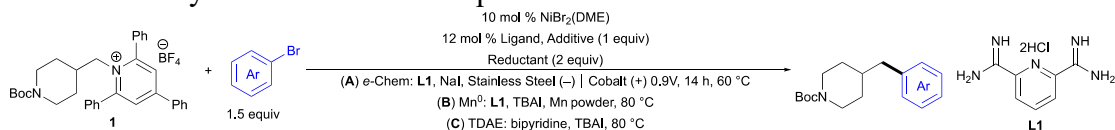
Results for the cross-coupling of 1° alkylpyridinium **1** with informer halides **X1–X13** are shown in Scheme 1.5A. The average LCAPs were 12%, 10%, and 15% for the electrochemical, Mn^0 , and TDAE conditions, respectively.

For all three sets of conditions, the scope was similar. An apparent limitation for the electrochemical conditions are pyridyl, fluorine and carboxylic acid containing

partners **X3**, **X4**, **X7** and **X9–11**, although it should be noted that simpler 3-bromo-5-phenylpyridine was successfully employed in our previous report and that the complexity of the informers makes such generalizations difficult.²⁹

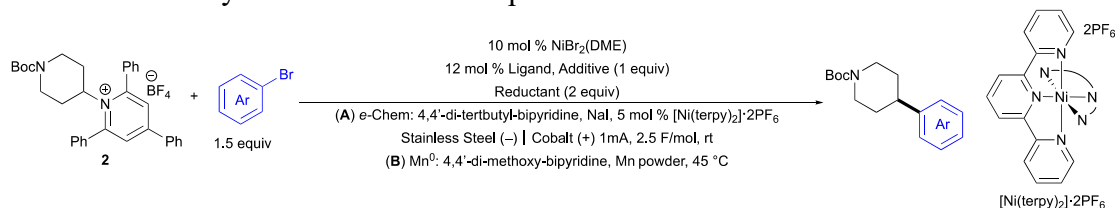
Scheme 1.5 Primary and Secondary Informer Halide Scope Results

A. Primary Informer Halide Scope



	Lowest LCAP					Highest LCAP								
Informer	1	2	3	4	5	6	7	8	9	10	11	12	13	Average
e-Chem Condition A	35	20	0	2	33	29	0	4	1	0	0	12	21	12
Mn Condition B	27	28	10	3	19	30	0	6	0	1	1	6	5	10
TDAE Condition C	0	67	15	12	3	56	0	15	0	0	0	25	2	15

B. Secondary Informer Halide Scope



Informer	1	2	3	4	5	6	7	8	9	10	11	12	13	Average
e-Chem Condition A	12	23	4	6	20	18	0	8	27	0	0	19	15	12
Mn Condition B	3	13	5	0	1	17	0	3	15	1	3	3	4	5

Percentages reflect product LCAPs that are the average of multiple runs (see Experimental). Formation of triphenylpyridine was not considered for LCAP determinations. (A) Primary substrate coupling conditions: (a) **e-Chem** = **1** (35 μmol, 1 equiv), ArBr (52.5 μmol, 1.5 equiv), NiBr₂(DME) (10 mol %), pyridine-2,6-bis(carboximidamide) dihydrochloride (12 mol %), NaI (1 equiv), DMA [0.1 M], 0.9V, 60 °C, 14 h. (b) **Mn** = **1** (10 μmol, 1 equiv), ArBr (15 μmol, 1.5 equiv), NiBr₂(DME) (10 mol %), pyridine-2,6-bis(carboximidamide) dihydrochloride (12 mol %), Mn⁰ (2 equiv), TBAI (1 equiv), DMA [0.1 M], 80 °C, 24 h. (c) **TDAE** = **1** (10 μmol, 1 equiv), ArBr (15 μmol, 1.5 equiv), NiBr₂•DME (10 mol %), bipyridine (12

mol %), TDAE (2 equiv), TBAI (1 equiv), DMA [0.1 M], 80 °C, 24 h. **(B)** Secondary substrate coupling conditions: (a) **e-Chem** = **2** (35 μ mol, 1 equiv), ArBr (52.5 μ mol, 1.5 equiv), NiBr₂(DME) (10 mol %), 4,4'-di-*tert*-butyl-bipyridine (12 mol %), [Ni(terpy)₂] \cdot 2PF₆ (5 mol%), NaI (1 equiv), DMA [0.1 M], 1mA constant current, 30V maximum 2.5 F/mol, rt. (b) **Mn** = **2** (10 μ mol, 1 equiv), ArBr (15 μ mol, 1.5 equiv), NiBr₂(DME) (10 mol %), 4,4'-di-methoxy-bipyridine (14 mol %), Mn⁰ (2 equiv), NMP [0.1 M], 45 °C, 24 h.

As shown in Scheme 1.5B, the couplings with 2° alkylpyridinium **2** were more challenging with average LCAPs of 12% and 5% for electrochemical and Mn⁰ conditions, respectively. Here, electrochemical conditions provided the broadest scope, with 6 informer halides leading to LCAPs \geq 15%.

1.3 Conclusions

In summary, this report describes a systematic comparison of the cross-electrophile couplings of two, nearly identical 1° and 2° alkylpyridinium salts under three different modes of reduction. The use of HTE techniques facilitated the cross-couplings and analysis of reactions using 24 diverse aryl bromides and 13 complex informer halides using electrochemical (using a sacrificial cobalt anode and stainless-steel cathode), and non-electrochemical conditions (using Mn⁰ and TDAE). Overall, the electrochemical conditions compare favorably with conditions using chemical reductants. In addition, and perhaps most importantly, the trends in ArBr scope were in general similar between the 1° and 2° alkylpyridinium salts, showing that one can extrapolate successes with one pyridinium class to the other with a reasonable level of confidence. This knowledge will be useful for chemists employing electrochemical

deaminative couplings in pharmaceutical discovery and other synthetic endeavors. It strengthens the confidence that methods developed with chemical reductants can be translated to electroreductive approaches, and that the scope of newly developed electroreductive deaminative methods is likely to be similar to those developed with Mn^0 . Perhaps even more importantly, this study provides future researchers with the knowledge that the scope of ArBr's is likely to be similar between 1° and 2° alkyipyridinium salts, facilitating the use of electrochemical deaminative cross-couplings broadly in parallel medicinal chemistry campaigns.

1.4 Experimental

1.4.1 General Information

Unless otherwise indicated, all Ni-catalyzed reactions were set up inside a nitrogen-purged glovebox and performed under an inert atmosphere of nitrogen, using Sure-seal (Sigma-Aldrich or Thermo Fisher) anhydrous solvents. $\text{NiBr}_2(\text{DME})$ was purchased from Strem Chemicals Inc. (catalog number 28-1145). Pyridine-2,6-dicarboxamide dihydrochloride was purchased from Sigma-Aldrich (catalog number 902047) and PharmaBlock (catalog number PBT3949-1). 4,4'-Di-*tert*-butyl-2,2'-bipyridine was purchased from Oakwood Chemical (catalog number 212480). All other commercial reagents were purchased from Sigma-Aldrich, Fisher, TCI, Combi-Blocks, Alfa Aesar and Ambeed and used as received.

The electrochemical mediator $[\text{Ni}(\text{terpy})_2]\cdot 2\text{PF}_6$ was prepared according to literature procedure.²⁶

High-throughput electrochemical experimentation (HTe-Chem) optimizations and scope evaluation were conducted using a 24-well electrochemical parallel reactor

from Analytical Sales and Services. Procedures for the assembly of HTe-Chem can be found at *ACS Cent. Sci.* **2021**, *7*, 1347. Cobalt electrodes were purchased from Surepure Chemicals L.L.C. (Product #10054, 1.60 mm diameter x 31.2 mm long), and stainless-steel electrodes were purchased from Analytical Sales (SKU: 700700, 1.63 mm diameter x 31.2 mm long). Within the undivided cells of the reactor, the cobalt sacrificial anode is 2 mm away from the stainless-steel cathode with a surface area of 34 mm². Non-electrochemical HTE experiments were performed in 1-mL glass vials secured in either a 96-well or 24-well aluminum block purchased from Analytical Sales and Services. For HTe-Chem experiments, electrodes and other consumables were purchased from Surepure Chemetals (Florham Park, New Jersey, USA) or Analytical Sales and Services (Flanders, New Jersey, USA). Electrodes were sonicated briefly in 0.1 M HCl solution then hexanes/acetone (1:1 v:v) mixture prior to use.

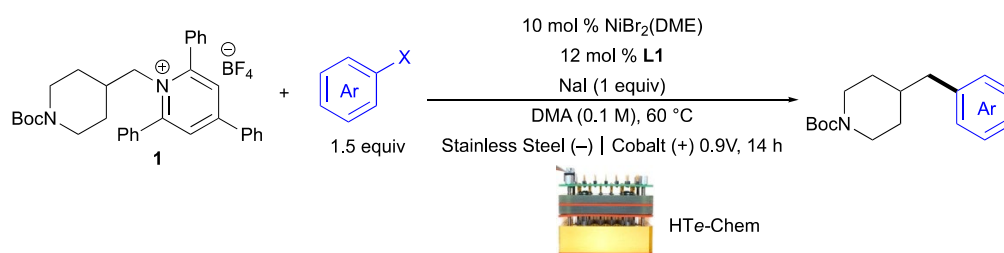
Analysis of all high throughput experimentation experiments was completed on a Waters Acquity Arc UHPLC-MS equipped with PDA and QDa detectors. A Waters 4.6 x 50 mm CORTECS column was used. The 5-minute analysis method used was 0 min, 10% B, 1.2 mL/min; 0.5 min, 10% B, 1.2 mL/min; 3.5 min, 100% B, 1.2 mL/min; 4.5 min, 100% B, 1.2 mL/min; 4.6 min, 10% B, 1.2 mL/min, where A = 0.1% formic acid in water and B = 0.1% formic acid in acetonitrile. Liquid chromatography area percentages (LCAPs) were determined from UV-Vis data collected from 210–400 nm and processed using PEAKSEL integration software. For more information visit <https://elsci.io/peaksel/index.html>.

Proton nuclear magnetic resonance spectra (¹H NMR), carbon nuclear magnetic resonance spectra (¹³C NMR), and fluorine nuclear magnetic resonance spectra (¹⁹F NMR) were recorded on a 400, 500, or 600 NMR spectrometer. Chemical

shifts for protons are recorded in parts per million and referenced to residual CHCl_3 ($\text{CHCl}_3 = \delta 7.26$) in deuterated chloroform. Chemical shifts for carbon are recorded in parts per million and referenced to carbon resonances of deuterated chloroform ($\text{CDCl}_3 = \delta 77.2$). Data are reported as follows: chemical shift, multiplicity (s = singlet, d = doublet, t = triplet, q = quartet, m = multiplet, etc.), coupling constants (Hz), integration.

1.4.2 High-Throughput Electrochemical (HTE-Chem) Procedures

1.4.2.1 Constant Voltage Procedure with Primary Alkylpyridinium Salt

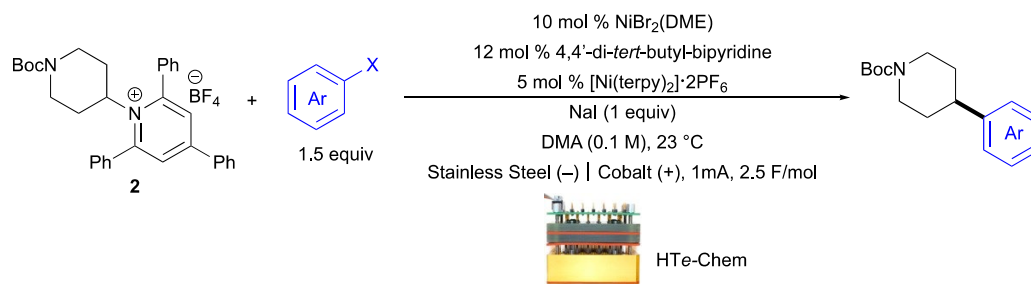


In a nitrogen-filled glovebox, to 1-mL vials (secured in a 24-well aluminum block) equipped with PTFE-covered 5 x 2 mm magnetic stir bars was added pyridinium **1** (175 μL , 0.2 M solution in DMA, 35 μmol , 1 equiv), aryl halide (105 μL , 0.5 M solution in DMA, 52.5 μmol , 1.5 equiv), NaI (50 μL , 0.7 M solution in DMA, 35 μmol , 1 equiv), and precomplexed $\text{NiBr}_2(\text{DME})$ catalyst/ligand **L1** mixture (23.3 μL , 0.15 M solution in DMA, 3.5 μmol , 10 mol %) sequentially. The electrodes were inserted, and the HTE-Chem reaction block was assembled inside the glovebox. The reactor was then connected to the external power supply inside the glovebox and heated to the appropriate temperature with 1000 rpm stirring on an IKA stir plate. Upon reaching the desired temperature, the reactions were electrolyzed under constant

voltage mode ($V = 0.9 \text{ V}$) for 14 h (overnight). After electrolysis, the HTe-Chem reactor was allowed to cool to room temperature, taken outside of the glovebox, and disassembled. Samples for analysis were prepared by transferring a $5 \mu\text{L}$ aliquot of the crude reaction mixture into a polypropylene analysis plate and diluting with $395 \mu\text{L}$ DMSO for LC-MS analysis.

Preparation of 0.15 M stock mixture of $\text{NiBr}_2(\text{DME})/\text{L1}$ mixture: In a nitrogen-filled glovebox, a 4-mL vial (equipped with a stir bar) was charged with $\text{NiBr}_2(\text{DME})$ catalyst ($239 \mu\text{mol}$, 73.6 mg) and L1 ($287 \mu\text{mol}$, 61.5 mg, 1.2 equiv with regard to Ni) and DMA ($1340 \mu\text{L}$) was added to prepare the final 0.15 M stock mixture. The mixtures were stirred for ~ 20 minutes (resulting in a slurry) before dosing into the reaction vials. The slurry was continually stirred at 1000 rpm while dosing.

1.4.2.2 Constant Current Procedure with Secondary Alkylpyridinium Salt



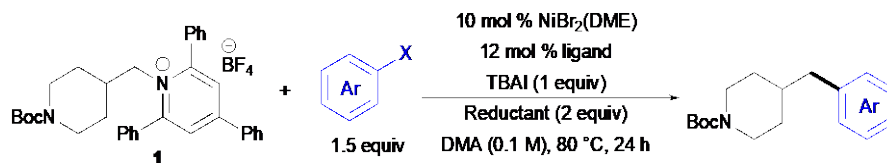
In a nitrogen-filled glovebox, to 1-mL vials (secured in a 24-well aluminum block) equipped with PTFE-covered $5 \times 2 \text{ mm}$ magnetic stir bars was added pyridinium **2** ($175 \mu\text{L}$, 0.2 M solution in DMA, $35 \mu\text{mol}$, 1 equiv), aryl halide ($105 \mu\text{L}$, 0.5 M solution in DMA, $52.5 \mu\text{mol}$, 1.5 equiv), NaI ($50 \mu\text{L}$, 0.7 M solution in DMA, $35 \mu\text{mol}$, 1 equiv), and precomplexed $\text{NiBr}_2(\text{DME})$ catalyst/ligand (4,4'-di-*tert*-butyl-

bipyridine)/mediator $[\text{Ni}(\text{terpy})_2]\cdot 2\text{PF}_6$ mixture (23.3 μL , 0.15 M solution in DMA, 3.5 μmol $\text{NiBr}_2(\text{DME})$, 10 mol % $\text{NiBr}_2(\text{DME})$ and 5 mol % $[\text{Ni}(\text{terpy})_2]\cdot 2\text{PF}_6$) sequentially. The electrodes were inserted, and the HTe-Chem reaction block was assembled inside the glovebox. The reactor was then connected to the external power supply inside the glovebox and heated to the appropriate temperature on an IKA stir plate. Upon reaching the desired temperature, the reactions were electrolyzed under constant current mode ($I = 1 \text{ mA}$, 2.5 F/mol). After electrolysis, the HTe-Chem reactor was taken outside of the glovebox and disassembled. Samples for analysis were prepared by transferring 5 μL aliquots of the crude reaction mixture into a polypropylene analysis plate and diluting with 395 μL of DMSO for LC-MS analysis.

Preparation of 0.15 M stock mixture of $\text{NiBr}_2(\text{DME})$ /ligand mixture: In a nitrogen-filled glovebox, a 4-mL vial (equipped with a stir bar) was charged with $\text{NiBr}_2(\text{DME})$ catalyst (239 μmol , 73.6 mg), 4,4'-di-*tert*-butyl-2,2'-bipyridine (287 μmol , 76.8 mg, 1.2 equiv with regard to $\text{NiBr}_2(\text{DME})$), $[\text{Ni}(\text{terpy})_2]\cdot 2\text{PF}_6$ (544 μmol , 97.9 mg, 0.5 equiv with regard to $\text{NiBr}_2(\text{DME})$), and DMA (1340 μL) to prepare the final 0.15 M stock mixture. The mixture was stirred for ~20 minutes (resulting in a slurry) before dosing into the reaction vials. The slurry was continually stirred at 1000 rpm while dosing.

1.4.3 High-Throughput Experimentation (HTE) Procedures with Chemical Reductants

1.4.3.1 General Procedure A for Primary Alkylpyridinium Salt 1

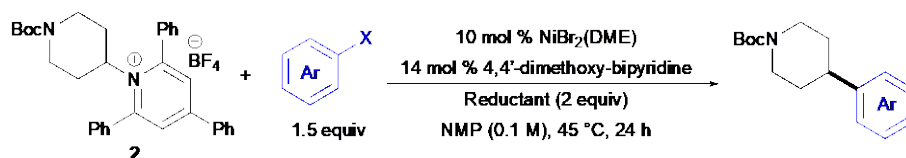


In a nitrogen-filled glovebox, to 1-mL vials (secured in a 24-well aluminum block) equipped with PTFE-covered 5 x 2 mm magnetic stir bars was added pyridinium (25 μ L, 0.4 M solution in DMA, 10 μ mol, 1 equiv), aryl halide (30 μ L, 0.5 M solution in solvent, 15 μ mol, 1.5 equiv), TBAI (14.3 μ L, 0.7 M solution in solvent, 10 μ mol, 1 equiv), precomplexed NiBr₂(DME) catalyst/ligand mixture (10 μ L, 0.1 M solution in solvent, 3.5 μ mol, 10 mol %), and appropriate reductant (33.3 μ L, 0.6 M in solvent, 20 μ mol, 2 equiv) sequentially. For Mn⁰ the mixture was added as a slurry stirred at 1000 rpm. The reaction block was sealed and placed on an IKA magnetic stir plate preheated at the appropriate temperature and stirred at 500 rpm for 24 h. The reaction block was allowed to cool to room temperature and taken out of the glovebox. Samples for analysis were prepared by transferring 5 μ L aliquots of the crude reaction mixture into a polypropylene analysis plate and diluting with 395 μ L DMSO for LC-MS analysis.

Preparation of 0.1 M stock mixture of NiBr₂(DME)/ligand mixture: In a nitrogen-filled glovebox, a 4-mL vial (equipped with a stir bar) was charged with NiBr₂(DME) catalyst (253 μ mol, 78.1 mg) and appropriate ligand (304 μ mol, 1.2 equiv regarding Ni) and solvent (2340 μ L) to prepare the final 0.1 M stock solution.

The mixtures were stirred for ~20 minutes (resulting in a slurry) before dosing into the reaction vials. The slurry was continually stirred at 1000 rpm while dosing.

1.4.3.2 General Procedure B using Mn⁰ with Secondary Alkylpyridinium Salt 2



In a nitrogen-filled glovebox, to 1-mL vials (secured in a 24-well aluminum block) equipped with PTFE-covered 5 x 2 mm magnetic stir bars was added pyridinium (25 μ L, 0.4 M solution in NMP, 10 μ mol, 1 equiv), aryl halide (30 μ L, 0.5 M solution in NMP, 15 μ mol, 1.5 equiv), precomplexed NiBr₂(DME) catalyst/ligand mixture (10 μ L, 0.1 M solution in NMP, 3.5 μ mol, 10 mol %), and Mn⁰ (47.6 μ L, 0.42 M in NMP, 20 μ mol, 2 equiv) sequentially. For Mn⁰ the mixture was added as a slurry stirred at 1000 rpm. The reaction block was sealed and placed on an IKA magnetic stir plate pre-heated at the appropriate temperature and stirred at 500 rpm for 24 h. The reaction block was allowed to cool to room temperature and taken out of the glovebox. Samples for analysis were prepared by transferring 5 μ L aliquots of the crude reaction mixture into a polypropylene analysis plate and diluting with 395 μ L DMSO for LC-MS analysis.

Preparation of 0.1 M stock mixture of NiBr₂(DME)/ligand mixture: In a nitrogen-filled glovebox, a 4-mL vial (equipped with a stir bar) was charged with NiBr₂(DME) catalyst (253 μ mol, 78.1 mg) and 4,4'-dimethoxy-bipyridine (354 μ mol, 76.6 mg, 1.4 equiv regarding Ni), and NMP (2340 μ L) to prepare the final 0.1 M stock solution. The mixtures were stirred for ~20 minutes (resulting in a slurry) before

dosing into the reaction vials. The slurry was continually stirred at 1000 rpm while dosing.

1.4.4 Reproducibility Data for Aryl Bromide Scope

Percentages reflect product LCAPs. Formation of triphenylpyridine was not considered for LCAP determinations. For chemical reduction conditions with both substrates, experiments for runs 2 and 3 were conducted at the same time. All data tables are color coded to depict lowest LCAP in blue, and highest LCAP in yellow.

Lowest LCAP Highest LCAP

1.4.4.1 Primary Alkylpyridinium Salt (Scheme 1.2A)

Table 1.1 Primary ArBr Reproducibility Data for Electrochemical Conditions (A)

ArBr	1	2	3	4	5	6	7	8	9	10	11	12	13	14	15	16	17	18	19	20	21	22	23	24	LCAP Average
Run 1	0	2	2	4	6	10	4	25	18	22	24	22	18	15	34	19	28	35	40	29	32	54	35	38	22
Run 2	0	2	2	4	11	11	12	12	16	20	20	20	20	21	24	25	21	28	31	32	39	40	41	44	21
Run Average	0	2	2	4	9	11	8	19	17	21	22	21	19	18	29	22	25	32	36	31	36	47	38	41	

Table 1.2 Primary ArBr Reproducibility Data for Mn⁰ Conditions (B)

ArBr	1	2	3	4	5	6	7	8	9	10	11	12	13	14	15	16	17	18	19	20	21	22	23	24	LCAP Average
Run 1	9	4	3	7	13	38	4	19	18	12	8	19	29	32	25	11	14	22	48	18	22	54	40	20	20
Run 2	21	3	4	25	10	19	6	27	17	20	3	16	10	26	28	18	27	18	40	23	36	24	43	40	21
Run 3	17	5	3	11	4	25	8	27	14	18	2	18	8	23	33	19	24	20	46	24	35	23	29	48	20
Run Average	16	4	3	14	9	27	6	24	16	17	4	18	16	27	29	16	22	20	45	22	31	34	37	36	

Table 1.3 Primary ArBr Reproducibility Data for TDAE Conditions (C)

ArBr	1	2	3	4	5	6	7	8	9	10	11	12	13	14	15	16	17	18	19	20	21	22	23	24	LCAP Average
Run 1	2	3	20	25	46	6	6	7	23	16	2	43	24	34	38	37	44	47	22	36	20	67	6	13	24
Run 2	2	3	20	21	48	26	11	12	30	12	0	34	22	32	48	38	41	45	24	38	17	56	16	17	26
Run 3	2	2	19	26	46	12	6	11	24	13	0	34	20	34	47	36	48	42	22	33	19	61	17	17	25
Run Average	2	3	20	24	47	15	8	10	26	14	1	37	22	33	44	37	44	45	23	36	19	61	13	16	

1.4.4.2 Secondary Alkylpyridinium Salt (Scheme 1.2B)

Table 1.4 Secondary ArBr Reproducibility Data for Electrochemical Conditions (A)

ArBr	1	2	3	4	5	6	7	8	9	10	11	12	13	14	15	16	17	18	19	20	21	22	23	24	LCAP Average
Run 1	4	0	23	5	30	7	21	10	3	11	2	12	22	4	24	17	26	29	4	28	13	13	28	23	15
Run 2	1	0	16	5	20	10	16	9	5	7	7	8	17	5	25	16	16	30	1	10	18	12	25	18	12
Run Average	3	0	20	5	25	9	19	10	4	9	5	10	20	5	25	17	21	30	3	19	16	13	27	21	

Table 1.5 Secondary ArBr Reproducibility Data for Mn⁰ Conditions (B)

ArBr	1	2	3	4	5	6	7	8	9	10	11	12	13	14	15	16	17	18	19	20	21	22	23	24	LCAP Average
Run 1	3	0	16	3	16	7	1	1	1	2	1	13	4	4	27	21	23	15	11	31	4	2	2	3	9
Run 2	4	0	13	3	15	8	3	2	1	2	1	12	3	2	22	12	24	15	12	28	3	1	1	7	8
Run 3	2	0	11	3	15	8	4	2	0	2	1	11	5	2	23	17	22	17	17	22	4	1	1	10	8
Run Average	3	0	13	3	15	8	3	2	1	2	1	12	4	3	24	17	23	16	13	27	4	1	1	7	

1.4.5 Reproducibility Data for Informer Halide Scope

Percentages reflect product LCAPs. Formation of triphenylpyridine was not considered for LCAP determinations. All data tables are color coded to depict lowest LCAP in blue, and highest LCAP in yellow.

Lowest LCAP	Highest LCAP
-------------	--------------

1.4.5.1 Primary Alkylpyridinium Salt (Scheme 1.3A)

Table 1.6 Primary Informer Reproducibility Data for Electrochemical Conditions (A)

Informer	1	2	3	4	5	6	7	8	9	10	11	12	13	LCAP Average
Run 1	36	19	0	2	32	26	0	4	1	0	0	15	21	12
Run 2	34	20	0	2	33	31	0	4	1	0	0	8	21	12
Run Average	35	20	0	2	33	29	0	4	1	0	0	12	21	

Table 1.7 Primary Informer Reproducibility Data for Mn⁰ Conditions (B)

Informer	1	2	3	4	5	6	7	8	9	10	11	12	13	LCAP Average
Run 1	23	28	10	3	19	34	0	6	0	1	1	9	5	11
Run 2	30	27	9	2	18	26	0	6	0	0	1	3	4	10
Run Average	27	28	10	3	19	30	0	6	0	1	1	6	5	

Table 1.8 Primary Informer Reproducibility Data for TDAE Conditions (C)

Informer	1	2	3	4	5	6	7	8	9	10	11	12	13	LCAP Average
Run 1	0	61	15	16	3	55	0	21	0	0	0	23	2	15
Run 2	0	72	15	7	2	56	0	8	0	0	0	26	2	14
Run Average	0	67	15	12	3	56	0	15	0	0	0	25	2	

1.4.5.2 Secondary Alkylpyridinium Salt (Scheme 1.3B)

Table 1.9 Primary Informer Reproducibility Data for Electrochemical Conditions (A)

Informer	1	2	3	4	5	6	7	8	9	10	11	12	13	LCAP Average
Run 1	13	22	4	6	23	19	0	8	25	0	0	20	12	12
Run 2	10	24	4	5	17	17	0	7	29	0	0	17	17	11
Run Average	12	23	4	6	20	18	0	8	27	0	0	19	15	

Table 1.10 Primary Informer Reproducibility Data for Mn⁰ Conditions (B)

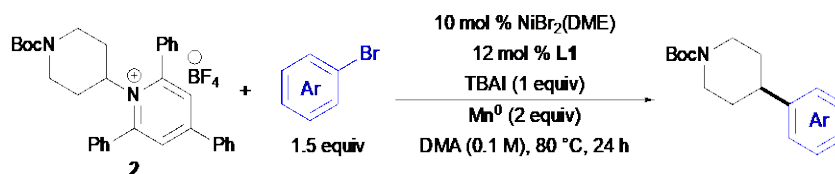
Informer	1	2	3	4	5	6	7	8	9	10	11	12	13	LCAP Average
Run 1	3	14	5	0	1	22	0	3	30	0	0	5	8	7
Run 2	3	12	5	0	1	12	0	2	0	1	5	0	0	3
Run Average	3	13	5	0	1	17	0	3	15	1	3	3	4	

1.4.6 Evaluation of Alternative Conditions with Mn⁰ and TDAE for Secondary Katritzky Pyridinium Salt 2

Percentages reflect product LCAPs. Formation of triphenylpyridine was not considered for LCAP determinations. All data tables are color coded to depict lowest LCAP in blue, and highest LCAP in yellow.

Lowest LCAP Highest LCAP

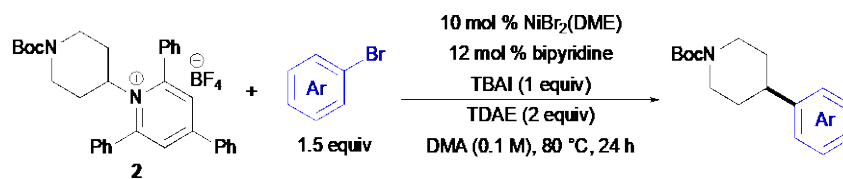
Scheme 1.6 Evaluation of Mn⁰ Conditions Optimal for 1° Alkylpyridinium Salt



ArBr	1	2	3	4	5	6	7	8	9	10	11	12	13	14	15	16	17	18	19	20	21	22	23	24	Average
LCAP	4	11	7	0	2	3	3	10	3	3	6	4	2	1	2	9	9	4	8	6	4	5	22	6	6

Informer	1	2	3	4	5	6	7	8	9	10	11	12	13	Average
LCAP	5	3	3	1	5	7	0	1	42	1	0	4	1	6

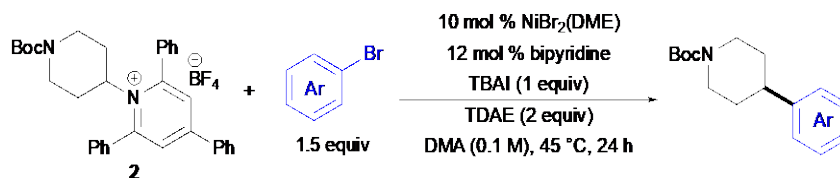
Scheme 1.7 Evaluation of TDAE Conditions Optimal for 1° Alkylpyridinium



ArBr	1	2	3	4	5	6	7	8	9	10	11	12	13	14	15	16	17	18	19	20	21	22	23	24	Average
LCAP	2	3	3	0	1	3	0	1	8	0	2	2	0	1	1	9	6	1	4	3	0	3	4	2	2

Informer	1	2	3	4	5	6	7	8	9	10	11	12	13	Average
LCAP	0	3	2	0	1	3	0	0	0	0	0	2	0	1

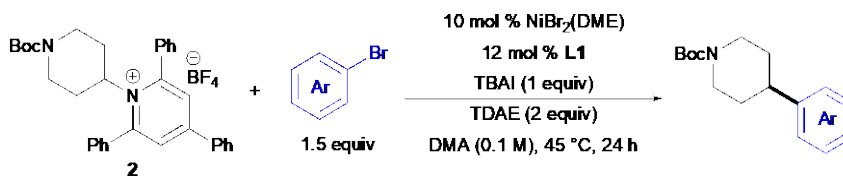
Scheme 1.8 Evaluation of TDAE Conditions at 45°C



ArBr	1	2	3	4	5	6	7	8	9	10	11	12	13	14	15	16	17	18	19	20	21	22	23	24	LCAP Average
Run 2	5	0	7	1	4	1	1	1	0	1	2	2	1	1	12	7	5	8	2	10	1	2	1	5	3
Run 3	6	0	7	1	5	1	1	1	0	1	2	2	1	1	11	6	2	8	2	9	1	2	1	5	3
Run Average	6	0	7	1	5	1	1	1	0	1	2	2	1	1	12	7	4	8	2	10	1	2	1	5	

Informer	1	2	3	4	5	6	7	8	9	10	11	12	13	Average
LCAP	0	3	2	0	1	3	0	0	0	0	0	2	0	1

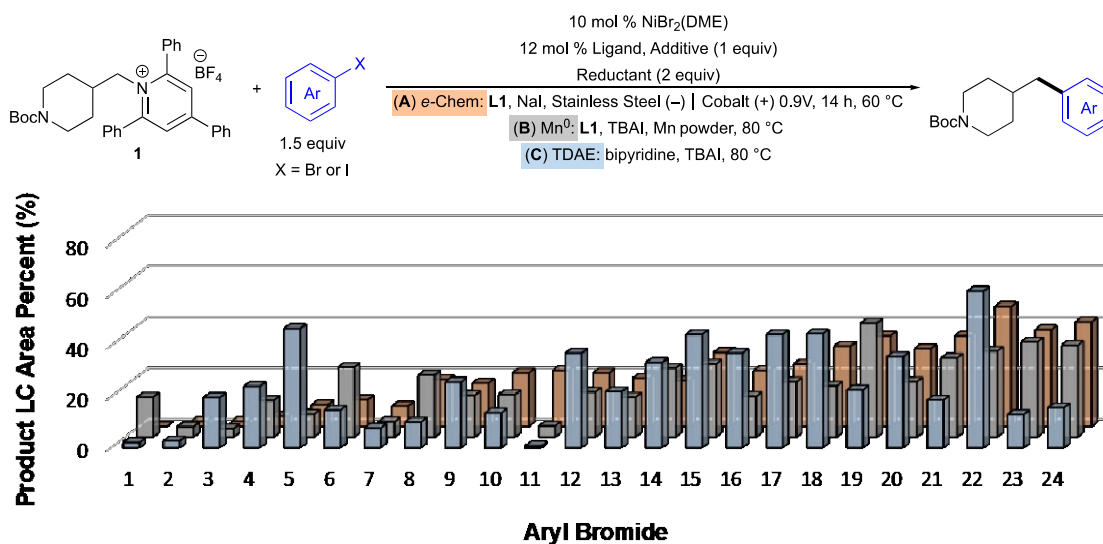
Scheme 1.9 Evaluation of TDAE Conditions with Ligand L1



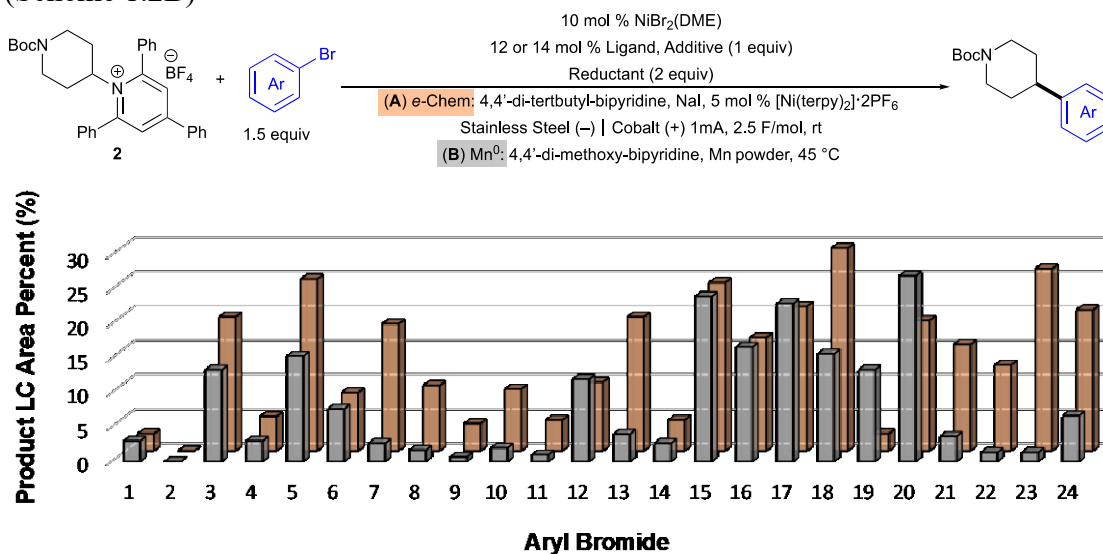
ArBr	1	2	3	4	5	6	7	8	9	10	11	12	13	14	15	16	17	18	19	20	21	22	23	24	Average
LCAP	0	4	6	0	0	0	2	0	0	0	1	0	0	0	0	3	5	0	4	5	1	3	2	0	2

1.4.7 Comparison of Electrochemical vs. Chemical Conditions for Aryl Bromide Scope

Scheme 1.10 ArBr Condition Comparison for Primary Alkylpyridinium Salt (Scheme 1.2A)



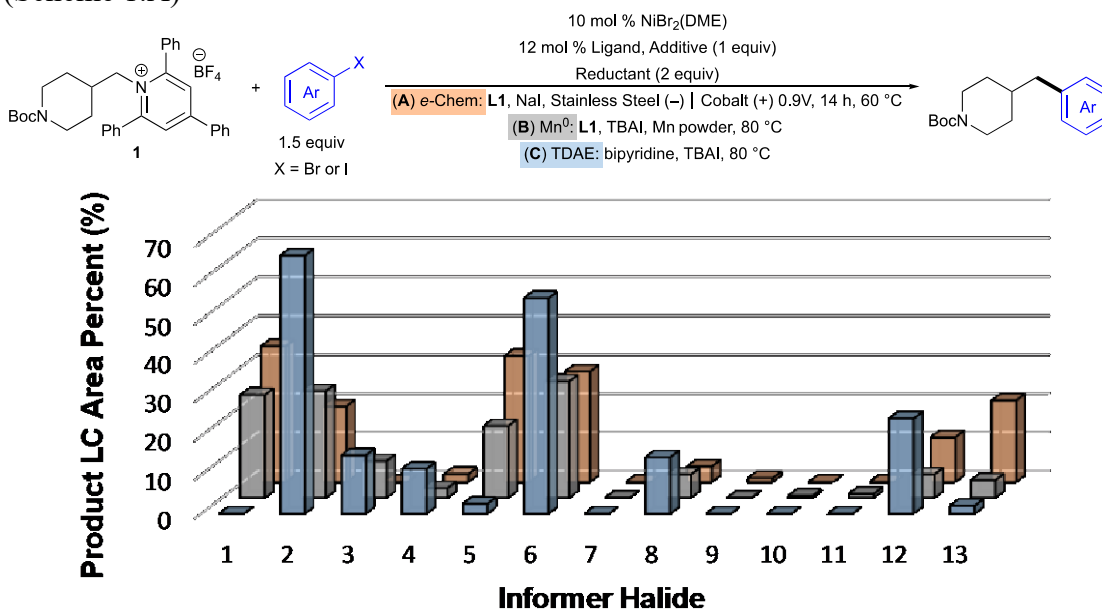
Scheme 1.11 ArBr Condition Comparison for Secondary Alkylpyridinium Salt (Scheme 1.2B)



1.4.8 Comparison of Electrochemical vs. Chemical Conditions for Informer Halide Scope

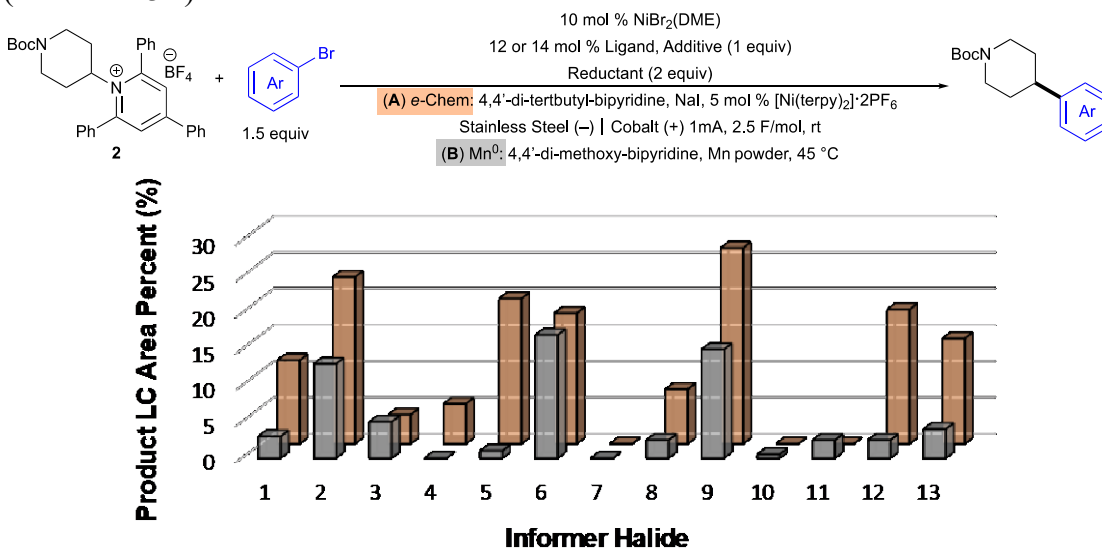
Scheme 1.12 Informer Condition Comparison for Primary Alkylpyridinium Salt

(Scheme 1.A)



Scheme 1.13 Informer Condition Comparison for Secondary Alkylpyridinium Salt

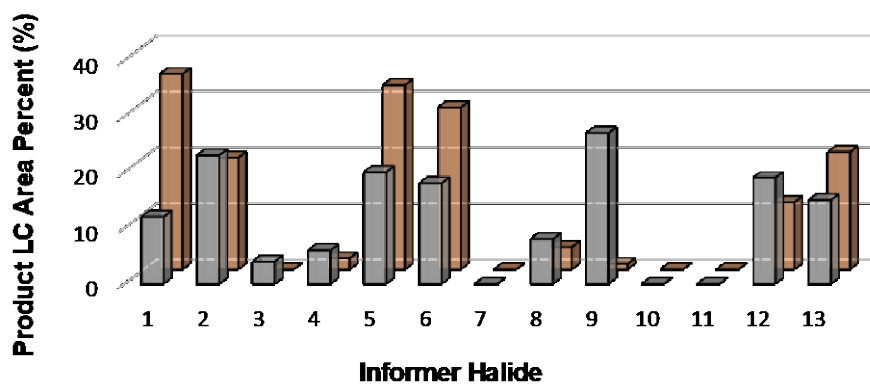
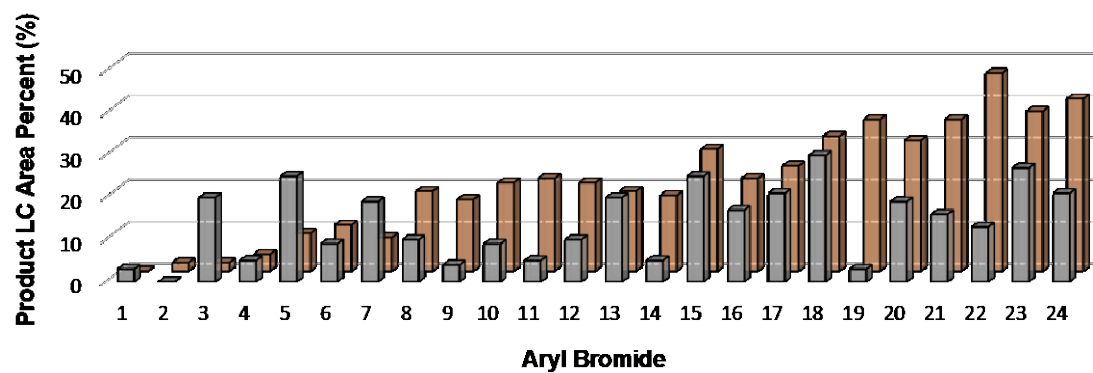
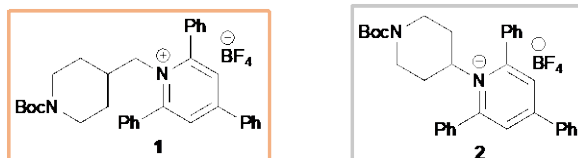
(Scheme 1.3B)



1.4.9 Comparison of ArBr Scope for 1° vs. 2° Alkylpyridinium Salts under Electrochemical Conditions

Scheme 1.14 Comparison of ArBr and Informer Halide Scope for 1° vs 2°

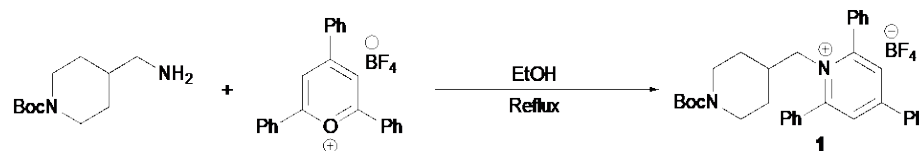
Alkylpyridinium Salts under Electrochemical Conditions



1.4.10 Preparation and Characterization of Katritzky Alkylpyridinium Salts

1.4.10.1 Synthesis of Primary Alkylpyridinium Salt 1

Primary pyridinium **1** was prepared as previously described.³⁵

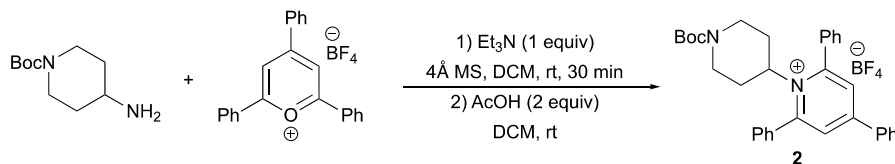


To a mixture of 2,4,6-triphenylpyrylium tetrafluoroborate (14.5 mmol, 5.8 g, 1.0 equiv) and 4-aminomethyl-1-Boc-piperidine (14.5 mmol, 3.1g, 1.0 equiv) was added EtOH (1.0 M) in a round-bottomed flask under air. The flask was fitted with a reflux condenser. The mixture was stirred and heated at reflux in an oil bath overnight. The mixture was then allowed to cool to room temperature. The mixture was diluted with Et₂O (2–3x volume of EtOH used) and vigorously stirred for 1 h. The resulting solid pyridinium salt was filtered and washed with Et₂O (3 x 25 mL).

¹H NMR (600 MHz, CDCl₃) δ 8.03 – 7.71 (m, 8H), 7.68 – 7.44 (m, 9H), 4.64 (d, J = 6.9 Hz, 2H), 3.81 (d, J = 13.5 Hz, 2H), 2.30 (t, J = 11.6 Hz, 2H), 1.69 – 1.51 (m, 1H), 1.35 (s, 9H), 1.00 (d, J = 11.7 Hz, 2H), 0.60 (qd, J = 12.2, 4.3 Hz, 2H). ¹³C NMR (151 MHz, CDCl₃) δ 157.4, 156.3, 154.6, 133.9, 133.3, 132.5, 131.5, 129.9, 129.72, 129.68, 128.3, 126.9, 79.9, 59.5, 43.1, 36.9, 29.3, 28.5. ¹⁹F NMR (565 MHz, CDCl₃) δ –153.0 (minor, ¹¹BF₄), –153.1 (major, ¹⁰BF₄). The spectral data of **1** is consistent with that previously reported in the literature.³⁵

1.4.10.2 Synthesis of Secondary Alkylpyridinium Salt 2

Secondary pyridinium **2** was prepared as previously described.³⁶



Under air, 2,4,6-triphenylpyrylium tetrafluoroborate (25 mmol, 9.9 g, 1.0 equiv), crushed activated 4Å molecular sieves (500 mg/mmol), and CH₂Cl₂ (0.5 M) were added to a round-bottomed flask with a stir bar. 4-Amino-1-Boc-piperidine (25 mmol, 5 g, 1.0 equiv) was added, and the flask was fitted with a septum. A vent needle was inserted, and Et₃N (25 mmol, 3.5 mL, 1.0 equiv) was added via syringe. The vent needle was removed, and the mixture was stirred at room temperature for 30 min. The vent needle was inserted again, and AcOH (50 mmol, 2.9 mL, 2.0 equiv) was added via syringe. The vent needle was removed, and the mixture was stirred at room temperature overnight. The mixture was filtered through a short pad of Celite, rinsing with CH₂Cl₂. The filtrate was then washed with aq. HCl (1.0 M, 2 x 30 mL), aq. NaHCO₃ (sat., 2 x 30 mL) and aq. NaCl (sat., 2 x 30 mL). The organic layer was dried (MgSO₄), filtered, and concentrated. Et₂O was added to the residue to precipitate the alkylpyridinium salt, which was collected by filtration and washed with Et₂O.

¹H NMR (600 MHz, CDCl₃) δ 7.87 (s, 2H), 7.84 – 7.71 (m, 6H), 7.64 – 7.47 (m, 9H), 4.81 (dd, J = 13.7, 10.8 Hz, 1H), 3.93 (d, J = 55.6 Hz, 2H), 2.43 – 1.65 (m, 6H), 1.31 (s, 9H). ¹³C NMR (151 MHz, CDCl₃) δ 157.35, 155.70, 154.36, 134.06, 133.88, 132.23, 131.25, 129.79, 129.47, 129.17, 128.45, 80.29, 70.10, 43.8 (br), 32.8 (br), 28.38. Note: one aromatic resonance is not observed due to coincidental overlap.

^{19}F NMR (565 MHz, CDCl_3) δ -153.04 (minor, $^{11}\text{BF}_4$), -153.09 (major, $^{10}\text{BF}_4$). The spectral data of **2** is consistent with that previously reported in the literature.³⁶

REFERENCES

1. Campeau, L.-C.; Hazari, N. Cross-Coupling and Related Reactions: Connecting Past Success to the Development of New Reactions for the Future. *Organometallics* **2019**, *38* (1), 3-35.
2. Gu, J. W., X.; Xue, W.; Gong, H. Nickel-catalyzed reductive coupling of alkyl halides with other electrophiles: concept and mechanistic considerations. *Org. Chem. Front.* **2015**, (2), 1411-1421.
3. Hu, X. Nickel-catalyzed cross coupling of non-activated alkyl halides: a mechanistic perspective. *Chem. Sci.* **2011**, (2), 1867-1886.
4. Dombrowski, A. W.; Gesmundo, N. J.; Aguirre, A. L.; Sarris, K. A.; Young, J. M.; Bogdan, A. R.; Martin, M. C.; Gedeon, S.; Wang, Y. Expanding the Medicinal Chemist Toolbox: Comparing Seven C(sp²)-C(sp³) Cross-Coupling Methods by Library Synthesis. *ACS Medicinal Chemistry Letters* **2020**, *11* (4), 597-604.
5. Everson, D. A.; Shrestha, R.; Weix, D. J. Nickel-Catalyzed Reductive Cross-Coupling of Aryl Halides with Alkyl Halides. *Journal of the American Chemical Society* **2010**, *132* (3), 920-921.
6. Everson, D. A.; Jones, B. A.; Weix, D. J. Replacing Conventional Carbon Nucleophiles with Electrophiles: Nickel-Catalyzed Reductive Alkylation of Aryl Bromides and Chlorides. *Journal of the American Chemical Society* **2012**, *134* (14), 6146-6159.
7. Wang, S.; Qian, Q.; Gong, H. Nickel-Catalyzed Reductive Coupling of Aryl Halides with Secondary Alkyl Bromides and Allylic Acetate. *Organic Letters* **2012**, *14* (13), 3352-3355.
8. Biswas, S. W., D. J. Mechanism and Selectivity in Nickel-Catalyzed Cross-Electrophile Coupling of Aryl Halides with Alkyl Halides. *J. Am. Chem. Soc.* **2013**, *135*, 16192-16197.
9. Everson, D. A. W., D.J. Cross-Electrophile Coupling: Principles of Reactivity and Selectivity. *J. Org. Chem.* **2014**, (79), 4793-4798.

10. Hansen, E. C.; Li, C.; Yang, S.; Pedro, D.; Weix, D. J. Coupling of Challenging Heteroaryl Halides with Alkyl Halides via Nickel-Catalyzed Cross-Electrophile Coupling. *The Journal of Organic Chemistry* **2017**, *82* (14), 7085-7092.
11. Charboneau, D. J.; Huang, H.; Barth, E. L.; Germe, C. C.; Hazari, N.; Mercado, B. Q.; Uehling, M. R.; Zultanski, S. L. Tunable and Practical Homogeneous Organic Reductants for Cross-Electrophile Coupling. *Journal of the American Chemical Society* **2021**, *143* (49), 21024-21036.
12. Cornella, J.; Edwards, J. T.; Qin, T.; Kawamura, S.; Wang, J.; Pan, C.-M.; Gianatassio, R.; Schmidt, M.; Eastgate, M. D.; Baran, P. S. Practical Ni-Catalyzed Aryl-Alkyl Cross-Coupling of Secondary Redox-Active Esters. *Journal of the American Chemical Society* **2016**, *138* (7), 2174-2177.
13. Huihui, K. M. M.; Caputo, J. A.; Melchor, Z.; Olivares, A. M.; Spiewak, A. M.; Johnson, K. A.; DiBenedetto, T. A.; Kim, S.; Ackerman, L. K. G.; Weix, D. J. Decarboxylative Cross-Electrophile Coupling of N-Hydroxyphthalimide Esters with Aryl Iodides. *Journal of the American Chemical Society* **2016**, *138* (15), 5016-5019.
14. Edwards, J. T.; Merchant, R. R.; McClymont, K. S.; Knouse, K. W.; Qin, T.; Malins, L. R.; Vokits, B.; Shaw, S. A.; Bao, D.-H.; Wei, F.-L.; et al. Decarboxylative alkenylation. *Nature* **2017**, *545* (7653), 213-218.
15. Salgueiro, D. C.; Chi, B. K.; Guzei, I. A.; García-Reynaga, P.; Weix, D. J. Control of Redox-Active Ester Reactivity Enables a General Cross-Electrophile Approach to Access Arylated Strained Rings**. *Angewandte Chemie International Edition* **2022**, *61* (33), e202205673.
16. Martin-Montero, R.; Yatham, V. R.; Yin, H.; Davies, J.; Martin, R. Ni-catalyzed Reductive Deaminative Arylation at sp³ Carbon Centers. *Organic Letters* **2019**, *21* (8), 2947-2951.
17. Yue, H.; Zhu, C.; Shen, L.; Geng, Q.; Hock, K. J.; Yuan, T.; Cavallo, L.; Rueping, M. Nickel-catalyzed C–N bond activation: activated primary amines as alkylating reagents in reductive cross-coupling. *Chemical Science* **2019**, *10* (16), 4430-4435.
18. Ni, S.; Li, C.-X.; Mao, Y.; Han, J.; Wang, Y.; Yan, H.; Pan, Y. Ni-catalyzed deaminative cross-electrophile coupling of Katritzky salts with halides via C–N bond activation. *Science Advances* **2019**, *5* (6), eaaw9516.

19. Liao, J.; Basch, C. H.; Hoerrner, M. E.; Talley, M. R.; Boscoe, B. P.; Tucker, J. W.; Garnsey, M. R.; Watson, M. P. Deaminative Reductive Cross-Electrophile Couplings of Alkylpyridinium Salts and Aryl Bromides. *Org. Lett.* **2019**, *21* (8), 2941-2946.
20. Yi, J.; Badir, S. O.; Kammer, L. M.; Ribagorda, M.; Molander, G. A. Deaminative Reductive Arylation Enabled by Nickel/Photoredox Dual Catalysis. *Organic Letters* **2019**, *21* (9), 3346-3351.
21. Twitty, J. C.; Hong, Y.; Garcia, B.; Tsang, S.; Liao, J.; Schultz, D. M.; Hanisak, J.; Zultanski, S. L.; Dion, A.; Kalyani, D.; et al. Diversifying Amino Acids and Peptides via Deaminative Reductive Cross-Couplings Leveraging High-Throughput Experimentation. *Journal of the American Chemical Society* **2023**, *145*, 5684-5695.
22. Jiao, K.-J.; Liu, D.; Ma, H.-X.; Qiu, H.; Fang, P.; Mei, T.-S. Nickel-Catalyzed Electrochemical Reductive Relay Cross-Coupling of Alkyl Halides to Aryl Halides. *Angewandte Chemie* **2020**, *132* (16), 6582-6586.
23. Truesdell, B. L.; Hamby, T. B.; Sevov, C. S. General C(sp²)–C(sp³) Cross-Electrophile Coupling Reactions Enabled by Overcharge Protection of Homogeneous Electrocatalysts. *Journal of the American Chemical Society* **2020**, *142* (12), 5884-5893.
24. Yan, M.; Kawamata, Y.; Baran, P. S. Synthetic Organic Electrochemical Methods Since 2000: On the Verge of a Renaissance. *Chemical Reviews* **2017**, *117* (21), 13230-13319.
25. Yi, L.; Ji, T.; Chen, K.-Q.; Chen, X.-Y.; Rueping, M. Nickel-Catalyzed Reductive Cross-Couplings: New Opportunities for Carbon–Carbon Bond Formations through Photochemistry and Electrochemistry. *CCS Chemistry* **2022**, *4* (1), 9-30.
26. Zackasee, J. L. S.; Al Zubaydi, S.; Truesdell, B. L.; Sevov, C. S. Synergistic Catalyst–Mediator Pairings for Electroreductive Cross-Electrophile Coupling Reactions. *ACS Catalysis* **2022**, *12* (2), 1161-1166.
27. Zhang, W.; Lu, L.; Zhang, W.; Wang, Y.; Ware, S. D.; Mondragon, J.; Rein, J.; Strotman, N.; Lehnher, D.; See, K. A.; et al. Electrochemically driven cross-electrophile coupling of alkyl halides. *Nature* **2022**, *604* (7905), 292-297.

28. Palkowitz, M. D.; Laudadio, G.; Kolb, S.; Choi, J.; Oderinde, M. S.; Ewing, T. E.-H.; Bolduc, P. N.; Chen, T.; Zhang, H.; Cheng, P. T. W.; et al. Overcoming Limitations in Decarboxylative Arylation via Ag–Ni Electrocatalysis. *Journal of the American Chemical Society* **2022**, *144* (38), 17709-17720.
29. Fu, J.; Lundy, W.; Twitty, C.; Sampson, J.; Watson, M.; Kalyani, D. Nickel-Catalyzed Electrochemical Reductive Cross-Electrophile Coupling of Alkylpyridinium Salts and Aryl Halides. *ACS Catalysis* **2023**, *13*, 9336-9345.
30. Liu, Y.; Tao, X.; Mao, Y.; Yuan, X.; Qiu, J.; Kong, L.; Ni, S.; Guo, K.; Wang, Y.; Pan, Y. Electrochemical C–N bond activation for deaminative reductive coupling of Katritzky salts. *Nature Communications* **2021**, *12* (1), 6745.
31. Wesenberg, L. J.; Sivo, A.; Vilé, G.; Noël, T. Ni-Catalyzed Electro-Reductive Cross-Electrophile Couplings of Alkyl Amine-Derived Radical Precursors with Aryl Iodides. *The Journal of Organic Chemistry* **2024**, *89*, 16121-16125.
32. Teyrulnikov, S.; Cai, Q.; Twitty, J. C.; Xu, J.; Atifi, A.; Bercher, O. P.; Yap, G. P. A.; Rosenthal, J.; Watson, M. P.; Kozłowski, M. C. Dissection of Alkylpyridinium Structures to Understand Deamination Reactions. *ACS Catalysis* **2021**, *11* (14), 8456-8466.
33. Rein, J.; Annand, J. R.; Wismer, M. K.; Fu, J.; Siu, J. C.; Klapars, A.; Strotman, N. A.; Kalyani, D.; Lehnher, D.; Lin, S. Unlocking the Potential of High-Throughput Experimentation for Electrochemistry with a Standardized Microscale Reactor. *ACS Central Science* **2021**, *7* (8), 1347-1355.
34. Kutchukian, P. S.; Dropinski, J. F.; Dykstra, K. D.; Li, B.; DiRocco, D. A.; Streckfuss, E. C.; Campeau, L.-C.; Cernak, T.; Vachal, P.; Davies, I. W.; et al. Chemistry informer libraries: a chemoinformatics enabled approach to evaluate and advance synthetic methods. *Chemical Science* **2016**, *7* (4), 2604-2613.
35. Sandfort, F.; Strieth-Kalthoff, F.; Klauck, F. J. R.; James, M. J.; Glorius, F. Deaminative Borylation of Aliphatic Amines Enabled by Visible Light Excitation of an Electron Donor–Acceptor Complex. *Chemistry – A European Journal* **2018**, *24* (65), 17210-17214.
36. Basch, C. H.; Liao, J.; Xu, J.; Pian, J. J.; Watson, M. P. Harnessing Alkyl Amines as Electrophiles for Nickel-Catalyzed Cross Couplings via C-N Bond Activation. *J Am Chem Soc* **2017**, *139* (15), 5313-5316.

Chapter 2

CROSS-ELECTROPHILE COUPLING OF PRIMARY ALKYL PYRIDINIUM SALTS AND ARYL CHLORIDES VIA NICKEL-CATALYZED ELECTROCHEMICAL REDUCTION

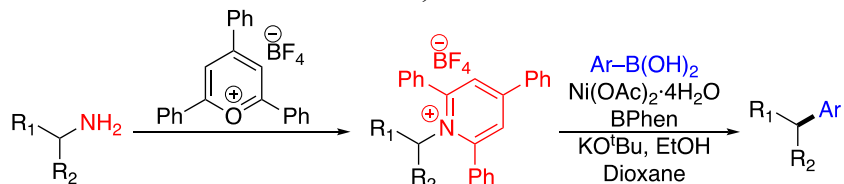
2.1 Introduction

Nickel-catalyzed deaminative cross-electrophile coupling reactions have become a vital tool to construct C(sp²)-C(sp³) bonds.^{1, 2} The first report of a deaminative cross coupling of n alkyl amine derivative with an unactivated alkyl group (not benzylic, allylic, α -carbonyl, or strained) was a redox neutral Suzuki-Miyara arylation of a Katritzky pyridinium salt (Scheme 2.1A). However, reductive methods are widely accepted over initially discovered redox-neutral protocols³⁻⁵ due to increased functional group tolerance of alkyl and aryl substituents. Reductive cross-couplings also avoid formation of an organometallic intermediate, which usually comes from an aryl halide precursor. The reported reductive deaminative arylations mainly focus on the use of aryl bromides and iodides.^{6-13, 29} For example, our group collaborated with researchers at Pfizer Inc. to develop a deaminative cross-coupling with aryl bromides (Scheme 2.1B). This reaction proceeded under neutral conditions, which allowed use of substrates with sensitive protic groups. Simultaneously, the Martin group published a similar nickel-catalyzed reductive coupling with aryl bromides (Scheme 2.1C), and the Molander group reported an iridium-photoredox-catalyzed approach (Scheme 2.1D). However, the use of aryl chlorides remains limited

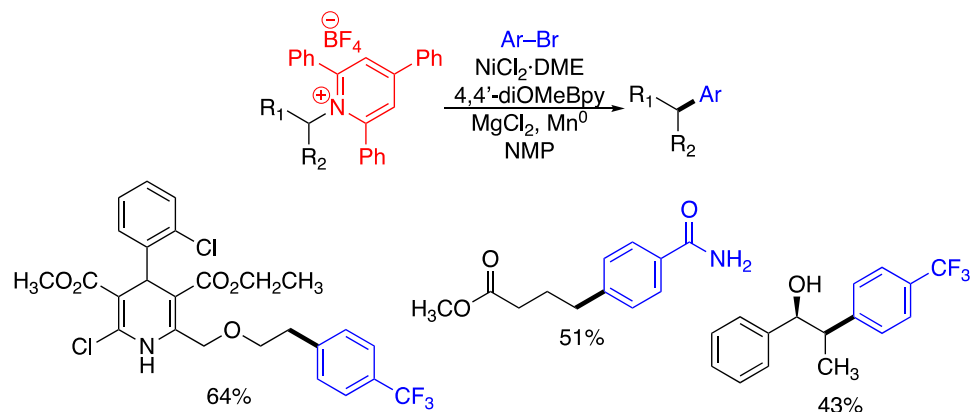
due to low reactivity.¹⁴ This suggests the activation of aryl chlorides in deaminative cross-coupling reactions may require more study to develop reaction conditions.

Scheme 2.1 Increased Functional Group Tolerance of Reductive Deaminative Cross-Couplings

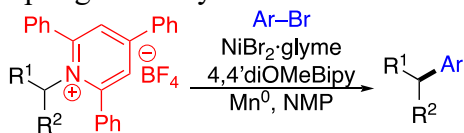
A. Initial Redox-Neutral Method – Watson, *et. al.* 2017



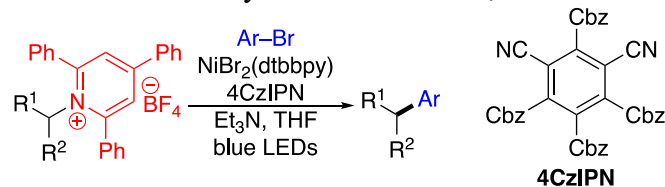
B. Improved Reductive Method and Tolerated Functional Groups – Watson, *et. al.* 2019



C. Deaminative Cross-Coupling with Aryl Bromides – Martin *et. al.* 2019



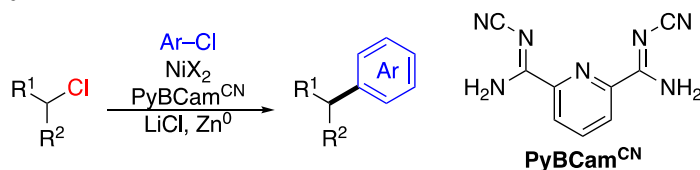
D. Nickel/Photoredox Reductive Arylation – Molander, *et. al.* 2019



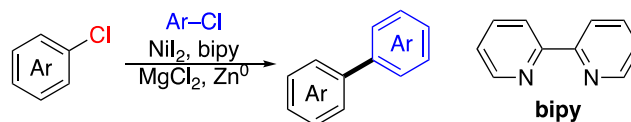
The incorporation of aryl chlorides in cross-coupling reactions is enticing due to their abundance and commercial availability in comparison to their aryl bromide counterparts (there are approximately 1,500,000 commercial aryl chlorides vs 640,000 commercially available aryl bromides).¹⁵ Methods to activate aryl chlorides for cross-electrophile coupling with alkyl^{16, 17} and aryl^{15, 18} coupling partners have been developed. For example, the Weix group demonstrated a reductive cross-electrophile coupling of alkyl chlorides and aryl chlorides and the Lautens group developed a method to couple aryl chlorides and heteroaryl chlorides (Scheme 2.2).

Scheme 2.2 Prior Activation Methods of Aryl Chlorides

Weix *et. al.* 2020



Lautens *et. al.* 2021

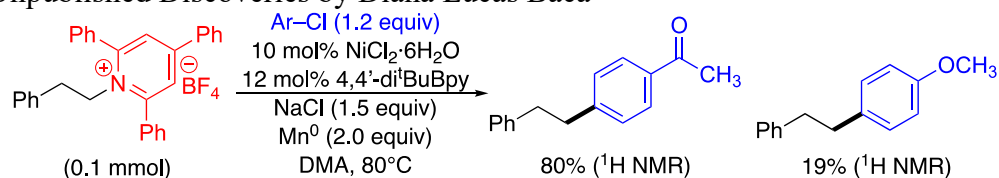


Although these procedures successfully engage aryl chlorides, the pursuit to incorporate aryl chlorides in deaminative cross-electrophile coupling reactions is ongoing,^{19, 20} to take advantage of two abundant feedstocks and form a variety of potentially bioactive, arylated compounds. A previous researcher in the M. Watson group, Diana Lucas Baca, investigated the use of chemical reductants in deaminative couplings with aryl chlorides (Scheme 2.3A). She discovered conditions that gave 80% yield in the coupling of 4-chloroacetophenone but were low yielding with 4-

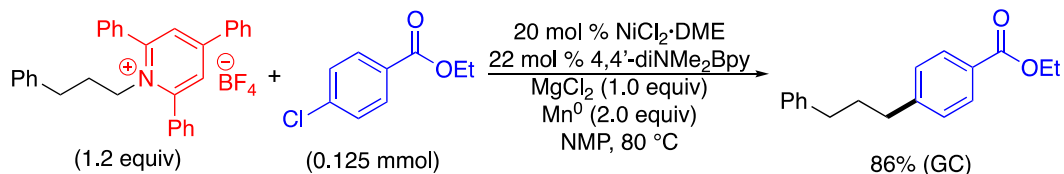
chloroanisole. Sigman, Hansen, and Weix also reported good yield for a coupling using an electron withdrawing aryl chloride and primary alkylpyridinium salt (Scheme 2.3B). However, this is limited to one example at 0.125 mmol scale.

Scheme 2.3 Investigations of Aryl Chlorides in Deaminative Cross-Coupling Reactions with Chemical Reductant

A. Unpublished Discoveries by Diana Lucas Baca



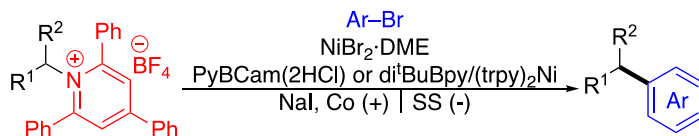
B. Coupling Example by Sigman, Hansen, and Weix



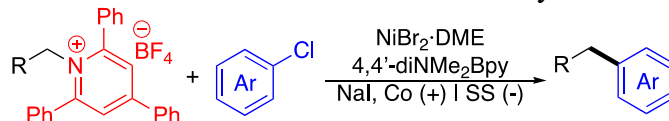
Electrochemical reductive methods have become an attractive alternative to reported chemical reductive procedures.²¹⁻²⁵ For deaminative cross-couplings electrochemical reduction has been utilized alongside aryl bromides²³ (Scheme 2.4A), and has shown to compare well to chemical reductants in comparative studies.⁹ Due to the tunability of electrochemical reduction and the aspiration to elucidate mild conditions to activate aryl chlorides, I sought to investigate the cross-electrophile coupling of aryl chlorides and alkylpyridinium salts using electrochemical methods (Scheme 2.4B).

Scheme 2.4 Previous Electrochemical Method and This Work

A. Electrochemical XEC of Alkylpyridinium Salts and Aryl Bromides – Watson, Kalyani, & Sevov *et. al.* 2023

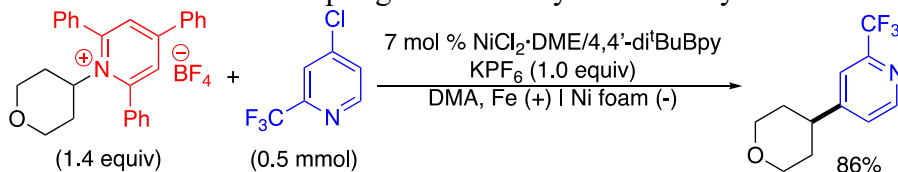


B. This Work: Electrochemical Deaminative XEC with Aryl Chlorides



Herein, a nickel-catalyzed electrochemical method for the cross-electrophile coupling of primary alkylpyridinium salts and aryl chlorides is reported. This work was performed in collaboration with Dr. Dipannita Kalyani (Merck & Co Inc.) and Dr. Christo Sevov (The Ohio State University). During the course of this research, the Stahl group included a single example of an electrochemical coupling of a secondary alkylpyridinium salt and an aryl chloride as part of a larger study comparing electroreduction to chemical reductants (Scheme 2.5). However, to our knowledge, this is the first reported account of an electrochemical cross-electrophile coupling of primary alkylpyridinium salts and aryl chlorides with large scale, isolated demonstrations.

Scheme 2.5 Electrochemical Coupling of Secondary Substrate by the Stahl Group

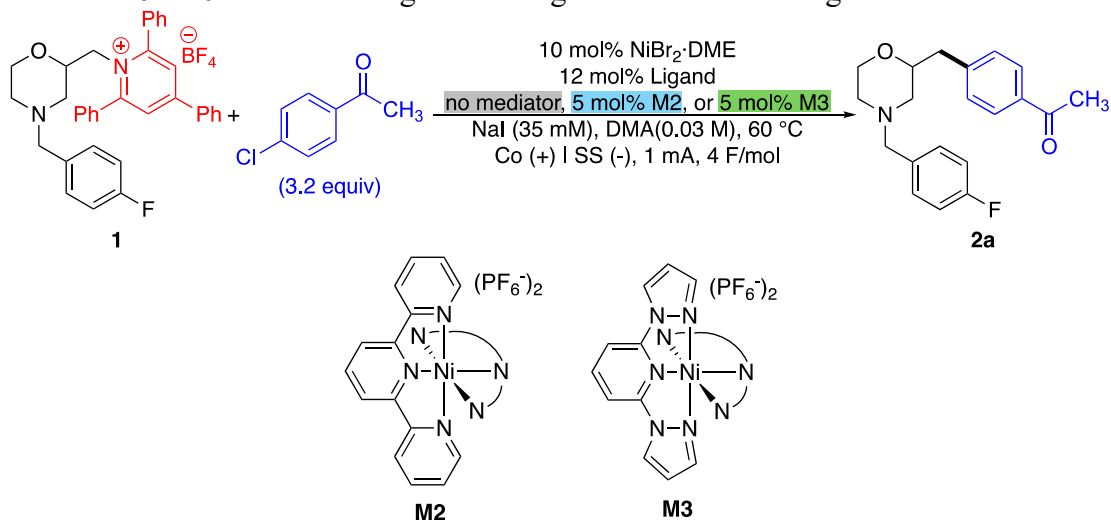


2.2 Results and Discussion

2.2.1 Reaction Development with Primary Alkylpyridinium Salt

The discovery of optimal reaction conditions began with a high-throughput electrochemical (H*T*e-Chem)²⁶ investigation of ligand-mediator pairings using primary alkylpyridinium salt **1a** and 4-chloroacetophenone (Scheme 2.6). Although electrochemical mediators were not required for the previously reported cross-electrophile coupling of primary alkylpyridinium salts and aryl bromides, it was hypothesized that aryl chloride coupling partners might benefit from increased electrochemical control.²⁷ In our previous study, mediator **M2** was used for the redox-matching of the radical initiation of secondary alkylpyridinium salts and the oxidative addition of aryl bromides. It was hypothesized that mediators would be beneficial towards matching the rate of radical initiation of a primary alkylpyridinium salts and the oxidative addition of an aryl chloride. It was also hypothesized that an electrochemical mediator might be beneficial to recycle reducing equivalents beyond those needed for productive reaction, as they were designed to protect against over oxidation of the anode.²⁷ In this H*T*e-Chem campaign, seven ligands (and one blank) were tested against two mediators (**M2** and **M3**), along with no mediator conditions. Both bidentate and tridentate nitrogen ligands were included; all have shown success in other reductive or deaminative couplings. Mediators **M2** and **M3** have been helpful in other electrochemical reactions.

Scheme 2.6 HTe-Chem Investigation of Ligand-Mediator Pairings^a



no mediator		5 mol % M2		5 mol % M3	
 L1 23%	 L5 14%	 L1 20%	 L5 18%	 L1 30%	 L5 16%
 L2 10%	 L6 31%	 L2 32%	 L6 25%	 L2 8%	 L6 12%
 L3 4%	 L7 3%	 L3 22%	 L7 13%	 L3 38%	 L7 3%
 L4 22%	no ligand 2%	 L4 11%	no ligand 14%	 L4 22%	no ligand 10%

^aReaction conditions: **1a** (10 μmol, 1.0 equiv), 4-Chloroacetophenone (32 μmol, 3.2 equiv), NiBr₂·DME (10 mol%), Ligand (12 mol%), NaI (10 μmol, 35 mM), **M2** or **M3** (5 mol%), DMA (0.03 M), 60 °C, cobalt (+), stainless steel (-), 1mA, 4F/mol. Yields determined by LC-MS analysis using 4,4-di-*tert*-butylbiphenyl as internal standard.

Several ligands showed promising results. Interestingly, pyridine-imidazoline ligand **L2** performed well only when used with **M2**, producing a 32% yield. In contrast, **L6** delivered a satisfactory yield of 31% without a mediator. It is noted that **L1** had consistent success across all conditions, while **L3** requires a mediator to provide favorable catalyst conditions.

Interest was taken in **L2** as it has not been used in deaminative cross-coupling reactions. Alongside **M2**, an investigation of electrolyte concentration was conducted (Table 2.1). It was observed that higher concentrations of electrolyte aided in the conduction of electrolysis, leading to increased yield of desired product (entries 1–3). A 70% yield was achieved using 350 mM of NaCl (entry 3).

At this point, reaction convenience became a priority. Although the combination of **L2** and **M2** was beneficial, **L2** was not commercially available and entailed a synthesis of multiple steps.²⁸ Although **M2** could be synthesized in one step, we hypothesized that the mediator may not be needed at such high concentrations of electrolyte. Utilizing **L6** in the absence of **M2** led to analogous yield of desired product (entry 4). In preparation of additional HTe-Chem campaigns, NaCl was substituted for NaI (entry 5), which afforded a comparable yield of 73%. A three-fold increase in reaction scale delivered a 77% yield of **2a** (entry 8). **L1** was also tested, with and without **M2**, as a potential alternative ligand on 0.1 mmol scale, yet did not give comparable product yields (entries 6 and 7). Using Mn⁰ as reductant in place of electrolysis resulted in 75% yield on 0.1-mmol scale (entry 5); however, yield decreased to 26% on 0.3-mmol scale (entry 8). This comparison demonstrates that an electrochemical approach is comparable to the use of chemical reductants but may be more easily scaled if electrode size and surface area are accounted for.

Table 2.1 Optimization of Reaction Conditions^a

Entry	Equiv Ar-Cl	L	mol% M2	NaX/mM	Yield 2a
0.1 mmol scale					
1	3.2	L2	10	NaCl/85mM	50
2	3.2	L2	10	NaCl/250mM	64
3	3.2	L2	10	NaCl/350mM	70
4	3.2	L6	0	NaCl/350mM	66
5	3.2	L6	0	NaI/350mM	73 (75) ^b
6	3.2	L1	5	NaI/350mM	48
7	3.2	L1	0	NaI/350mM	35
0.3 mmol scale					
8	3.2	L6	0	NaI/1M	77 (26) ^b
9	3.2	L6	0	NaI/100mM	40
10	1.5	L6	0	NaI/1M	46
11 ^c	3.2	L6	0	NaI/1M	0
12 ^d	3.2	L6	0	NaI/1M	0

^aReaction Conditions: 0.1 mmol = **1a** (0.1 mmol, 1.0 equiv), 4-Chloroacetophenone (0.32 mmol, 3.2 equiv), NiBr₂·DME (10 mol%), **L** (12 mol%), **M2** (5-10 mol%), NaX (x mmol, xx mM), DMA (0.03 M), 60 °C, cobalt (+), stainless steel (-), 1mA, 4F/mol. 0.3 mmol = **1a** (0.3 mmol, 1.0 equiv), 4-Chloroacetophenone (0.96 mmol, 3.2 equiv), NiBr₂·DME (10 mol%), **L6** (12 mol%), NaI (x mmol, xx mM), DMA (0.1 M), 60 °C, cobalt (+), stainless steel (-), 2mA, 4F/mol. Yields determined by ¹H NMR analysis using 1,3,5-trimethoxybenzene as internal standard. ^b(2.0 equiv) Mn⁰ added, no

electrolysis. ^cAbsence of NiBr₂·DME and **L6**. ^dElectrodes were inserted but no electrolysis was delivered.

Control experiments were conducted to test the effects of manipulated reaction parameters (Table 1, entries 9–12). Again, it was observed that a high concentration of sodium electrolyte is beneficial towards reaction efficiency (entries 8 vs. 9). It should be noted that only NaCl and NaI were tested as electrolytes; future work could include a more thorough investigation of the impact of electrolyte identity. When half the amount of ArCl is used (1.5 equiv) low yield is also observed. Biaryl homocoupling and unreacted aryl chloride are observed in the crude reaction mixture. The increased concentration of aryl chloride is beneficial to combat formation of side product and lack of reactivity. In absence of the nickel catalyst or electrolysis, no desired arylated product is observed (entries 11 and 12).

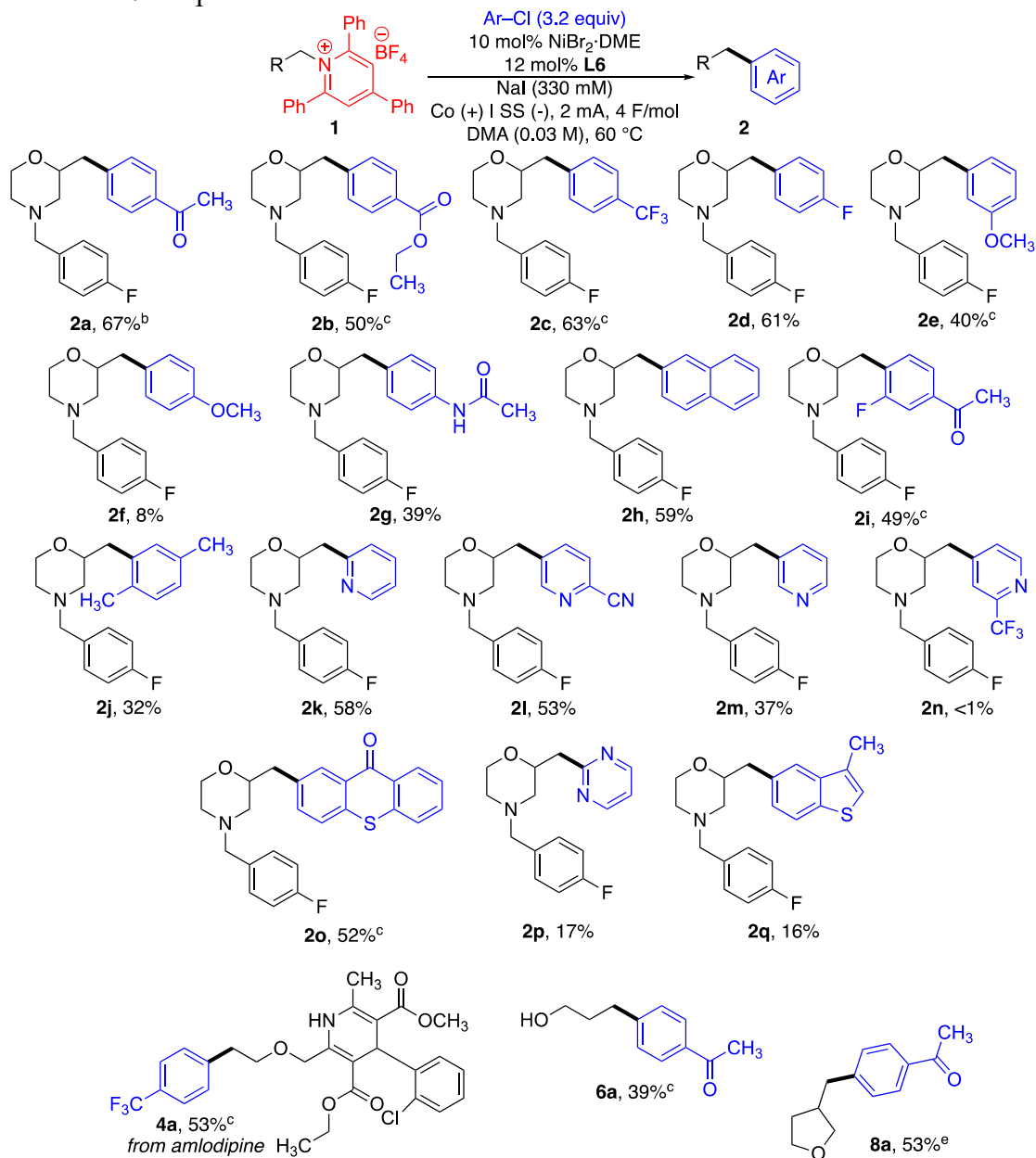
2.2.2 Aryl Chloride and Alkylpyridinium Salt Scope

With the newly optimized conditions in hand, the new focus was to demonstrate the scope of the method (Scheme 2.7). The model reaction was conducted on 1.0 mmol scale and desired product **2a** was isolated in 67% yield.

Exploration of the aryl chloride scope was done at 0.1 mmol scale. Other electron withdrawing aryl chlorides (**2b** and **2c**) were tolerated. Use of an electron neutral aryl chloride afforded product **2d** in 61% yield. While 3-chloroanisole gave product **2e** in 40% yield, 4-chloroanisole delivered product **2f** in 8% yield. A protic functional group are modestly tolerated (**2g**), which is expected as possible side reactions with the free proton may occur. Extended π -systems are decently tolerated as product **2h** was formed in 59% yield. Regarding *ortho*-substituted aryl chlorides, small

substituents in conjugation with electron withdrawing groups are tolerated, as product **2i** was formed in 49% yield. In comparison, product **2j**, containing an *ortho*-methyl substituent resulted in a 32% yield. When pyridyl substrates are incorporated, additional observations are made. Unsubstituted 2-pyridyl coupling partners, **2k**, are tolerated in 58% yield. 3-pyridyl coupling partners of electron deficient, **2l**, and electron neutral nature, **2m**, resulted in yields of 53% and 37% respectively. 4-Pyridyl substrates are not tolerated, see **2n**. Other aryl chlorides that performed poorly included pyrimidine aryl chloride coupling partners and sulfur containing heteroaromatics, **2p** and **2q**. The method is tolerable of xanthene derivatives, **2o**, and additional alkylpyridinium salt substrates containing secondary amines, **4a**, alcohols, **6a**, and heterocycles, **8a**.

Scheme 2.7 Scope and Limitations^a

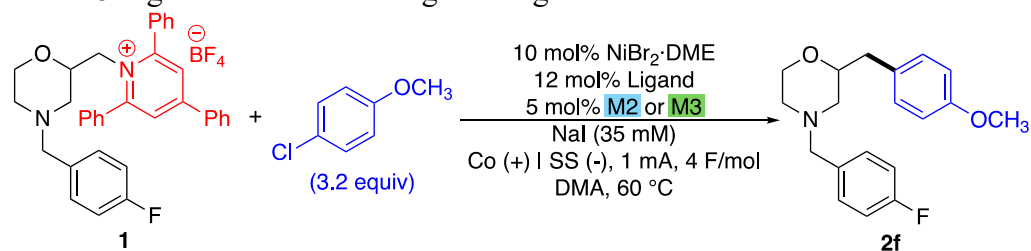


^aReaction Conditions: **1** (0.1 mmol, 1.0 equiv), aryl chloride (0.32 mmol, 3.2 equiv), NiBr₂·DME (10 mol%), L6 (12 mol%), NaI (1 mmol, 330 mM), DMA (0.03 M), 60 °C, cobalt (+), stainless steel (-), 1mA, 4F/mol. Yields determined by ¹H NMR analysis using 1,3,5-trimethoxybenzene as internal standard. ^bReaction Conditions: **1**

(1.0 mmol, 1.0 equiv), 4-chloroacetophenone (0.32 mmol, 3.2 equiv), NiBr₂·DME (10 mol%), **L6** (12 mol%), NaI (10 mmol, 1 M), DMA (0.1 M), 60 °C, cobalt (+), stainless steel (-), 1mA, 4F/mol. Isolated yield. °Reaction Conditions: alkylpyridinium salt (0.3 mmol, 1.0 equiv), aryl chloride (0.96 mmol, 3.2 equiv), NiBr₂·DME (10 mol%), **L6** (12 mol%), NaI (3 mmol, 1 M), DMA (0.1 M), 60 °C, cobalt (+), stainless steel (-), 2mA, 4F/mol. Isolated yield. ^d0.3 mmol scale, 70 °C. ^e0.3 mmol scale, Yield determined by ¹H NMR analysis using 1,3,5-trimethoxybenzene as internal standard.

The use of electron-rich aryl chlorides remains a challenge. High-throughput experiments were conducted with electron-rich aryl chloride, 4-chloroanisole, under electrochemical conditions (Scheme 2.8). However, low yields were still observed across all conditions surveyed. It is noted that the combination of **L2** with **M2** or **M3** shows promising results compared to other ligand-mediator combinations. At 0.1 mmol scale a 17% yield was observed when using **L2** and **M2**.

Scheme 2.8 Ligand-Mediator Pairing Investigation with 4-Chloroanisole^a



5 mol % M2			5 mol % M3		
 L1 <1%	 L5 <1%	 L10 <1%	 L1 <1%	 L5 <1%	 L10 <1%
 L2 9%	 L7 <1%	 L11 <1%	 L2 8%	 L7 <1%	 L11 <1%
 L3 4%	 L8 5%	 L12 2%	 L3 3%	 L8 2%	 L12 <1%
 L4 1%	 L9 2%	no ligand <1%	 L4 <1%	 L9 1%	no ligand <1%

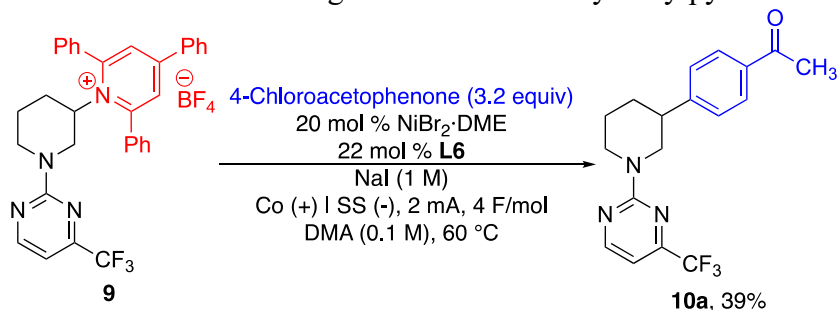
^aReaction conditions: **1** (10 μmol, 1.0 equiv), 4-Chloroacetophenone (32 μmol, 3.2 equiv), NiBr₂·DME (10 mol%), Ligand (12 mol%), NaI (10 μmol, 35 mM), **M2** or **M3** (5 mol%), DMA (0.03 M), 60 °C, cobalt (+), stainless steel (-), 1mA, 4F/mol. Yields determined by LC-MS analysis using 4,4-di-*tert*-butylbiphenyl as internal standard.

2.2.3 Investigations with Secondary Alkylpyridinium Salt

Preliminary investigations were conducted for the cross-electrophile coupling of secondary alkylpyridinium salt **9** (Scheme 2.9). A modest 39% yield of product **10a** is observed when using 20 mol % catalyst.

We have previously demonstrated that secondary alkylpyridinium salts can be utilized under electrochemical reductive conditions, and electron-deficient aryl chlorides can be activated using the current developed method. It is hypothesized the rate of radical initiation of the secondary alkylpyridinium salt is misaligned with the rate of oxidative addition of the aryl chloride under the current electrochemical system. An investigation of alternate anode and cathode combinations may be beneficial towards further optimizing this reaction, as different reduction potentials can be accessed and tested.

Scheme 2.9 Electrochemical Investigations for Secondary Alkylpyridinium Salt^a



^aReaction conditions: **9** (0.3 mmol, 1.0 equiv), 4-Chloroacetophenone (0.96 mmol, 3.2 equiv), NiBr₂·DME (10 mol%), **L6** (12 mol%), NaI (10 mmol, 1 M), DMA (0.1 M), 60 °C, cobalt (+), stainless steel (-), 2mA, 4F/mol. Yield determined by ¹H NMR analysis using 1,3,5-trimethoxybenzene as internal standard.

2.3 Conclusions

In conclusion, a nickel-catalyzed electrochemical method for the cross-electrophile coupling of primary alkylpyridinium salts and electron-poor aryl chlorides has been developed. This work shows that electrochemical conditions compare favorable to those using Mn^0 , but did not solve the challenge of electron-rich aryl chlorides. It is also observed that the benefit of electrochemical mediators depends on the ligand employed. The cross-electrophile coupling of secondary alkylpyridinium salts requires additional investigation and alternate reaction conditions.

2.4 Experimental

2.4.1 General Information

Unless otherwise indicated, all Ni-catalyzed reactions were set up inside a nitrogen-purged glovebox and performed under an inert atmosphere of nitrogen, using Sure-seal (Sigma-Aldrich or Thermo Fisher) anhydrous solvents. $\text{NiBr}_2(\text{DME})$ was purchased from Strem Chemicals Inc. (catalog number 28-1145). All other commercial reagents were purchased from Sigma-Aldrich, Acros, Thermo Fisher, Strem, TCI, Oakwood, Combi-Blocks, Alfa Aeser, Ambeed, or Cambridge Isotopes Laboratories and used as received.

Electrochemical redox mediators **M2** and **M3** were prepared according to literature procedure (*ACS Catal.* **2022**, *12* (2), 1161-1166). Racemic pyridine-oxazoline ligand, **L9**, was prepared according to literature procedure (*J. Am. Chem. Soc.* **2024**, *146* (26), 17606-17612).

High-throughput electrochemical experimentation (HTe-Chem) optimizations were conducted using a 24-well electrochemical parallel reactor from Analytical Sales and Services. Procedures for the assembly of HTe-Chem can be found at *ACS Cent.*

Sci. **2021**, *7*, 1347. Cobalt electrodes were purchased from Surepure Chemicals L.L.C. (Product# 10054, 1.60 mm diameter x 31.2 mm long), and stainless-steel electrodes were purchased from Analytical Sales (SKU: 700700, 1.63 mm diameter x 31.2 mm long). Within the undivided cells of the reactor, the cobalt sacrificial anode is 2 mm away from the stainless-steel cathode. Electrodes and other consumables were purchased from Surepure Chemetals (Florham Park, New Jersey, USA) or Analytical Sales and Services (Flanders, New Jersey, USA). Electrodes were sonicated briefly in 0.1 M HCl solution then hexanes/acetone (1:1 v:v) mixture prior to use.

Analysis of high throughput experimentation experiments was completed on a Waters Acquity Arc UHPLC-MS equipped with PDA and QDa detectors. A Waters 4.6 x 50 mm CORTECS column was used. The 5-minute analysis method used was 0 min, 10% B, 1 mL/min; 0.5 min, 10% B, 1.2 mL/min; 3.5 min, 100% B, 1.2 mL/min; 4.5 min, 100% B, 1.2 mL/min; 4.6 min, 10% B, 1.2 mL/min, where A = 0.1% formic acid in water and B = 0.1% formic acid in acetonitrile. The data was processed using a Mass Lynx program with TargetLynx software or PEAKSEL integration software. For more information visit <https://elsci.io/peaksel/index.html>

Electrodes were prepared according to literature procedure (*ACS Catal.* **2022**, *12* (2), 1161-1166). Materials used: 2-dram vial, green open-top cap with Polypropylene SURE-Link TFE Septa, copper wire (18 ga), Co wire (5 x 3 cm), Stainless steel (SS) Sheet, PTFE tubing (3/16" ID, 1/4" OD, 1/32" WT), plyers, hole punch, and aviation snips. Reactions were conducted as two-electrode cells with a Landt Battery Testing System (model number: CT3002A).

Proton nuclear magnetic resonance spectra (^1H NMR), carbon nuclear magnetic resonance spectra (^{13}C NMR), and fluorine nuclear magnetic resonance spectra (^{19}F NMR) were recorded on a 400, 500, or 600 NMR spectrometer. Chemical shifts for protons are recorded in parts per million and referenced to residual CHCl_3 ($\text{CHCl}_3 = \delta 7.26$) in deuterated chloroform. Chemical shifts for carbon are recorded in parts per million and referenced to carbon resonances of deuterated chloroform ($\text{CDCl}_3 = \delta 77.2$). Data are reported as follows: chemical shift, multiplicity (s = singlet, d = doublet, t = triplet, q = quartet, m = multiplet, etc.), coupling constants (Hz), integration. Infrared (IR) spectra were obtained using FTIR spectrophotometers with material loaded onto a NaCl plate. The mass spectral data were obtained at the University of Delaware using a Q-Exactive Orbitrap Mass Spectrometer (Thermo Scientific). Melting points were taken on a Thomas-Hoover Uni-Melt Capillary Melting Point Apparatus.

2.4.2 General Procedures

2.4.2.1 General Procedure A: High-Throughput Electrochemical (HTE-Chem) Investigation

In a nitrogen-filled glovebox, to 1-mL vials (secured in a 24-well aluminum block) equipped with PTFE-covered 5 x 2 mm magnetic stir bars was added pyridinium salt 1 (100 μL , 0.2 M solution in DMA, 10 μmol , 1.0 equiv), aryl chloride (50 μL , 0.6 M solution in DMA, 32 μmol , 3.2 equiv), NaI (50 μL , 0.2 M solution in DMA, 10 μmol , 1.0 equiv), $\text{NiBr}_2(\text{DME})$ (40 μL , 0.02 M solution in DMA, 1 μmol , 10 mol%), ligand (100 μL , 0.02 M solution in DMA, 1.2 μmol , 12 mol%), and mediator, if applicable, (20 μL , 0.03 M solution in DMA, 0.5 μmol , 5 mol%). The electrodes were inserted, and the HTE-Chem reaction block was assembled inside the

glovebox. The reactor was then connected to the external power supply inside the glovebox and heated to 60 °C with 1200 RPM stirring on an IKA stir plate. Upon reaching the desired temperature, the reactions were electrolyzed under constant current mode (1mA, $V_{\max} = 30$ V) for 64.3 min. After electrolysis, the HTe-Chem reactor was allowed to cool to room temperature, taken outside of the glovebox, and disassembled. Samples for analysis were prepared by diluting the reactions with 4,4'-di-tert-butylbiphenyl internal standard (200 μ L, 0.005 M solution in LC-MS MeCN, 1 μ mol, 10 mol%), transferring a 20 μ L aliquot of the crude reaction mixture and internal standard into a polypropylene analysis plate and diluting with 580 μ L MeCN for LC-MS analysis.

2.4.2.2 General Procedure B: Optimization Studies Using Electrochemical Reduction

In a nitrogen-filled glovebox: To an oven-dried 2-dram vial fitted with a magnetic stir bar was added NiBr₂·DME (10 mol %), ligand (12 mol %), mediator, if applicable, (5-10 mol %), sodium electrolyte, pyridinium salt **1** (1.0 equiv), aryl chloride, if solid, (3.2 equiv), DMA (3 mL), aryl chloride, if liquid, (3.2 equiv). The undivided reaction cell was removed from the glovebox and transferred to a preheated stir plate. After stirring for approx. 5 minutes to let warm and ensuring all solids have dissolved, the resulting mixture was stirred vigorously at 60 °C with enough electrolysis to deliver 4 F/mol (0.1 mmol reactions: 1 mA for 10.72 mAh. 0.3 mmol reactions: 2 mA for 32.16 mAh). The mixture was then diluted with EtOAc (2 mL), transferred to a 20 mL scintillation vial, and washed with a 1:1 mixture of water and sat. NaCl (2 x 5 mL), then washed with water (5 mL). The solution was then dried

with (MgSO₄), and concentrated. 1,3,5-Trimethoxybenzene (internal standard) and CDCl₃ were added, and the yield was determined by ¹H NMR analysis.

2.4.2.3 General Procedure C: Investigations Using Mn⁰

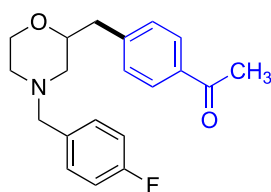
In a nitrogen-filled glovebox, to an oven-dried 1-dram vial fitted with a magnetic stir bar was added NiBr₂·DME (3.1 mg, 0.010 mmol, 10 mol %), 4,4'-dimethylamino-bipyridine (2.7 mg, 0.012 mmol, 12 mol %), NaI (151 mg, 1.0 mmol, 10 equiv), pyridinium salt **1** (60 mg, 0.10 mmol, 1.0 equiv), DMA (3 mL, 0.03 M), 4-chloroacetophenone (42 μL, 0.32 mmol, 3.2 equiv), then Mn⁰ (11 mg, 0.20 mmol, 2.0 equiv). The vial was then capped with a Teflon-coated cap and removed from the glovebox. The resulting mixture was stirred vigorously at 60 °C for 22 h. The mixture was then diluted with EtOAc (1 mL), filtered through a short plug of silica gel, and the filter cake was washed with EtOAc (5 mL). The filtrate was then washed with a 1:1 mixture of water and sat. NaCl (2 x 5 mL), then washed with water (5 mL). The solution was then dried with (MgSO₄), and concentrated. 1,3,5-Trimethoxybenzene (internal standard) and CDCl₃ were added, and the yield was determined by ¹H NMR analysis.

2.4.2.4 General Procedure D: Optimization and Investigation at 0.3 mmol Scale

In a nitrogen-filled glovebox: To an oven-dried 2-dram vial fitted with a magnetic stir bar was added NiBr₂·DME (9.3 mg, 0.030 mmol, 10 mol %), 4,4'-dimethylamino-bipyridine (8.1 mg, 0.036 mmol, 12 mol %), NaI (453 mg, 1.0 mmol, 10 equiv), pyridinium salt (0.30 mmol, 1.0 equiv), aryl chloride, if solid, (0.96 mmol, 3.2 equiv), DMA (3 mL, 0.1 M), aryl chloride, if liquid, (0.96 mmol, 3.2 equiv). The undivided reaction cell was removed from the glovebox. The resulting mixture was

stirred vigorously at 60 °C, at 2 mA for 32.16 mAh. The mixture was then diluted with EtOAc (2 mL), transferred to a 20 mL scintillation vial, and washed with a 1:1 mixture of water and sat. NaCl (2 x 5 mL), then washed with water (5 mL). The solution was then dried with (MgSO₄), and concentrated. 1,3,5-Trimethoxybenzene (internal standard) and CDCl₃ were added, and the yield was determined by ¹H NMR analysis.

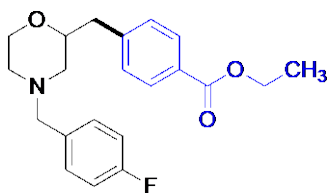
2.4.3 Characterization of Isolated Products



1-(4-((4-(4-fluorobenzyl)morpholin-2-yl)methyl)phenyl)ethan-1-one (2a).

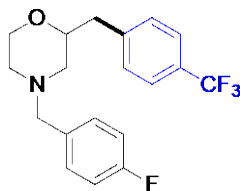
In a nitrogen-filled glovebox: To an oven-dried 20 mL scintillation vial was added NiBr₂·DME (31 mg, 0.10 mmol, 10 mol %), 4,4'-dimethylamino-bipyridine (27 mg, 0.12 mmol, 12 mol %), NaI (1.49 g, 10.0 mmol, 10 equiv), pyridinium salt 1 (600 mg, 1.0 mmol, 1.0 equiv), DMA (10 mL, 0.1 M), 4-chloroacetophenone (420 μL, 3.2 mmol, 3.2 equiv). The undivided reaction cell was removed from the glovebox. The resulting mixture was stirred vigorously at 60 °C, at 8 mA for 107.2 mAh. The mixture was then diluted with EtOAc (5 mL) and transferred to a separatory funnel and washed with a 1:1 mixture of water and sat. NaCl (2 x 10 mL), then washed with water (10 mL). The solution was then dried with MgSO₄, and concentrated. The crude mixture was columned using silica gel chromatography (0–50% ethyl acetate/hexanes) to give 2a (219 mg, 67%) as a yellow oil: ¹H NMR (400 MHz, CDCl₃) δ 7.91 – 7.84 (m, 2H), 7.33 – 7.28 (m, 2H), 7.28 – 7.21 (m, 2H, overlaps with CHCl₃), 7.03 – 6.95 (m, 2H), 3.86 – 3.80 (m, 1H), 3.80 – 3.73 (m, 1H), 3.59 (td, J = 11.3, 2.5 Hz, 1H), 3.50

– 3.36 (m, 2H), 2.86 (dd, $J = 13.9, 7.7$ Hz, 1H), 2.77 – 2.67 (m, 2H), 2.63 – 2.59 (m, 1H), 2.58 (s, 3H), 2.16 – 2.09 (m, 1H), 1.98 – 1.90 (m, 1H); $^{13}\text{C}\{^1\text{H}\}$ NMR (101 MHz, CDCl_3) δ 197.95 (C), 163.42 (C), 160.99 (C), 144.18 (C), 135.60 (C), 133.55 (C), 133.52 (C), 130.75 (C), 130.67 (CH), 129.62 (CH), 128.58 (CH), 115.34 (CH), 115.13 (CH), 76.23 (CH), 67.01 (CH_2), 62.55 (CH_2), 58.45 (CH_2), 52.87 (CH_2), 40.28 (CH_2), 26.70 (CH_3); ^{19}F NMR (376 MHz, CDCl_3) δ –115.64. The spectral data matches that of the literature.⁶

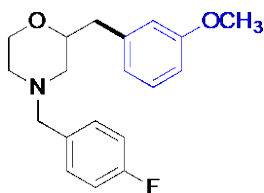


ethyl 4-((4-(4-fluorobenzyl)morpholin-2-yl)methyl)benzoate (2b). Prepared via General Procedure D using pyridinium salt **1**. The crude mixture was purified by silica gel chromatography (run 1: 0–50% ethyl acetate/hexanes, run 2: 0–50% ethyl acetate/hexanes) to give **2b** (38 mg, 50%) as a yellow oil: ^1H NMR (400 MHz, CDCl_3) δ 7.99 – 7.94 (m, 2H), 7.30 – 7.22 (m, 4H, *overlaps with CHCl_3*), 7.03 – 6.96 (m, 2H), 4.36 (q, $J = 7.1$ Hz, 2H), 3.87 – 3.80 (m, 1H), 3.80 – 3.73 (m, 1H), 3.60 (td, $J = 11.4, 2.5$ Hz, 1H), 3.47 (d, $J = 13.0$ Hz, 1H), 3.39 (d, $J = 13.0$ Hz, 1H), 2.87 (dd, $J = 13.9, 7.5$ Hz, 1H), 2.77 – 2.67 (m, 2H), 2.64 – 2.57 (m, 1H), 2.13 (td, $J = 11.3, 3.3$ Hz, 1H), 1.94 (dd, $J = 11.2, 9.8$ Hz, 1H), 1.38 (t, $J = 7.1$ Hz, 3H); $^{13}\text{C}\{^1\text{H}\}$ NMR (101 MHz, CDCl_3) δ 166.72 (C), 163.42 (C), 160.99 (C), 143.69 (C), 130.76 (CH), 130.68 (CH), 129.72 (CH), 129.39 (CH), 128.80 (C), 115.33 (CH), 115.12 (CH), 76.27 (CH), 66.97 (CH_2), 62.53 (CH_2), 60.94 (CH_2), 58.41 (CH_2), 52.83 (CH_2), 40.31 (CH_2), 14.49 (CH_3); ^{19}F NMR (376 MHz, CDCl_3) δ -75.79, -115.66; FTIR (neat): 2933, 2855, 2805,

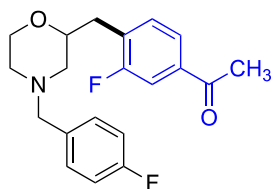
1716, 1510, 1276, 1107, 1023, 765 cm^{-1} ; HRMS (ESI+) calculated for $\text{C}_{19}\text{H}_{22}\text{FNO}_2$: 357.1740, found 357.1814.



4-(4-fluorobenzyl)-2-(4-(trifluoromethyl)benzyl)morpholine (2c). Prepared via General Procedure D using pyridinium salt **1**. The crude mixture was purified by silica gel chromatography (0–40% ethyl acetate/hexanes) to give **2c** (67 mg, 63%) as a pink oil: ^1H NMR (400 MHz, CDCl_3) δ 7.51 (d, $J = 8.0$ Hz, 2H), 7.29 (d, $J = 8.0$ Hz, 2H), 7.26 – 7.19 (m, 2H, *overlaps with CHCl₃*), 7.02 – 6.93 (m, 2H), 3.86 – 3.78 (m, 1H), 3.78 – 3.68 (m, 1H), 3.57 (td, $J = 11.3, 2.5$ Hz, 1H), 3.50 – 3.34 (m, 2H), 2.83 (dd, $J = 14.0, 7.8$ Hz, 1H), 2.70 (ddd, $J = 13.1, 6.6, 3.5$ Hz, 2H), 2.59 (dq, $J = 11.4, 2.0$ Hz, 1H), 2.12 (td, $J = 11.3, 3.3$ Hz, 1H), 1.93 (dd, $J = 11.2, 9.8$ Hz, 1H); $^{13}\text{C}\{^1\text{H}\}$ NMR (101 MHz, CDCl_3) δ 163.44 (C), 161.00 (C), 142.58 (C), 142.56 (C), 133.55 (C), 133.52 (C), 130.75 (CH), 130.67 (CH), 129.70 (CH), 125.39 (CH), 125.35 (CH), 125.31 (CH), 125.28 (CH), 115.34 (CH), 115.13 (CH), 76.20 (CH), 66.99 (CH_2), 62.54 (CH_2), 58.41 (CH_2), 52.86 (CH_2), 40.07 (CH_2); ^{19}F NMR (376 MHz, CDCl_3) δ -62.35, -115.61; FTIR (neat): 2935, 2857, 2806, 1510, 1325, 1114, 1034, 843 cm^{-1} ; HRMS (ESI+) calculated for $\text{C}_{19}\text{H}_{19}\text{F}_4\text{NO}$: 353.1402, found 354.1474.

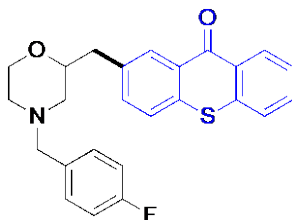


4-(4-fluorobenzyl)-2-(3-methoxybenzyl)morpholine (2e). Prepared via General Procedure D (at 70 °C) using pyridinium salt **1**. The crude mixture was purified by silica gel chromatography (0–80% ethyl acetate/hexanes) to give **2e** (38 mg, 40%) as a yellow oil: ^1H NMR (600 MHz, CDCl_3) δ 7.28 – 7.23 (m, 2H), 7.20 (dd, $J = 8.9, 7.5$ Hz, 1H), 7.01 – 6.96 (m, 2H), 6.81 – 6.77 (m, 1H), 6.77 – 6.73 (m, 2H), 3.87 – 3.82 (m, 1H), 3.79 (s, 3H), 3.78 – 3.73 (m, 1H), 3.61 (td, $J = 11.4, 2.4$ Hz, 1H), 3.49 (d, $J = 13.0$ Hz, 1H), 3.37 (d, $J = 13.0$ Hz, 1H), 2.82 (dd, $J = 13.9, 7.1$ Hz, 1H), 2.75 – 2.70 (m, 1H), 2.64 (dd, $J = 13.8, 6.1$ Hz, 1H), 2.59 (dt, $J = 11.4, 2.2$ Hz, 1H), 2.12 (td, $J = 11.3, 3.3$ Hz, 1H), 1.94 (dd, $J = 11.2, 9.8$ Hz, 1H); $^{13}\text{C}\{^1\text{H}\}$ NMR (101 MHz, CDCl_3) δ 163.40 (C), 160.97 (C), 159.71 (C), 139.85 (C), 133.63 (C), 130.76 (CH), 130.69 (CH), 129.40 (CH), 121.80 (CH), 115.30 (CH), 115.14 (CH), 115.09 (CH), 111.79 (CH), 76.60 (CH), 66.99 (CH_2), 62.58 (CH_2), 58.57 (CH_2), 55.29 (CH_3), 52.84 (CH_2), 40.45 (CH_2); ^{19}F NMR (376 MHz, CDCl_3) δ -115.79; FTIR (neat): 2936, 2854, 2804, 1509, 1220, 1113, 697 cm^{-1} ; HRMS (ESI+) calculated for $\text{C}_{19}\text{H}_{22}\text{FNO}_2$: 315.1634, found 315.1705.



1-(3-fluoro-4-((4-(4-fluorobenzyl)morpholin-2-yl)methyl)phenyl)ethan-1-one (2i). Prepared via General Procedure D using pyridinium salt **1**. The crude mixture was purified by silica gel chromatography (0–50% ethyl acetate/hexanes) to give **2i** (51 mg, 49%) as a yellow oil: ^1H NMR (400 MHz, CDCl_3) δ 7.66 (dd, $J = 7.9, 1.8$ Hz, 1H), 7.60 (dd, $J = 10.4, 1.7$ Hz, 1H), 7.34 (t, $J = 7.6$ Hz, 1H), 7.29 – 7.23 (m, 2H,

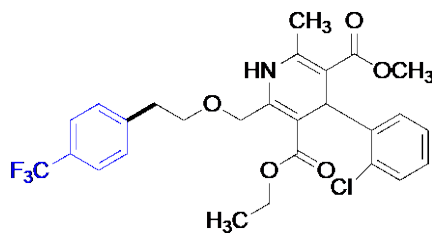
overlaps with $CHCl_3$), 7.02 – 6.96 (m, 2H), 3.85 – 3.75 (m, 2H), 3.59 (td, $J = 11.3, 2.5$ Hz, 1H), 3.48 (d, $J = 13.0$ Hz, 1H), 3.40 (d, $J = 13.0$ Hz, 1H), 2.90 – 2.77 (m, 2H), 2.73 (dt, $J = 11.1, 2.0$ Hz, 1H), 2.63 – 2.58 (m, 1H), 2.57 (s, 3H), 2.13 (td, $J = 11.3, 3.3$ Hz, 1H), 1.97 (dd, $J = 11.2, 9.8$ Hz, 1H); $^{13}C\{^1H\}$ NMR (101 MHz, $CDCl_3$) δ 196.73 (C), 163.43 (C), 162.51 (C), 161.00 (C), 160.06 (C), 137.64 (C), 137.58 (C), 133.52 (C), 132.11 (CH), 132.06 (CH), 131.20 (C), 131.04 (C), 130.75 (CH), 130.67 (CH), 124.11 (CH), 124.08 (CH), 115.34 (CH), 115.13 (CH), 115.08 (CH), 114.85 (CH), 75.16 (CH), 66.98 (CH_2), 62.54 (CH_2), 58.42 (CH_2), 52.79 (CH_2), 33.35 (CH_2), 26.72 (CH_3); ^{19}F NMR (376 MHz, $CDCl_3$) δ -115.65, -116.52; FTIR (neat): 2932, 2857, 2807, 1687, 1509, 1221, 1114, 839 cm^{-1} ; HRMS (ESI+) calculated for $C_{20}H_{21}F_2NO_2$: 345.1540, found 345.1614.



2-((4-(4-fluorobenzyl)morpholin-2-yl)methyl)-9H-thioxanthen-9-one (2o).

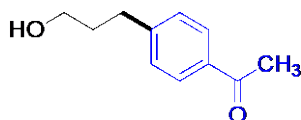
Prepared via General Procedure D using pyridinium salt **1**. The crude mixture was purified by silica gel chromatography (0–50% ethyl acetate/hexanes) to give **2o** (65 mg, 52%) as a yellow oil: 1H NMR (600 MHz, $CDCl_3$) δ 8.64 – 8.61 (m, 1H), 8.47 – 8.45 (m, 1H), 7.64 – 7.57 (m, 2H), 7.52 (d, $J = 0.9$ Hz, 2H), 7.50 – 7.46 (m, 1H), 7.28 – 7.26 (m, 1H), 7.26 – 7.24 (m, 1H), 7.01 – 6.96 (m, 2H), 3.86 – 3.80 (m, 2H), 3.61 (td, $J = 11.4, 2.5$ Hz, 1H), 3.48 (d, $J = 13.0$ Hz, 1H), 3.39 (d, $J = 13.0$ Hz, 1H), 2.94 (dd, $J = 14.1, 7.6$ Hz, 1H), 2.83 (dd, $J = 14.1, 5.4$ Hz, 1H), 2.77 – 2.72 (m, 1H), 2.60 (dq, $J = 11.4, 2.0$ Hz, 1H), 2.13 (td, $J = 11.3, 3.3$ Hz, 1H), 1.98 (dd, $J = 11.3, 9.8$ Hz,

1H); $^{13}\text{C}\{^1\text{H}\}$ NMR (101 MHz, CDCl_3) δ 180.05 (C), 163.46 (C), 161.03 (C), 137.44 (C), 136.81 (C), 135.31 (C), 133.89 (CH), 132.29 (CH), 130.87 (CH), 130.79 (CH), 130.14 (CH), 129.98 (CH), 129.35 (C), 129.18 (C), 126.31 (CH), 126.12 (CH), 115.37 (CH), 115.16 (CH), 76.13 (CH), 66.78 (CH_2), 62.37 (CH_2), 58.21 (CH_2), 52.68 (CH_2), 39.86 (CH_2); ^{19}F NMR (376 MHz, CDCl_3) δ -115.74; FTIR (neat): 2927, 2855, 2806, 1601, 1439, 1121, 1115, 743 cm^{-1} ; HRMS (ESI+) calculated for $\text{C}_{25}\text{H}_{22}\text{FNO}_2\text{S}$: 419.1355, found 419.1429.



3-Ethyl 5-methyl 4-(2-chlorophenyl)-6-methyl-2-((4-(trifluoromethyl)phenoxy)methyl)-1,4-dihydro-pyridine-3,5-dicarboxylate (4a). Prepared via General Procedure D using pyridinium salt **3**. The crude mixture was purified by silica gel chromatography (0–40% ethyl acetate/hexanes) to give **4a** (85.3 mg, 53%) as a yellow oil: ^1H NMR (400 MHz, CDCl_3) δ 7.60 (d, $J = 8.0$ Hz, 2H), 7.38 (d, $J = 8.0$ Hz, 2H), 7.31 (dd, $J = 7.8, 1.7$ Hz, 1H), 7.22 (dd, $J = 7.9, 1.4$ Hz, 1H), 7.15 – 7.08 (m, 1H), 7.08 – 7.01 (m, 1H), 6.68 (s, 1H), 5.37 (s, 1H), 4.79 – 4.64 (m, 2H), 4.10 – 3.97 (m, 2H), 3.88 – 3.75 (m, 2H), 3.60 (s, 3H), 3.02 (t, $J = 6.3$ Hz, 2H), 2.09 (s, 3H), 1.17 (t, $J = 7.1$ Hz, 3H); $^{13}\text{C}\{^1\text{H}\}$ NMR (101 MHz, CDCl_3) δ 168.05 (C), 167.27 (C), 145.74 (C), 145.23 (C), 143.71 (C), 143.08 (C), 132.55 (C), 131.61 (CH), 129.43 (CH), 129.40 (CH), 127.52 (CH), 126.94 (CH), 125.77 (CH), 125.73 (CH), 125.69 (CH), 125.65, 104.10 (C), 101.61 (C), 71.57 (CH_2), 67.83 (CH_2), 59.95

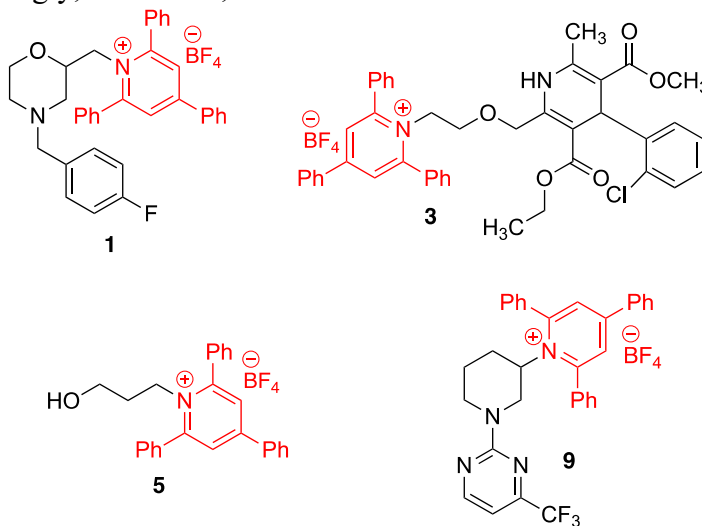
(CH₂), 50.93 (CH₃), 37.41 (CH₃), 36.09 (CH₂), 19.36 (CH₃), 14.40 (CH); ¹⁹F NMR (376 MHz, CDCl₃) δ -62.47. The spectral data matches that of the literature.⁶



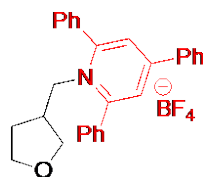
1-(4-(3-hydroxypropyl)phenyl)ethan-1-one (6a). Prepared via General Procedure D using pyridinium salt **5**. The crude mixture was purified by silica gel chromatography (0–60% ethyl acetate/hexanes) to give **6a** (21 mg, 39%) as a brown oil: ¹H NMR (400 MHz, CDCl₃) δ 7.88 (d, *J* = 8.3 Hz, 2H), 7.29 (d, 2H), 3.68 (t, *J* = 6.3 Hz, 2H), 2.77 (dd, *J* = 8.7, 6.8 Hz, 2H), 2.58 (s, 3H), 1.97 – 1.84 (m, 2H), 1.52 (s, 1H); ¹³C {¹H} NMR (101 MHz, CDCl₃) δ 198.02 (C), 147.90 (C), 135.26 (C), 128.78 (CH), 128.72 (CH), 62.10 (CH₂), 33.93 (CH₂), 32.22 (CH₂), 26.68 (CH₃). The spectral data matches that of the literature.³¹

2.4.4 Preparation of Alkylpyridinium Salt Substrates

Alkylpyridinium salts **1** and **5** have been reported in the literature and were prepared accordingly,³ as were **3**,⁶ and **9**.³²



2.4.4.1 Synthesis of Alkylpyridinium Salt 7



3-((methyl)tetrahydrofuran)-2,4,6-triphenylpyridin-1-ium tetrafluoroborate (7).

3-(Aminomethyl)-tetrahydrofuran hydrochloride (1.5 g, 11 mmol, 1.0 equiv) was added to a suspension of 2,4,6-triphenylpyrylium tetrafluoroborate (4.5 g, 11 mmol, 1.04 equiv), powdered activated 4Å molecular sieves (~500 mg/mmol), and CH₂Cl₂ (0.5 M) in a round-bottomed flask equipped with a stirbar. The flask was fitted with a septum and a vent needle. The mixture was stirred as Et₃N (3.15 mL, 22 mmol, 2.1 equiv) was added by syringe. The vent needle was removed, and the mixture was stirred at room temperature for 30 min. The vent needle was reinserted before the addition of acetic acid (1.3 mL, 22 mmol, 2.1 equiv). The needle was again removed, and the mixture was stirred at room temperature overnight. The mixture was then filtered through a short pad of Celite using CH₂Cl₂ to rinse the flask and Celite pad. The filtrate was then washed successively with aq. HCl (1.0 M, 2 x 30 mL), aq. NaHCO₃ (sat. 2 x 30 mL), then sat. NaCl (2 x 30 mL), dried (MgSO₄), filtered, and concentrated. Et₂O (200 mL) was added, and the mixture was stirred vigorously overnight to induce trituration. The resulting solid pyridinium salt was filtered and washed with Et₂O (3 x 25 mL) to give **7** (4.2 g, 81%) as an off-white powder (mp 195–199 °C): ¹H NMR (600 MHz, CDCl₃) δ 7.94 (d, J = 6.6 Hz, 6H), 7.81 (d, J = 7.4 Hz, 2H), 7.69 – 7.62 (m, 6H), 7.62 – 7.53 (m, 3H), 4.86 (dd, J = 14.7, 6.9 Hz, 1H), 4.77 (dd, J = 14.7, 7.2 Hz, 1H), 3.50 – 3.42 (m, 1H), 3.35 – 3.26 (m, 2H), 2.84 (dd, J = 9.0, 5.7 Hz, 1H), 2.19 – 2.12 (m, 1H), 1.65 – 1.54 (m, 2H), 1.10 – 1.02 (m, 1H);

$^{13}\text{C}\{^1\text{H}\}$ NMR (101 MHz, CDCl_3) δ 157.29 (C), 156.26 (C), 133.92 (C), 133.14 (C), 132.50 (CH), 131.49 (CH), 129.94 (CH), 129.74 (CH), 129.72 (CH), 128.28, 126.94 (CH), 70.32 (CH_2), 67.15 (CH_2), 56.83 (CH_2), 39.53 (CH), 29.99 (CH_2); ^{19}F NMR (565 MHz, CDCl_3) δ -153.16 (minor, $^{11}\text{BF}_4$), -153.18 (major, $^{10}\text{BF}_4$.); FTIR (neat): 3061, 2926, 2870, 1621, 1056, 704 cm^{-1} ; HRMS (ESI+) $[\text{M}-\text{BF}_4]^+$ calculated for $\text{C}_{28}\text{H}_{26}\text{NO}$: 392.2014, found 392.2006.

REFERENCES

1. He, F. S. Y., S.; Wu, J. Recent Advances in Pyridinium Salts as Radical Reservoirs in Organic Synthesis. *ACS Catal.* **2019**, (9), 8943-8960.
2. Li, Y.-N.; Xiao, F.; Guo, Y.; Zeng, Y.-F. Recent Developments in Deaminative Functionalization of Alkyl Amines. *Eur. J. Org. Chem.* **2021**, 2021 (8), 1215-1228.
3. Basch, C. H.; Liao, J.; Xu, J.; Piane, J. J.; Watson, M. P. Harnessing Alkyl Amines as Electrophiles for Nickel-Catalyzed Cross Couplings via C-N Bond Activation. *J. Am. Chem. Soc.* **2017**, 139 (15), 5313-5316.
4. Guan, W.; Liao, J.; Watson, M. P. Vinylation of Benzylic Amines via C-N Bond Functionalization of Benzylic Pyridinium Salts. *Synthesis (Stuttg)* **2018**, 50 (16), 3231-3237.
5. Liao, J.; Guan, W.; Boscoe, B. P.; Tucker, J. W.; Tomlin, J. W.; Garnsey, M. R.; Watson, M. P. Transforming Benzylic Amines into Diarylmethanes: Cross-Couplings of Benzylic Pyridinium Salts via C-N Bond Activation. *Org. Lett.* **2018**, 20 (10), 3030-3033.
6. Liao, J.; Basch, C. H.; Hoerrner, M. E.; Talley, M. R.; Boscoe, B. P.; Tucker, J. W.; Garnsey, M. R.; Watson, M. P. Deaminative Reductive Cross-Electrophile Couplings of Alkylpyridinium Salts and Aryl Bromides. *Org. Lett.* **2019**, 21 (8), 2941-2946.
7. Martin-Montero, R.; Yatham, V. R.; Yin, H.; Davies, J.; Martin, R. Ni-catalyzed Reductive Deaminative Arylation at sp³ Carbon Centers. *Org. Lett.* **2019**, 21 (8), 2947-2951.
8. Ni, S.; Li, C.-X.; Mao, Y.; Han, J.; Wang, Y.; Yan, H.; Pan, Y. Ni-catalyzed deaminative cross-electrophile coupling of Katritzky salts with halides via C-N bond activation. *Science Advances* **2019**, 5 (6), eaaw9516.
9. Garcia, B.; Sampson, J.; Watson, M. P.; Kalyani, D. Primary vs. secondary alkylpyridinium salts: a comparison under electrochemical and chemical reduction conditions. *Faraday Discuss.* **2023**, 247 (0), 324-332, 10.1039/D3FD00120B.

10. Twitty, J. C.; Hong, Y.; Garcia, B.; Tsang, S.; Liao, J.; Schultz, D. M.; Hanisak, J.; Zultanski, S. L.; Dion, A.; Kalyani, D.; et al. Diversifying Amino Acids and Peptides via Deaminative Reductive Cross-Couplings Leveraging High-Throughput Experimentation. *J. Am. Chem. Soc.* **2023**, *145* (10), 5684-5695.
11. Yousif, A. M.; Colarusso, S.; Bianchi, E. Katritzky Salts for the Synthesis of Unnatural Amino Acids and Late-Stage Functionalization of Peptides. *Eur. J. Org. Chem.* **2023**, *26* (12), e202201274.
12. Charboneau, D. J.; Huang, H.; Barth, E. L.; Germe, C. C.; Hazari, N.; Mercado, B. Q.; Uehling, M. R.; Zultanski, S. L. Tunable and Practical Homogeneous Organic Reductants for Cross-Electrophile Coupling. *J. Am. Chem. Soc.* **2021**, *143* (49), 21024-21036.
13. Yue, H.; Zhu, C.; Shen, L.; Geng, Q.; Hock, K. J.; Yuan, T.; Cavallo, L.; Rueping, M. Nickel-catalyzed C–N bond activation: activated primary amines as alkylating reagents in reductive cross-coupling. *Chem. Sci.* **2019**, *10* (16), 4430-4435, 10.1039/C9SC00783K.
14. Bajo, S.; Laidlaw, G.; Kennedy, A. R.; Sproules, S.; Nelson, D. J. Oxidative Addition of Aryl Electrophiles to a Prototypical Nickel(0) Complex: Mechanism and Structure/Reactivity Relationships. *Organomet.* **2017**, *36* (8), 1662-1672.
15. Liangbin, H. A., L. K. G.; Kang, K.; Parsons, A. M.; Weix, D. J. LiCl-Accelerated Multimetallic Cross-Coupling of Aryl Chlorides with Aryl Triflates. *J. Am. Chem. Soc.* **2019**, *141*, 10978-10983.
16. Kim, S.; Goldfogel, M. J.; Gilbert, M. M.; Weix, D. J. Nickel-Catalyzed Cross-Electrophile Coupling of Aryl Chlorides with Primary Alkyl Chlorides. *Journal of the American Chemical Society* **2020**, *142* (22), 9902-9907. DOI: 10.1021/jacs.0c02673.
17. Sakai, H. A.; Liu, W.; Le, C. C.; MacMillan, D. W. C. Cross-Electrophile Coupling of Unactivated Alkyl Chlorides. *J. Am. Chem. Soc.* **2020**, *142* (27), 11691-11697.
18. Mirabi, B. M., A. D.; Lautens, M. Nickel-Catalyzed Reductive Cross-Coupling of Heteroaryl Chlorides and Aryl Chlorides. *ACS Catal.* **2021**, (11), 12785-12793.

19. Akana, M. E.; Tcyrulnikov, S.; Akana-Schneider, B. D.; Reyes, G. P.; Monfette, S.; Sigman, M. S.; Hansen, E. C.; Weix, D. J. Computational Methods Enable the Prediction of Improved Catalysts for Nickel-Catalyzed Cross-Electrophile Coupling. *J. Am. Chem. Soc.* **2024**, *146* (5), 3043-3051. DOI: 10.1021/jacs.3c09554.
20. Su, Z.-M.; Deng, R.; Stahl, S. S. Zinc and manganese redox potentials in organic solvents and their influence on nickel-catalysed cross-electrophile coupling. *Nat. Chem.* **2024**.
21. Liu, Y.; Tao, X.; Mao, Y.; Yuan, X.; Qiu, J.; Kong, L.; Ni, S.; Guo, K.; Wang, Y.; Pan, Y. Electrochemical C–N bond activation for deaminative reductive coupling of Katritzky salts. *Nat. Comm.* **2021**, *12* (1), 6745.
22. Yi, L.; Ji, T.; Chen, K.-Q.; Chen, X.-Y.; Rueping, M. Nickel-Catalyzed Reductive Cross-Couplings: New Opportunities for Carbon–Carbon Bond Formations through Photochemistry and Electrochemistry. *CCS Chemistry* **2022**, *4* (1), 9-30.
23. Fu, J.; Lundy, W.; Chowdhury, R.; Twitty, J. C.; Dinh, L. P.; Sampson, J.; Lam, Y.-h.; Sevov, C. S.; Watson, M. P.; Kalyani, D. Nickel-Catalyzed Electroreductive Coupling of Alkylpyridinium Salts and Aryl Halides. *ACS Catal.* **2023**, 9336-9345.
24. Wesenberg, L. J.; Sivo, A.; Vilé, G.; Noël, T. Ni-Catalyzed Electro-Reductive Cross-Electrophile Couplings of Alkyl Amine-Derived Radical Precursors with Aryl Iodides. *J. Org. Chem.* **2024**, *89* (22), 16121-16125.
25. Palkowitz, M. D.; Laudadio, G.; Kolb, S.; Choi, J.; Oderinde, M. S.; Ewing, T. E.-H.; Bolduc, P. N.; Chen, T.; Zhang, H.; Cheng, P. T. W.; et al. Overcoming Limitations in Decarboxylative Arylation via Ag–Ni Electrocatalysis. *J. Am. Chem. Soc.* **2022**, *144* (38), 17709-17720.
26. Rein, J.; Annand, J. R.; Wismer, M. K.; Fu, J.; Siu, J. C.; Klapars, A.; Strotman, N. A.; Kalyani, D.; Lehnerr, D.; Lin, S. Unlocking the Potential of High-Throughput Experimentation for Electrochemistry with a Standardized Microscale Reactor. *ACS Central Science* **2021**, *7* (8), 1347-1355.
27. Zackasee, J. L. S.; Al Zubaydi, S.; Truesdell, B. L.; Sevov, C. S. Synergistic Catalyst–Mediator Pairings for Electroreductive Cross-Electrophile Coupling Reactions. *ACS Catal.* **2022**, *12* (2), 1161-1166.

28. Kim, R. S.; Kgoadi, L. O.; Hayes, J. C.; Rainboth, D. P.; Mudd, C. M.; Yap, G. P. A.; Watson, D. A. Nickel-Catalyzed Atroposelective Cross-Electrophile Coupling of Aryl Halides: A General and Practical Route to Diverse MOP-Type Ligands. *J. Am. Chem. Soc.* **2024**, *146* (26), 17606-17612.
29. Yi, J.; Badir, S. O.; Kammer, L. M.; Ribagorda, M.; Molander, G. A. Deaminative Reductive Arylation Enabled by Nickel/Photoredox Dual Catalysis. *Organic Letters* **2019**, *21* (9), 3346-3351.
30. Sandfort, F.; Strieth-Kalthoff, F.; Klauck, F. J. R.; James, M. J.; Glorius, F. Deaminative Borylation of Aliphatic Amines Enabled by Visible Light Excitation of an Electron Donor–Acceptor Complex. *Chemistry – A European Journal* **2018**, *24* (65), 17210-17214.
31. Mori, Y.; Hayashi, M.; Sato, R.; Tai, K.; Nagase, T. Development of Photoredox Cross-Electrophile Coupling of Strained Heterocycles with Aryl Bromides Using High-Throughput Experimentation for Library Construction. *Organic Letters* **2023**, *25* (30), 5569-5573.
32. Plunkett, S.; Basch, C. H.; Santana, S. O.; Watson, M. P. Harnessing Alkylpyridinium Salts as Electrophiles in Deaminative Alkyl-Alkyl Cross-Couplings. *J. Am. Chem. Soc.* **2019**, *141* (6), 2257-2262.

Chapter 3

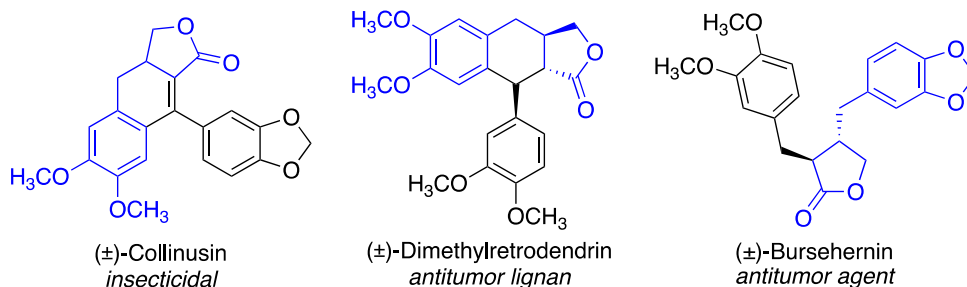
NICKEL-CATALYZED CASCADE CYCLIZATION OF ALKENE-TETHERED ALKYL PYRIDINIUM SALTS AND ARYL HALIDES

3.1 Introduction

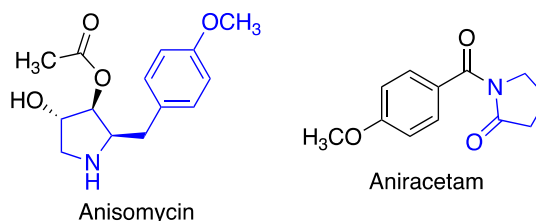
Heterocycles, specifically saturated 5-membered rings, represent an important motif in many bioactive molecules. For example, lignan natural products are a class of compounds that possess the saturated cyclic motif. They have been used in traditional and conventional medicine for antioxidant, antitumor, anti-inflammatory, and antiviral bioactive properties (Scheme 3.1A).¹⁻³ In addition to the synthesis of lignans and their derivatives, efficient methods to synthesize a variety of highly substituted saturated heterocycles are desired to obtain bioactive molecules such as pyrrolidines, that are prevalent in pharmaceuticals (Scheme 3.1B).²⁵ A particularly efficient approach to these scaffolds is an intramolecular dicarbofunctionalization of alkenes.⁴⁻⁸

Scheme 3.1 Heterocyclic Natural Products

A. Lignan Natural Products



B. Pyrrolidine-Based Pharmaceuticals

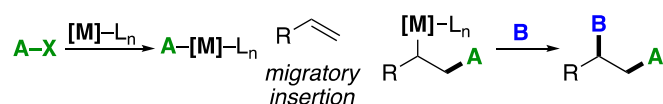


Dicarbofunctionalization of alkenes is a special synthetic tool that can construct complex carbon skeletons by forming two C–C bonds in a one-pot reaction.⁹ Generally, nickel-catalyzed dicarbofunctionalization of alkenes takes place either through a carbometallation/cross-coupling or a radical addition/cross-coupling process (Scheme 3.2A).^{7, 10} Dicarbofunctionalization protocols that employ nickel-catalyzed reductive conditions follow the proposed radical addition/cross-coupling process as alkyl electrophiles are prone generating radicals via single electron transfer (SET).¹¹⁻¹⁷ Although dicarbofunctionalization of alkenes can occur intramolecularly or intermolecularly (Scheme 3.2B), the intramolecular approach is of interest as it can form cyclic structures (Scheme 3.2C).¹⁸

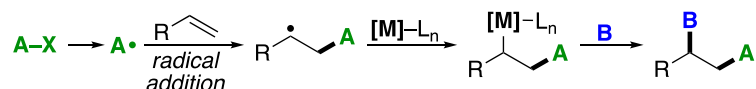
Scheme 3.2 Dicarbofunctionalization of Alkenes

A. Possible Reaction Pathways

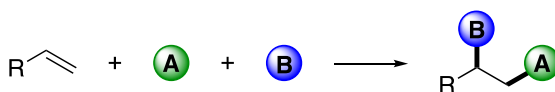
Carbometalation/Cross-Coupling Process



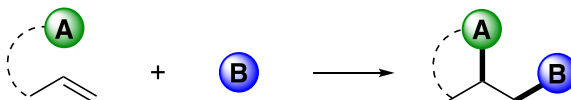
Radical Addition/Cross-Coupling Process



B. Intermolecular Process



C. Intramolecular Process

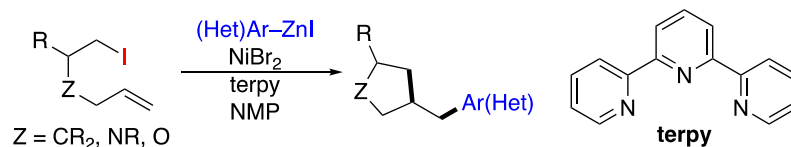


The literature includes several inspirational examples of dicarbofunctionalization to form heterocycles. Giri and coworkers demonstrated a nickel-catalyzed Negishi cross-coupling that employs unactivated alkenes tethered to alkyl halides (Scheme 3.3A).⁴ Through this methodology, with minimal sequential synthetic steps, several natural lignan products were formed (Scheme 3.1). The Diao group reported reductive conditions for the dicarbofunctionalization of unactivated alkenes also tethered to alkyl halides (Scheme 3.3B).⁵ Although the mild conditions tolerated various aryl coupling partners, many of the cyclized products formed were all-carbon, five-membered rings containing a geminal diester moiety that was hypothesized to aid cyclization.¹⁹ More recently, Adiyala was able to incorporate Katritzky pyridinium salts in a light-induced alkylation/cyclization of *N*-methacryloyl-

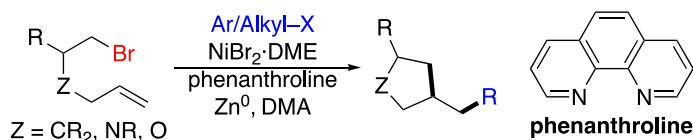
2-phenylbenzimidazoles (Scheme 3.3C).²⁰ Primary and secondary alkylpyridinium salts were used in the cross-coupling reaction. Notably, although this is a dicarbofunctionalization using a pyridinium salt, in this case, the pyridinium is not coupled to the alkene, leading to a different reaction design from the current work.

Scheme 3.3 Prior Art Utilizing Dicarbofunctionalization of Alkenes

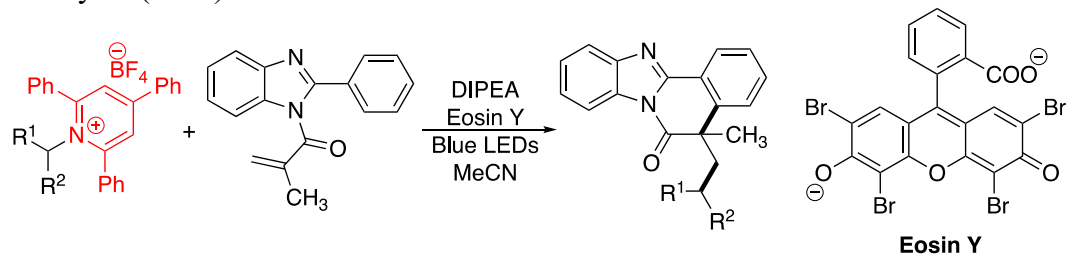
A. Giri (2018)



B. Diao (2018)



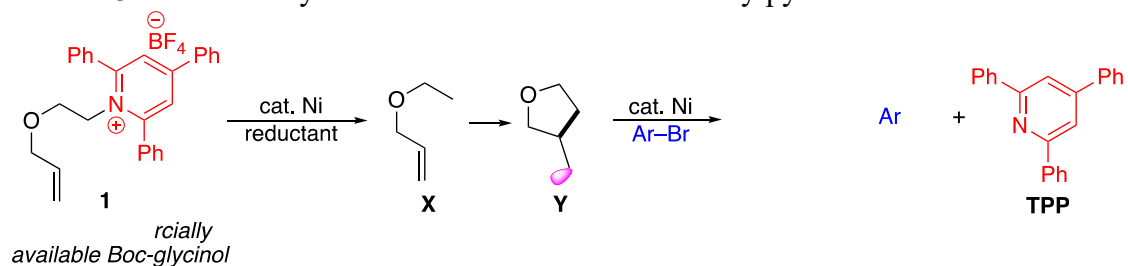
C. Adiyala (2021)



Noting that reductive conditions support dicarbofunctionalization methods and alkylpyridinium salts can partake in radical cascade reactions,²¹⁻²³ a cascade cyclization of alkene-tethered alkylpyridinium salts was developed (Scheme 3.4). This method provides an attractive route to heterocyclic targets. A key advantage of this approach is the ease of synthesis of the alkene-bearing alkylpyridinium salts. The first substrate investigated was ether pyridinium salt **1**, readily made from a 1,2-amino

alcohol (see Experimental Section). It was hypothesized that after being subjected to reductive conditions, the initial radical may intramolecularly cyclize on the pendant alkene. Subsequent radical capture by a nickel arene and reductive elimination would afford a heterocyclic product. An expected challenge was achieving fast enough intramolecular cyclization before the radical is captured by the aryl nickel species. Otherwise, arylation of radical **X** will lead to undesired uncyclized arylated product.

Scheme 3.4 Cascade Cyclization of Alkene-Tethered Alkylpyridinium Salts



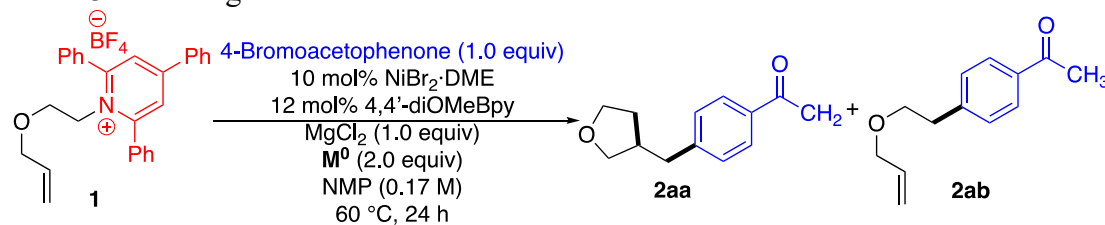
3.2 Results and Discussion

3.2.1 Initial Optimization Investigations

Initial studies performed by colleague, Jianyu Xu, demonstrated the feasibility of this cascade, albeit in low yields of the desired cyclized product **2aa**. A large competing factor in this cascade reaction is the generation of the undesired uncyclized product **2ab**, generated from coupling of acyclic radical **X** before cyclization to form radical **Y**. 2,4,6-Triphenylpyridine (**TPP**) is the byproduct generated after radical formation, and is quantified to determine success of carbon–nitrogen bond cleavage (Scheme 3.4). Reductants, ligands, and nickel sources were examined to determine their effect on the reaction.

Metallic reductants were screened first. It was observed that manganese and zinc were sufficient reductants for the cyclization transformation (Table 3.1, entries 1 and 5). At this stage, Mn^0 was selected for further studies.

Table 3.1 Investigation of Reductant^a



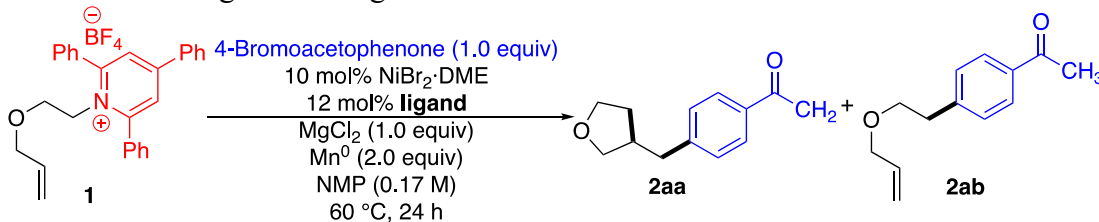
Entry	Reductant	2aa	2ab	2aa : 2ab	TPP
1	Mn^0	17	13	1:1	40
2	Fe^0	1	not detected	-	2
3	Cu^0	3	1	3:1	6
4	Mg^0	not detected	not detected	-	1
5	Zn^0	13	4	3:1	66

^aReaction conditions: **1** (0.1 mmol, 1.0 equiv), 4-bromoacetophenone (0.1 mmol, 1.0 equiv), $\text{NiBr}_2 \cdot \text{DME}$ (10 mol%), 4,4'-diOMeBpy (12 mol%), MgCl_2 (0.1 mmol, 1.0 equiv), Reductant (0.2 mmol, 2.0 equiv), NMP (0.17 M), 60 °C. Yields determined by ¹H NMR analysis using 1,3,5-trimethoxybenzene as internal standard.

The next parameter tested was ligand. A variety of electron-rich, bidentate bipyridine ligands afforded desired product **2aa** in 12-25% yield (Table 3.2, entries 1-5). Tridentate ligand terpyridine was not beneficial towards reaction efficiency, giving the desired cyclized product in only 4% yield (entry 6). Although entries 2 and 3 delivered about the same amount of reaction products, 4,4'-di^tBuBpy (entry 3) was

chosen to proceed forward with reaction optimization. It is noted that 4,4'-diMeBpy would have been a satisfactory ligand choice as well.

Table 3.2 Investigation of Ligands^a

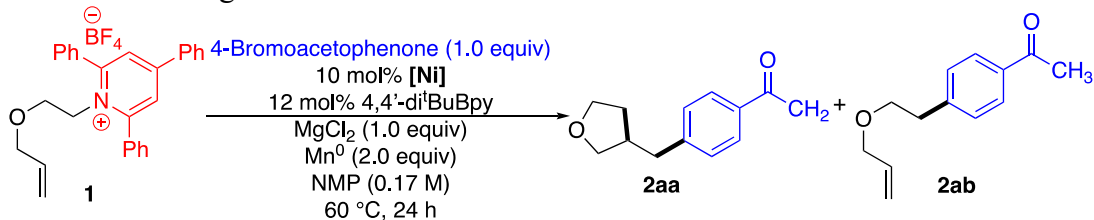


Entry	Reductant	2aa	2ab	2aa : 2ab	TPP
1	4,4'-diOMeBpy	12	n.d.	12:1	54
2	4,4'-diMeBpy	26	21	1.2:1	65
3	4,4'-di ^t BuBpy	25	24	1.2:1	66
4	bipyridine	24	n.d.	24:1	72
5	phenanthroline	25	5	25:5	47
6	terpyridine	4	n.d.	4:1	49

^aReaction conditions: **1** (0.1 mmol, 1.0 equiv), 4-bromoacetophenone (0.1 mmol, 1.0 equiv), NiBr₂·DME (10 mol%), ligand (12 mol%), MgCl₂ (0.1 mmol, 1.0 equiv), Mn⁰ (0.2 mmol, 2.0 equiv), NMP (0.17 M), 60 °C. Yields determined by ¹H NMR analysis using 1,3,5-trimethoxybenzene as internal standard.

In continuation of investigating catalyst, nickel sources were tested. Except for NiCl₂·DME, all nickel salts examined gave similar yield of product **2aa**. Because they were all similar, NiBr₂·DME was chosen arbitrarily to move forward with optimization studies.

Table 3.3 Investigation of Nickel Sources^a



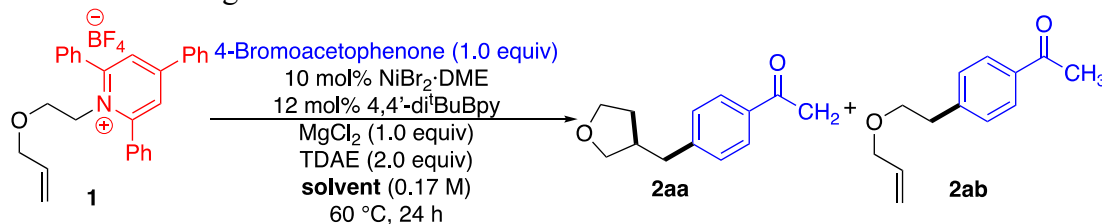
Entry	Reductant	2aa	2ab	2aa : 2ab	TPP
1	NiBr ₂ ·DME	28	n.d.	28:1	62
2	NiCl ₂ ·DME	15	n.d.	15:1	49
3	NiI ₂	24	n.d.	24:1	66
4	NiCl ₂ ·6H ₂ O	26	17	2:1	59
5	Ni(OAc) ₂ ·4H ₂ O	26	n.d.	26:1	60
6	Ni(acac) ₂	30	n.d.	30:1	77

^aReaction conditions: **1** (0.1 mmol, 1.0 equiv), 4-bromoacetophenone (0.1 mmol, 1.0 equiv), nickel salt (10 mol%), 4,4'-di^tBuBpy (12 mol%), MgCl₂ (0.1 mmol, 1.0 equiv), Mn⁰ (0.2 mmol, 2.0 equiv), NMP (0.17 M), 60 °C. Yields determined by ¹H NMR analysis using 1,3,5-trimethoxybenzene as internal standard.

At this point, it was hypothesized that a homogenous reductant could be a potential benefit towards achieving more desired product.²⁴ Thus, tetrakis-(dimethylamino)ethylene (TDAE) was tested in place of Mn⁰ as a reductant during a screen of solvents (Table 3.4). Overall, there was an increase in product yield; this data supports the hypothesis that a homogenous reaction is advantageous. With more than 50% of desired product observed with TDAE as reductant (Table 3.4, entries 1, 3, and 6), the focus turned to optimizing the formation of cyclized vs uncyclized product.

DMPU was taken forward for further investigations as the boiling solvent, N,N-Diisopropylacetamide, was not commercially available and was difficult to remove via rotary evaporation.

Table 3.4 Investigation of Solvent with TDAE as Reductant^a



Entry	Solvent	2aa	2ab	2aa : 2ab	TPP
1	NMP	56	8	7:1	73
2	DMA	41	16	3:1	71
3	DMPU	57	11	5:1	86
4	DMF	47	15	3:1	75
5	Toluene	38	21	2:1	78
6	N,N-Diisopropylacetamide	54	26	2:1	73

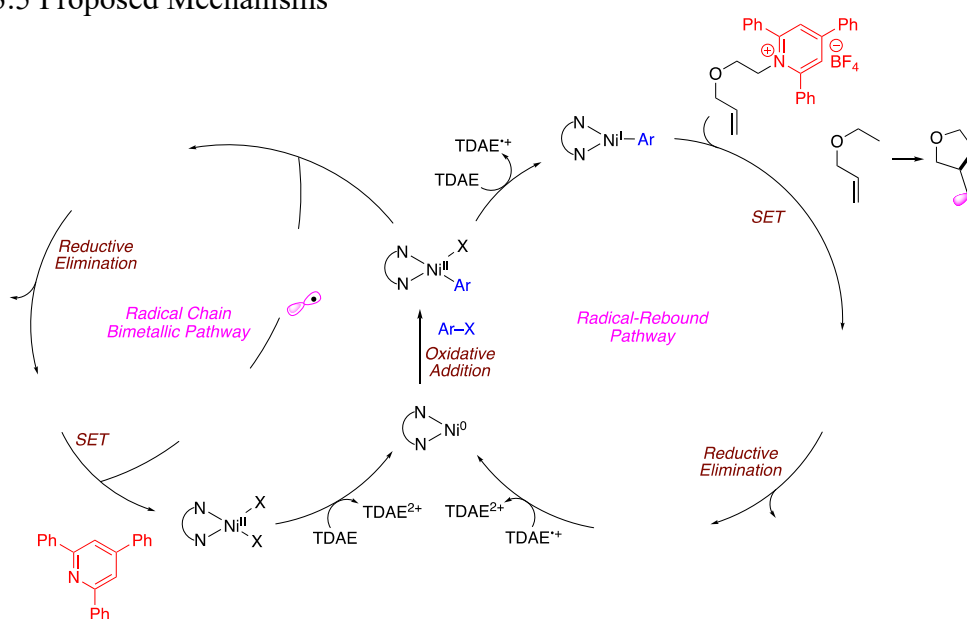
^aReaction conditions: **1** (0.1 mmol, 1.0 equiv), 4-bromoacetophenone (0.1 mmol, 1.0 equiv), NiBr₂·DME (10 mol%), 4,4'-di^tBuBpy (12 mol%), MgCl₂ (0.1 mmol, 1.0 equiv), TDAE (0.2 mmol, 2.0 equiv), solvent (0.17 M), 60 °C. Yields determined by ¹H NMR analysis using 1,3,5-trimethoxybenzene as internal standard.

3.2.2 Mechanistic Experiments

In considering how to optimize selectivity for the cyclized product over uncyclized product, it is helpful to consider the potential reaction pathways. There are two potential mechanisms for the cross-electrophile coupling of alkylpyridinium salts and aryl halides (Scheme 3.5).^{25, 26} The radical cascade reaction is proposed to proceed

via either reaction pathway, with additional consideration towards the cyclization event after radical generation. In the radical-rebound pathway, one nickel center participates in the radical initiation and recombination process. Meanwhile, in the radical chain bimetallic pathway, one nickel center generates the initial uncyclized radical and a second nickel center captures the cyclized radical. As both reaction pathways are possible, this consideration sparks an interest in uncovering whether the radical initiation and recombination occurs via a mono- (radical-rebound) or bimetallic (radical chain bimetallic) process.

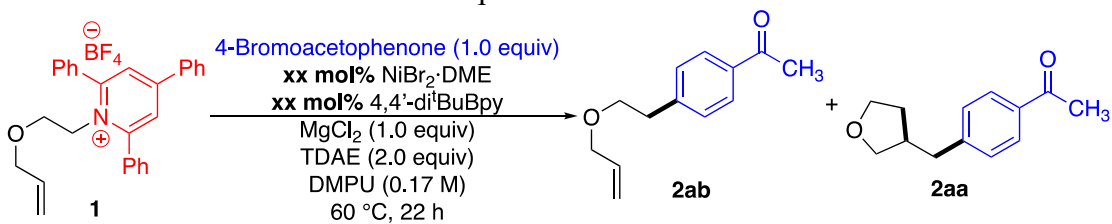
Scheme 3.5 Proposed Mechanisms



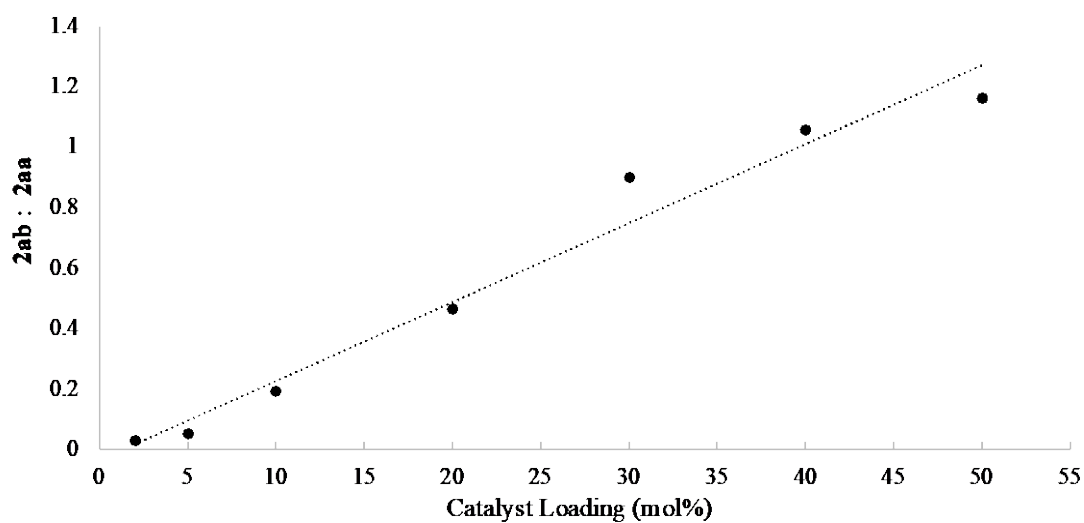
The alkene-tethered substrate is an ideal compound to use for the investigation of this phenomenon. If the radical initiation, cyclization, and recombination events were to occur via a mono-metallic process, where the radical does not escape the solvent cage of nickel, the concentration of nickel catalyst would not affect the ratio of

uncyclized to cyclized product. However, it is evident that increased nickel concentration leads to increased uncyclized product (Scheme 3.6), while low concentrations lead to low generation of uncyclized product. Because the abundance of nickel catalyst impacts the radical cyclization event, it is likely that pyridinium reduction and radical recombination proceed through the bimetallic, radical-rebound mechanism. This trend is observed in other mechanistic investigations of radical clock substrates of alkyl halides.^{6, 25}

Scheme 3.6 Nickel Concentration Experiments^a



Entry	mol% Catalyst	2ab	2aa	2ab : 2aa	TPP
1	2	1	35	1:35	69
2	5	2	40	1:20	63
3	10	8	42	1:5	71
4	20	13	28	1:2	69
5	30	18	20	0.9:1	80
6	40	19	18	1:1	71
7	50	21	18	1.2:1	78

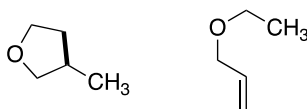


^aReaction conditions: **1** (0.1 mmol, 1.0 equiv), 4-bromoacetophenone (0.1 mmol, 1.0 equiv), NiBr₂·DME (xx mol%), 4,4'-di^tBuBpy (xx mol%), MgCl₂ (0.1 mmol, 1.0

equiv), TDAE (0.2 mmol, 2.0 equiv), DMPU (0.17 M), 60 °C. Yields determined by ¹H NMR analysis using 1,3,5-trimethoxybenzene as internal standard.

One additional consideration with pyridinium salts, however, is that they can be directly reduced by the reductant (TDAE or Mn⁰), in addition to being reduced by nickel intermediates. In addition to understanding the mechanism, it was an aim that increasing the ratio of cyclized to uncyclized product would also lead to a high yield of desired product. However, even though the ratio can be increased to ≥20:1 (entries 1 and 2), the yield of **2aa** remains around 40%. This observation suggests that the formed radical could be going through an additional reaction pathway. A hypothesized route was that the formed radicals could undergo hydrogen atom abstraction, where 3-methyltetrahydrofuran and the uncyclized derivative would form (Scheme 3.7). However, both products would be too volatile to survive work up procedures and would not be quantified via ¹H NMR analysis. Even if GC analysis were used, these species would likely come off in the solvent front under typical GC conditions.

Scheme 3.7 Possible Side Products of Cascade Cyclization

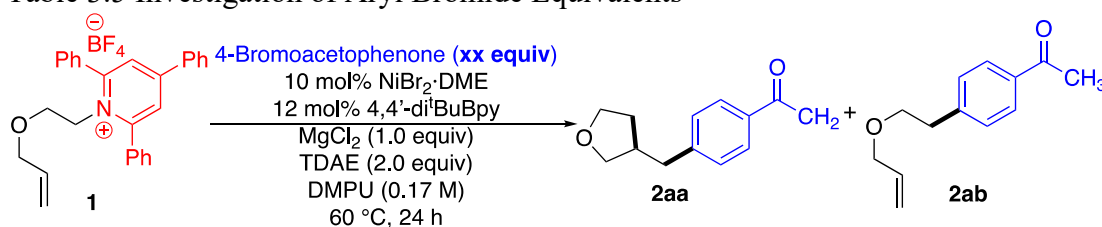


3.2.3 Additional Optimization and Effect of the Tether

The effect of using starting material in excess to further investigate possible side reactions was examined. A slight drop in yield of desired product **2aa** was

observed when increasing aryl bromide equivalents (Table 3.5). It is unclear why this occurred, but it may be due in part to a slight increase in the yield of uncyclized product **2ab**. When increasing pyridinium equivalents, an increase in yield is observed (Table 3.6, entry 5). This may suggest that pyridinium **1** is the partner undergoing a detrimental side reaction.

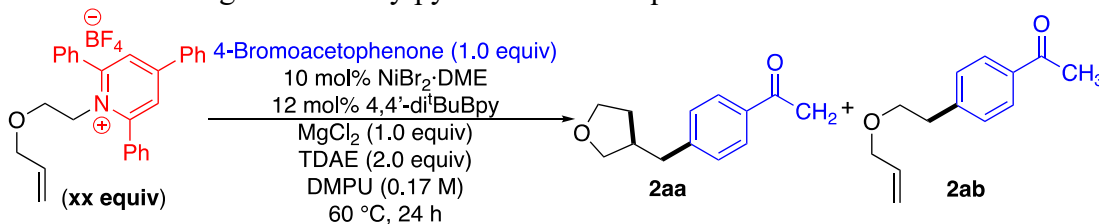
Table 3.5 Investigation of Aryl Bromide Equivalents^a



Entry	Equiv ArBr	2aa	2ab	2aa : 2ab	TPP
1	1.0	50	14	4:1	85
2	1.2	44	14	3:1	78
3	1.5	42	16	3:1	74
4	1.7	39	16	2:1	73
5	2.0	40	17	2:1	72

^aReaction conditions: **1** (0.1 mmol, 1.0 equiv), 4-bromoacetophenone (xx mmol, xx equiv), NiBr₂·DME (10 mol%), 4,4'-di^tBuBpy (12 mol%), MgCl₂ (0.1 mmol, 1.0 equiv), TDAE (0.2 mmol, 2.0 equiv), DMPU (0.17 M), 60 °C. Yields determined by ¹H NMR analysis using 1,3,5-trimethoxybenzene as internal standard.

Table 3.6 Investigation of Alkylpyridinium Salt Equivalents^a



Entry	XX equiv	2aa	2ab	2aa : 2ab	TPP
1	1.0	50	14	4:1	85
2	1.2	49	11	4:1	83
3	1.5	58	11	5:1	95
4	1.7	44	18	2:1	82
5	2.0	78	11	7:1	128

^aReaction conditions: **1** (xx mmol, xx equiv), 4-bromoacetophenone (0.1 mmol, 1.0 equiv), NiBr₂·DME (10 mol%), 4,4'-di^tBuBpy (12 mol%), MgCl₂ (0.1 mmol, 1.0 equiv), TDAE (0.2 mmol, 2.0 equiv), DMPU (0.17 M), 60 °C. Yields determined by ¹H NMR analysis using 1,3,5-trimethoxybenzene as internal standard.

Seeking to maintain a 1:1 ratio of alkylpyridinium salt and aryl bromide, an alternative alkene-tethered substrate **3** was initially investigated. Using N,N-diisopropylacetamide as solvent (entry 1), the desired cyclic product was delivered in 66% yield (Table 3.7). Additional optimization efforts (Table 3.7 entries 2-6) led to no further increase in yield. When DMA was used as the solvent, a slight increase was observed, with the desired cyclized product formed in 69% yield (entry 7). Upon scale up to 1.0 mmol, 67% yield of desired cyclized product **4aa** was achieved (Table 3.7, entry 8). Excitingly, with this substrate, undesired uncyclized product **4ab** was not

observed under any reaction conditions. It is possible that the tosyl protecting group has a steric influence, as it is much larger than an ether. This slight Thorpe-Ingold effect may aid in the cyclization event.

Table 3.7 Optimization of NTs Substrate^a

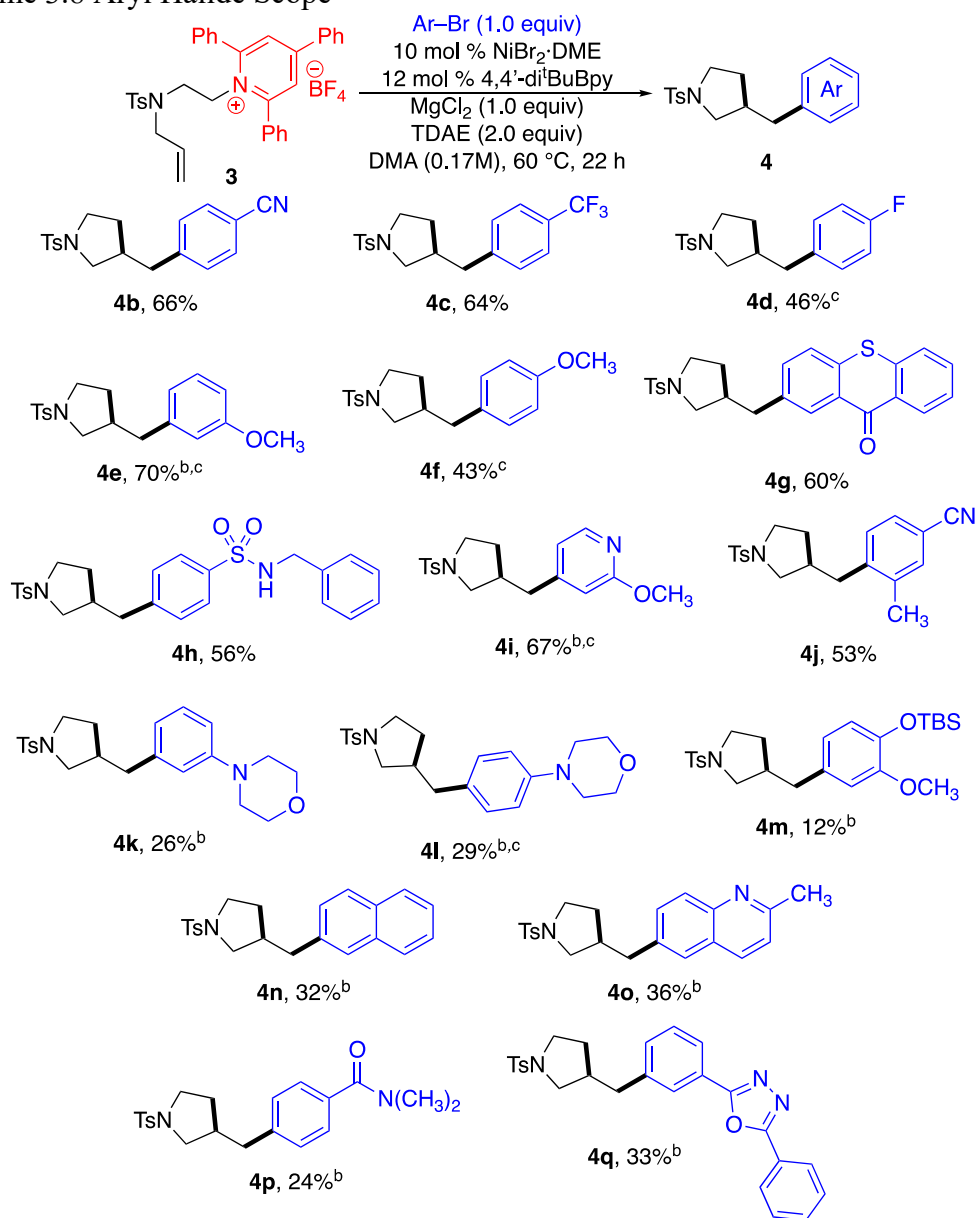
Entry	Deviation	4aa	4ab	TPP
1	None	66	Not detected	79
2	48 h	52	Not detected	78
3	70 °C	61	Not detected	75
4	50 °C	54	Not detected	67
5	1.2 equiv Pyridinium	58	Not detected	82
6	1.2 equiv ArBr	62	Not detected	76
7	DMA as solvent	69	Not detected	70
8	DMA as solvent, 1.0 mmol scale	67	Not detected	75

^aReaction conditions without deviation: **3** (0.1 mmol, 1.0 equiv), 4-bromoacetophenone (0.1 mmol, 1.0 equiv), NiBr₂·DME (10 mol%), 4,4'-di^tBuBpy (12 mol%), MgCl₂ (0.1 mmol, 1.0 equiv), TDAE (0.2 mmol, 2.0 equiv), N,N-diisopropylacetamide (0.17 M), 60 °C. Yields determined by ¹H NMR analysis using 1,3,5-trimethoxybenzene as internal standard.

3.2.4 Scope in Aryl Halide

Having demonstrated the feasibility of this transformation, colleagues Pankti Mehta and Dr. Roberto Silva Villatoro were recruited to help with demonstrating the scope of the transformation (Scheme 3.8). Additional electron-deficient aryl bromides were tolerated (**4b** and **4c**). When utilizing an aryl iodide, electron-neutral aryl (**4d**), electron-rich methoxy groups (**4e** and **4f**), and 4-pyridyl (**4i**) substrates are tolerated. Presumably the iodide is required in these cases because it undergoes oxidative addition more easily than the aryl bromide. Xanthene (**4g**) and sulfonamide (**4h**) aryl bromides react in sufficient yields, as well as *ortho*-substituted arenes (**4j**). Morpholine aryl halides are not well tolerated (**4k** and **4l**). Other limitations include alcohol derivatives (**4m**), extended π -systems (**4n** and **4o**), amides (**4p**), and five-membered heterocycles (**4q**).

Scheme 3.8 Aryl Halide Scope^a



^aReaction conditions: **3** (0.5 mmol, 1.0 equiv), aryl bromide (0.5 mmol, 1.0 equiv), NiBr₂·DME (10 mol%), 4,4'-di^tBuBpy (12 mol%), MgCl₂ (0.5 mmol, 1.0 equiv), TDAE (1.0 mmol, 2.0 equiv), DMA (0.17 M), 60 °C. Yields determined by ¹H NMR analysis using 1,3,5-trimethoxybenzene as internal standard. ^bReaction conditions: **3**

(0.1 mmol, 1.0 equiv), aryl bromide (0.1 mmol, 1.0 equiv), NiBr₂·DME (10 mol%), 4,4'-di^tBuBpy (12 mol%), MgCl₂ (0.1 mmol, 1.0 equiv), TDAE (0.2 mmol, 2.0 equiv), DMA (0.17 M), 60 °C. Yields determined by ¹H NMR analysis using 1,3,5-trimethoxybenzene as internal standard. ^cAryl iodide was used instead of aryl bromide.

3.2.5 Conclusions

In conclusion alkene-tethered alkylpyridinium salts can be utilized in reductive cascade reactions to afford heterocyclic, arylated products. Electron-poor aryl bromides are effective coupling partners, and the use of aryl iodides allows for electron-rich aryl groups to be tolerated. The dependence of the cyclized to uncyclized ratio on catalyst loading suggests that the radical formation and cyclization event occurs via a bimetallic mechanism. This unique reaction can be completed on 1.0 mmol scale, without a decrease in reaction efficiency.

3.2.6 Experimental

3.2.6.1 General Information

Unless otherwise indicated, all Ni-catalyzed reactions were set up inside a nitrogen-purged glovebox and performed under an inert atmosphere of nitrogen, using Sure-seal (Sigma-Aldrich or Thermo Fisher) anhydrous solvents. NiBr₂·DME was purchased from Strem Chemicals Inc. (catalog number 28-1145). 4,4'-di-*tert*-butyl-2,2'-bipyridine was purchased from Oakwood Chemical (catalog number 212480). All other commercial reagents were purchased from Sigma-Aldrich, Acros, Fisher, Strem, TCI, Combi-Blocks, Alfa Aesar, Ambeed, or Cambridge Isotopes Laboratories and used as received.

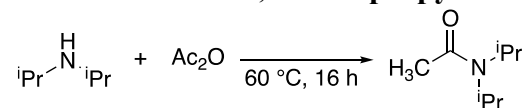
Proton nuclear magnetic resonance spectra (^1H NMR), carbon nuclear magnetic resonance spectra (^{13}C NMR), and fluorine nuclear magnetic resonance spectra (^{19}F NMR) were recorded on a 400, 500, or 600 NMR spectrometer. Chemical shifts for protons are recorded in parts per million and referenced to residual CHCl_3 ($\text{CHCl}_3 = \delta$ 7.26) in deuterated chloroform. Chemical shifts for carbon are recorded in parts per million and referenced to carbon resonances of deuterated chloroform ($\text{CDCl}_3 = \delta$ 77.2). Data are reported as follows: chemical shift, multiplicity (s = singlet, d = doublet, t = triplet, q = quartet, m = multiplet, etc.), coupling constants (Hz), integration. Infrared (IR) spectra were obtained using FTIR spectrophotometers with material loaded onto a NaCl plate. The mass spectral data were obtained at the University of Delaware using a Q-Exactive Orbitrap Mass Spectrometer (Thermo Scientific). Melting points were taken on a Thomas-Hoover Uni-Melt Capillary Melting Point Apparatus.

3.2.6.2 General Optimization Procedure

In a nitrogen-filled glovebox: To an oven-dried 1-dram vial fitted with a magnetic stir bar was added nickel salt (0.010 mmol, 10 mol%) and ligand (0.012 mmol, 12 mol %) the vial was stirred at room temperature for 5 minutes then additive (0.10 mmol, 1.0 equiv), aryl bromide, if solid, (0.10 mmol, 1.0 equiv), pyridinium salt (0.10 mmol, 1.0 equiv), solvent (0.6 mL, 0.17M), and aryl bromide, if liquid, (0.1 mmol, 1.0 equiv). The mixture was stirred at room temperature for 5 minutes then reductant (0.20 mmol, 2.0 equiv) was added. The reaction was then capped with a Teflon-coated cap, taken out of the glovebox, and stirred at the appropriate temperature for 22 to 24 h. The mixture was cooled to room temperature, diluted with 2 mL of Et_2O , and filtered through a short plug of silica gel. The filter cake was

washed with Et₂O (4 mL). The filtrate was then washed with sat. NaCl (5 mL), washed with deionized water (5 mL), dried using MgSO₄, and concentrated. 1,3,5-Trimethoxybenzene (internal standard) and CDCl₃ were added, and the yield was determined by ¹H NMR analysis.

3.2.6.3 Synthesis and Purification of N,N-Diisopropylacetamide



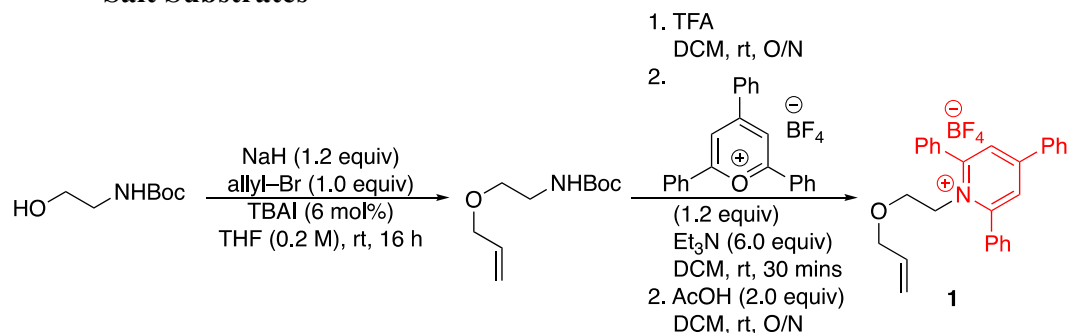
Under air, diisopropylamine (2.1 mol, 294 mL, 1.5 equiv), was added to a 3-neck round bottom flask, equipped with a dropping funnel and two vent needles. With water bath cooling, acetic anhydride (1.4 mol, 132 mL, 1.0 equiv) was added via dropping funnel. The solution went from clear and homogenous, to white with precipitation, then yellow and homogenous as the acetic anhydride was added. The solution was then stirred at 60 °C for 16 h. The yellow, homogenous solution was allowed to cool to room temperature and quenched with 200 mL water. Brine solution was added to separate the organic and aqueous layers. The aqueous layer was extracted with ether, and the organic layers were combined and stirred with saturated sodium bicarbonate to quench the AcOH formed during the reaction. The organic layer was dried with MgSO₄, filtered, and concentrated. ¹H NMR showed desired solvent and remaining diethyl ether. CaH₂ was added, and the solution was stirred under nitrogen overnight. Distillation under nitrogen (oil bath temperature: 40 °C) was done to remove excess ether that was not removed under vacuum concentration. Vapor distillation (400 millitorr, oil bath temperature: 60 °C, ca. 40 °C) gave pure product as a colorless liquid. The product was freeze-pump-thawed then stored in a nitrogen-

filled glovebox. The spectral data of the synthesized solvent is consistent with that previously reported in the literature.²⁶

3.2.6.4 General Procedure for Cross-Coupling of Alkene-Tethered Alkylpyridinium Salts and Aryl Halides

In a nitrogen-filled glovebox: To an oven-dried 2-dram vial fitted with a magnetic stir bar was added NiBr₂·DME (15.5 mg, 0.050 mmol, 10 mol%) and 4,4'-di-tert-butyl-2,2'-bipyridine (16 mg, 0.06 mmol, 12 mol %). The vial was stirred at room temperature for 5 minutes then MgCl₂ (48 mg, 0.50 mmol, 1.0 equiv), aryl bromide, if solid, (0.50 mmol, 1.0 equiv), pyridinium salt (0.50 mmol, 1.0 equiv), DMA (3 mL, 0.17M), and aryl bromide, if liquid, (0.50 mmol, 1.0 equiv). The mixture was stirred at room temperature for 5 minutes, then TDAE (240 μL, 1.0 mmol, 2.0 equiv) was added. The reaction was then capped with a Teflon-coated cap, taken out of the glovebox, and stirred at 60 °C for 22 h. The mixture was cooled to room temperature, diluted with 5 mL of Et₂O, and filtered through a short plug of silica gel. The filter cake was washed with Et₂O (10 mL). The filtrate was then washed with sat. NaCl (20 mL), washed with deionized water (20 mL), dried using MgSO₄, and concentrated. 1,3,5-Trimethoxybenzene (internal standard) and CDCl₃ were added, and the yield was determined by ¹H NMR analysis.

3.2.6.5 Synthesis and Characterization of Alkene-Tethered Alkylpyridinium Salt Substrates



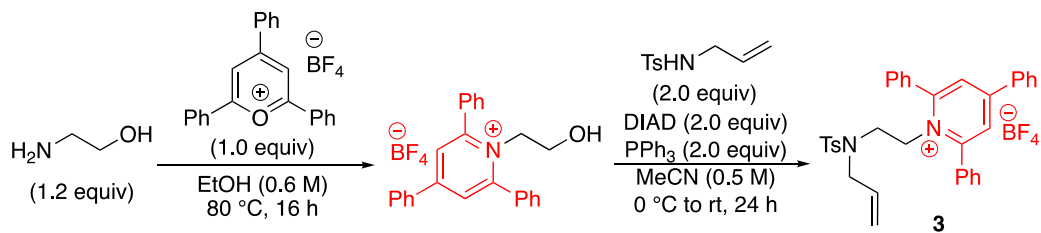
(2-(prop-2-en-1-yloxy)ethyl)-2,4,6-triphenylpyridinium tetrafluoroborate (1).

Boc-glycinol (8 g, 49 mmol, 1.0 equiv) and THF (0.2 M) were added to a round bottom flask. Sodium hydride (1.4 g, 58 mmol, 1.2 equiv) was then added, and the mixture was stirred at room temperature until the formation of bubbles subsided. Allyl bromide (4.5 mL, 52 mmol, 1.1 equiv) and TBAI (1.1 g, 3 mmol, 6 mol%) were added, and the mixture was stirred vigorously at room temperature for 16 hours. The resulting solution was washed with a 1:1 solution of H₂O and saturated NaCl. The aqueous layer was extracted with EtOAc (2 x 20 mL). The combined organic layers were dried over MgSO₄, filtered, and concentrated under reduced pressure resulting in 7.74 g of a crude product that was used without further purification.

Trifluoroacetic acid (60 mL) and CH₂Cl₂ (60 mL) were added, and the reaction mixture was stirred vigorously at room temperature overnight. The solvent was reduced under pressure. 50 mL CH₂Cl₂ was added to the mixture and evaporated under pressure. This was repeated two additional times to remove remaining acid. The crude mixture was used without further purification.

The crude product was solvated in 200 mL CH₂Cl₂ then 4Å molecular sieves (24 g, 630 mg/mmol) and 2,4,6-triphenylpyrylium tetrafluoroborate (18 g, 45 mmol, 1.2 equiv) were added to the round bottom flask equipped with a stir bar. The flask was

fitted with a septum and a vent needle. The mixture was stirred as Et₃N (20 mL, 198 mmol, 5.0 equiv) was added by syringe. The vent needle was removed, and the mixture was stirred at room temperature for 30 minutes. The vent needle was reinserted before the addition of acetic acid (6 mL, 100 mmol, 2.6 equiv). The needle was removed, and the mixture was stirred at room temperature overnight. The mixture was filtered through a short pad of Celite using CH₂Cl₂ to rinse the flask and Celite pad. The filtrate was washed successively with aq. HCl (1.0 M, 2 x 50 mL), aq. NaHCO₃ (sat., 2 x 50 mL) and aq. NaCl (sat., 2 x 50 mL). The organic layer was dried over MgSO₄, filtered, and concentrated under reduced pressure. Et₂O (200 mL) was added to precipitate the alkyipyridinium salt, which was isolated by filtration in 72% yield (16.87 g) over three steps as an off-white solid (mp 161–165 °C): ¹H NMR (600 MHz, CDCl₃) δ 7.89 (s, 2H), 7.86 – 7.81 (m, 4H), 7.81 – 7.77 (m, 2H), 7.63 – 7.52 (m, 9H), 5.62 – 5.54 (m, 1H), 5.08 (dq, J = 10.4, 1.3 Hz, 1H), 4.99 (dq, J = 17.2, 1.6 Hz, 1H), 4.86 (t, J = 5.7 Hz, 2H), 3.59 (dt, J = 5.7, 1.4 Hz, 2H), 3.25 (t, J = 5.7 Hz, 2H); ¹³C{¹H} NMR (101 MHz, CDCl₃) δ 157.7 (C), 155.8 (C), 133.9 (C), 133.6 (CH), 133.2 (C), 132.4 (CH), 131.1 (CH), 129.9 (CH), 129.8 (CH), 129.4 (CH), 128.2 (CH), 126.5 (CH), 117.9 (CH₂), 71.9 (CH₂), 66.4 (CH₂), 54.4 (CH₂); ¹⁹F NMR (376 MHz, CDCl₃) δ – 153.09 (minor, ¹¹BF₄), – 153.15 (major, ¹⁰BF₄); FTIR (neat): 3064, 2866, 1622, 1565, 1070, 767, 702 cm⁻¹; HRMS (ESI+) [M–BF₄]⁺ calculated for C₂₈H₂₆NO: 392.2014 found 392.2008.



(2-(prop-2-en-1-yl-*p*-toluenesulfonamide)ethyl)-2,4,6-triphenylpyridin-1-ium

tetrafluoroborate (3). Ethanolamine (4.32 mL, 72 mmol, 1.2 equiv), 2,4,6-triphenylpyrylium tetrafluoroborate (23.76 g, 60 mmol, 1.0 equiv), and ethanol (0.6 M) were added to the round bottom flask equipped with a stir bar. The mixture was refluxed at 80 °C for 16h. The crude reaction solution was cooled to room temperature and diluted with Et₂O (2–3x volume of EtOH used) and vigorously stirred for 1 h to induce trituration. The resulting solid pyridinium salt was filtered and washed with Et₂O (3 x 25 mL). The white solid was used without further purification and added to a round bottom flask (2.2 g, 5 mmol, 1.0 equiv) with 4-methyl-N-(2-propenyl)benzenesulfonamide (2.1 g, 10 mmol, 2.0 equiv), triphenylphosphine (2.62 g, 10 mmol, 2.0 equiv) and acetonitrile (0.5 M). The reaction mixture was cooled to 0 °C. Diisopropyl azodicarboxylate (1.97 mL, 10 mmol, 2.0 equiv) was added dropwise, and the reaction was stirred for 16 h at room temperature. The solution was concentrated under vacuum to remove the acetonitrile. Et₂O (100 mL) was added to precipitate the alkylpyridinium salt, which was isolated by filtration in 89% yield (16.87 g) over two steps as a white solid (mp 220–223 °C): ¹H NMR (600 MHz, CDCl₃) δ 8.06 – 8.01 (m, 4H), 7.95 (s, 2H), 7.84 – 7.80 (m, 2H), 7.72 – 7.67 (m, 4H), 7.67 – 7.62 (m, 2H), 7.60 – 7.53 (m, 3H), 7.40 – 7.36 (m, 2H), 7.24 (d, J = 8.2 Hz, 2H), 5.00 (t, J = 5.3 Hz, 2H), 4.83 (dd, J = 10.0, 1.2 Hz, 1H), 4.74 (d, J = 1.7 Hz, 1H), 4.54 (ddt, J = 16.9, 10.0, 6.8 Hz, 1H), 3.04 (d, J = 6.9 Hz, 2H), 3.00 (t, J = 5.4 Hz, 2H), 2.39 (s, 3H); ¹³C{¹H} NMR (101 MHz, CDCl₃) δ 157.64 (C), 156.13 (C), 144.25

(C), 135.76 (C), 134.15 (C), 133.27 (C), 132.31 (CH₂), 131.28 (CH₂), 130.11 (CH₂), 129.98 (CH₂), 129.86 (CH₂), 129.70 (CH₂), 128.24 (CH₂), 127.05 (CH₂), 126.92 (CH₂), 121.63 (C), 52.81 (CH₂), 51.52 (CH₂), 45.36 (CH₂), 21.63 (CH₃); ¹⁹F NMR (376 MHz, CDCl₃) δ – 152.91 (minor, ¹¹BF₄), – 152.96 (major, ¹⁰BF₄); FTIR (neat): 2919, 2849, 1622, 1343, 1056, 768, 548 cm⁻¹; HRMS (ESI+) [M–BF₄]⁺ calculated for C₃₅H₃₃N₂O₂S: 545.2263 found 545.2263.

REFERENCES

1. Teponno, R. B.; Kusari, S.; Spitteller, M. Recent advances in research on lignans and neolignans. *Natural Product Reports* **2016**, *33* (9), 1044-1092, 10.1039/C6NP00021E.
2. Wang, H. G., C.; Xu, H. Huang, X.; Ma, Y.; Yang, C.; Zhang, X.; Chen, J. Lignans from the Fruits of *Melia toosendan* and Their Agonistic Activities on Melatonin Receptor MT1. *Planta Med.* **2015**, *81* (10), 847-854.
3. Fang, X.; Hu, X. Advances in the Synthesis of Lignan Natural Products. *Molecules* **2018**, *23* (12), 3385.
4. KC, S. B., P.; Thapa, S.; Shrestha, B.; Giri, R. Ni-Catalyzed Regioselective Dicarbofunctionalization of Unactivated Olefins by Tandem Cyclization/Cross-Coupling and Application to the Concise Synthesis of Lignan Natural Products. *J. Org. Chem.* **2018**, *83* (5), 2920-2936.
5. Kuang, Y. W., X.; Anthony, D.; Diao, T. . Nickel-Catalyzed Reductive Dicarbofunctionalization of Alkenes via Radical Cyclization. *Chem. Commun.* **2018**, *54*, 2558-2561.
6. Lin, Q. D., T. Mechanism of Ni-Catalyzed Reductive 1,2-Dicarbofunctionalization of Alkenes. *J. Am. Chem. Soc.* **2019**, *141* (44), 17937-17948.
7. Dhungana, R. K. K., S.; Basnet, P.; Giri, R. Transition Metal-Catalyzed Dicarbofunctionalization of Unactivated Olefins. *Chem. Rec.* **2018**, *18*, 1314-1340.
8. Xiao, J. C., X.; Yang, G.; Wang, Y.; Peng, Y. Stereoselective synthesis of a *Podophyllum* lignan core by intramolecular reductive nickel-catalysis. *Chem. Commun.* **2018**, *54*, 2040-2043.
9. Wickham, L. M.; Giri, R. Transition Metal (Ni, Cu, Pd)-Catalyzed Alkene Dicarbofunctionalization Reactions. *Accounts of Chemical Research* **2021**, *54* (17), 3415-3437.

10. Luo, Y. X., C.; Zhang, X. Nickel-Catalyzed Dicarbofunctionalization of Alkenes. *Chin. J. Chem.* **2020**, (38), 1371-1394.
11. Dhungana, R. K. S., R. R.; Wickham, L. M.; Niroula, D.; Giri, R. Ni-Catalyzed Regioselective 1,2-Dialkylation of Alkenes Enabled by the Formation of Two C(sp³)-C(sp³) Bonds. *J. Am. Chem. Soc.* **2020**, *142*, 20930-20936.
12. García-Domínguez, A.; Li, Z.; Nevado, C. Nickel-Catalyzed Reductive Dicarbofunctionalization of Alkenes. *Journal of the American Chemical Society* **2017**, *139* (20), 6835-6838.
13. Hewitt, K. A.; Herbert, C. A.; Jarvo, E. R. Synthesis of Vicinal Carbocycles by Intramolecular Nickel-Catalyzed Conjunctive Cross-Electrophile Coupling Reaction. *Organic Letters* **2022**, *24* (32), 6093-6098.
14. Jin, Y.; Wang, C. Nickel-Catalyzed Asymmetric Reductive Arylalkylation of Unactivated Alkenes. *Angew. Chem. Int. Ed. Engl.* **2019**, *58* (20), 6722-6726.
15. Jin, Y.; Yang, H.; Wang, C. Nickel-Catalyzed Reductive Arylalkylation via a Migratory Insertion/Decarboxylative Cross-Coupling Cascade. *Organic Letters* **2019**, *21* (18), 7602-7608.
16. Jin, Y.; Yang, H.; Wang, C. Nickel-Catalyzed Asymmetric Reductive Arylbenzylation of Unactivated Alkenes. *Organic Letters* **2020**, *22* (7), 2724-2729.
17. Shu, W.; García-Domínguez, A.; Quirós, M. T.; Mondal, R.; Cárdenas, D. J.; Nevado, C. Ni-Catalyzed Reductive Dicarbofunctionalization of Nonactivated Alkenes: Scope and Mechanistic Insights. *Journal of the American Chemical Society* **2019**, *141* (35), 13812-13821.
18. Zhang, J. L., L.; Chen, T.; Han, L. Transition-Metal-Catalyzed Three-Component Difunctionalizations of Alkenes. *Chem. Asian. J.* **2018**, (13), 2277-2291.
19. Beesley, R. M.; Ingold, C. K.; Thorpe, J. F. CXIX.—The formation and stability of spiro-compounds. Part I. spiro-Compounds from cyclohexane. *Journal of the Chemical Society, Transactions* **1915**, *107* (0), 1080-1106, 10.1039/CT9150701080.
20. Ramesh, V. G., M.; Nanubolu, J. B.; Adiyala, P. R. Visible-Light-Induced Deaminative Alkylation/Cyclization of Alkyl Amines with N-Methacryloyl-2-phenylbenzimidazoles in Continuous-Flow Organo-Photocatalysis. *J. Org. Chem.* **2021**, *86*, 12908-12921.

21. Chen, S.-J.; Chen, G.-S.; Deng, T.; Li, J.-H.; He, Z.-Q.; Liu, L.-S.; Ren, H.; Liu, Y.-L. 1,2-Dicarbonylfunctionalization of Trifluoromethyl Alkenes with Pyridinium Salts via a Cycloaddition/Visible-Light-Enabled Fragmentation Cascade. *Organic Letters* **2022**, *24* (2), 702-707.
22. Klauck, F. J. R.; Yoon, H.; James, M. J.; Lautens, M.; Glorius, F. Visible-Light-Mediated Deaminative Three-Component Dicarbonylfunctionalization of Styrenes with Benzylic Radicals. *ACS Catalysis* **2019**, *9* (1), 236-241.
23. Yang, J.; Yang, L.; Gu, J.; Shuai, L.; Wang, H.; Ouyang, Q.; Li, Y.-L.; Liu, H.; Gong, L. Nickel-Catalyzed Reductive Cascade Arylalkylation of Alkenes with Alkylpyridinium Salts. *Organic Letters* **2022**, *24* (12), 2376-2380.
24. Biswas, S. W., D. J. Mechanism and Selectivity in Nickel-Catalyzed Cross-Electrophile Coupling of Aryl Halides with Alkyl Halides. *J. Am. Chem. Soc.* **2013**, *135*, 16192-16197.
25. Poyraz, S.; Döndaş, H. A.; Döndaş, N. Y.; Sansano, J. M. Recent insights about pyrrolidine core skeletons in pharmacology. *Frontiers in Pharmacology* **2023**, *14*, Review.
26. Ma, Y.; Pang, Y.; Chhabra, S.; Reijerse, E. J.; Schnegg, A.; Niski, J.; Leutzsch, M.; Cornella, J. Radical C–N Borylation of Aromatic Amines Enabled by a Pyrylium Reagent. *Chem. Eur. J.* **2020**, *26* (17), 3738-3743.

Appendix A

PERMISSIONS

The work discussed in Chapter 1 of this thesis dissertation has been published (Garcia, B.; Sampson, J.; Watson, M. P.; Kalyani, D. *Faraday Discuss.* **2023**, *247*, 324-332). It is reprinted with permission from the *Royal Society of Chemistry*.

Rights Link: <https://www.rsc.org/journals-books-databases/author-and-reviewer-hub/authors-information/licences-copyright-permissions-journal-articles/#about-licence>

Appendix B

FUNDAMENTAL OBSERVATIONS

As the electrochemical reduction method for the cross electrophile coupling of primary alkylpyridinium salts and aryl chlorides required the use of non-traditional electrochemical set ups, many lessons were learned during optimization investigations.

1. Although cobalt electrodes are sacrificial, they can be reused if they are lightly sanded and inverted during the subsequent run. It is not recommended to reuse the cobalt electrode more than two times, as the surface area does decrease due to erosion. Stainless steel electrodes, when serving as the cathode, can be reused multiple times as the electrodes are not sacrificial. The electrodes must be lightly sanded and have a metallic shine after cleaning.

2. Helpful equations that can be used to calculate reaction time (in minutes) and mAh required include:

$$\text{Reaction time (min)} = [\text{mmol substrate}] \left[\frac{\# \text{ Faradays}}{\text{mol}} \right] \left[\frac{96485 \text{ C mol}^{-1}}{\left(\frac{\text{current mA}}{1} \right) \left(\frac{60 \text{ min}}{1 \text{ hour}} \right)} \right]$$

$$\text{mAh} = \left[\frac{\# \text{ Faradays}}{\text{mol}} \right] [\text{moles reaction}] \left[\frac{96485 \text{ C}}{\text{mol}} \right] \left[\frac{1000 \text{ mA}}{1 \text{ A}} \right] \left[\frac{1 \text{ min}}{60 \text{ seconds}} \right] \left[\frac{1 \text{ hour}}{60 \text{ minutes}} \right]$$

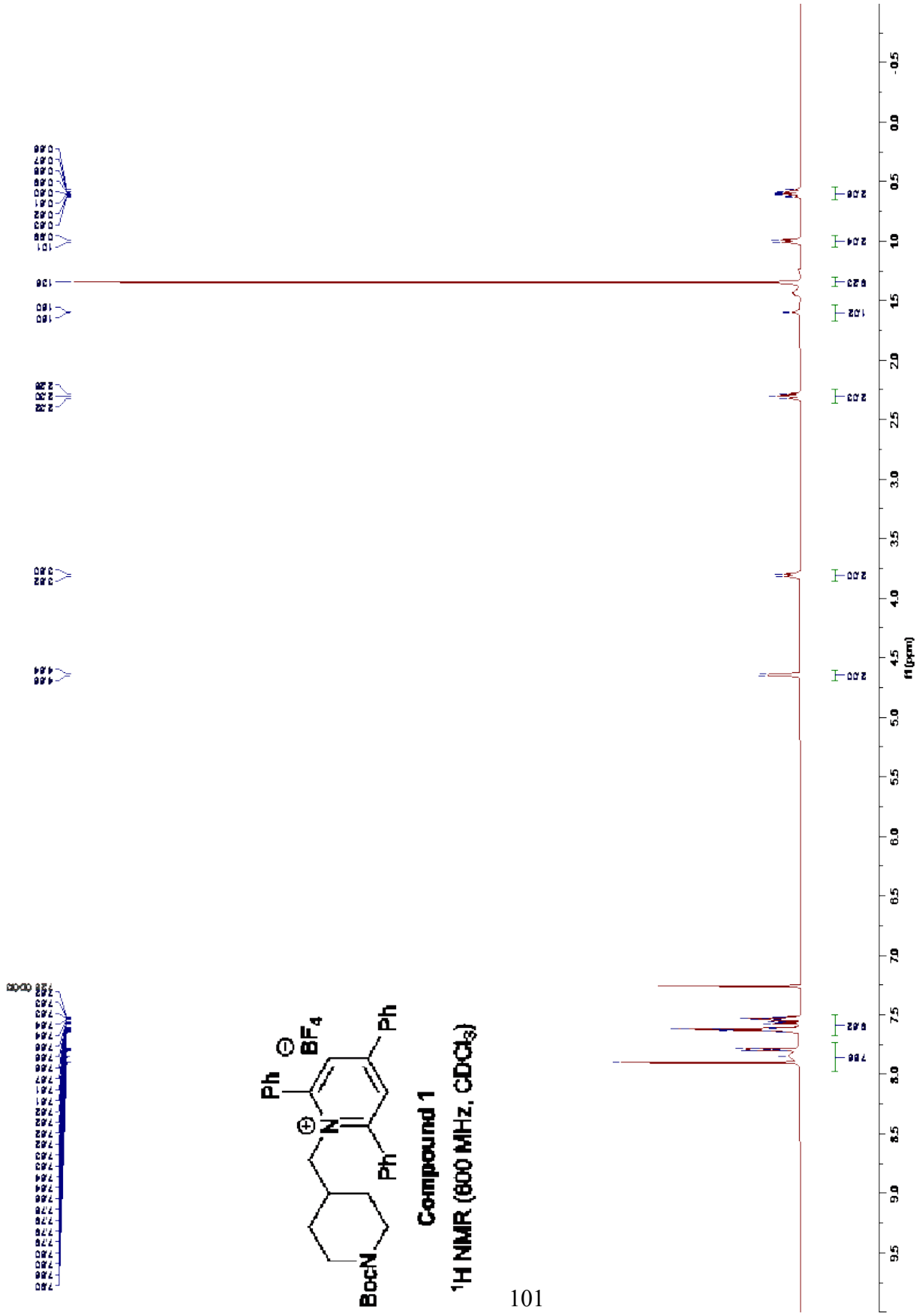
3. The additive, or electrolyte, should be treated as a component analogous to solvent. When electrolyte concentration is too low, electrolysis is compromised.

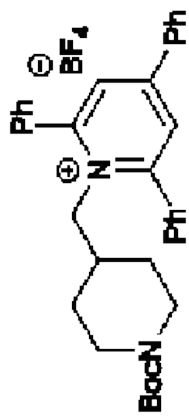
4. When scaling up to large scale: the electrode must also increase in surface area to account for the increase of material and maintain sufficient electrolysis. With

minimal electrode surface area, there is a risk of complete erosion of the sacrificial anode and increased resistance throughout electrolysis. Increased electrode surface area can allow electrolysis at higher currents.

5. When utilizing HTe⁻Chem set ups: The HTe⁻Chem reactor consists of 4 rows that with 6 reaction wells in each row. During the constant current mode, each well runs is connected in series thus, the resistance of one well will affect the electrolysis of the others. Investigation of reaction variables that may change resistance (such as electrochemical mediator, electrolyte, or ligand) may be difficult, as the risk of reaching the maximum resistance capacity becomes greater.

Appendix C
SPECTRAL DATA FOR CHAPTER 1

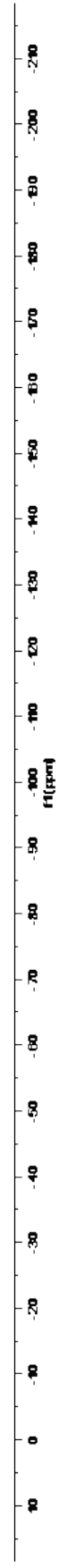


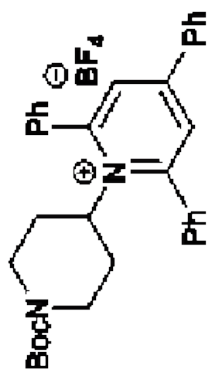


Compound 1

¹⁹F NMR (565 MHz, CDCl₃)

42.08
10.08

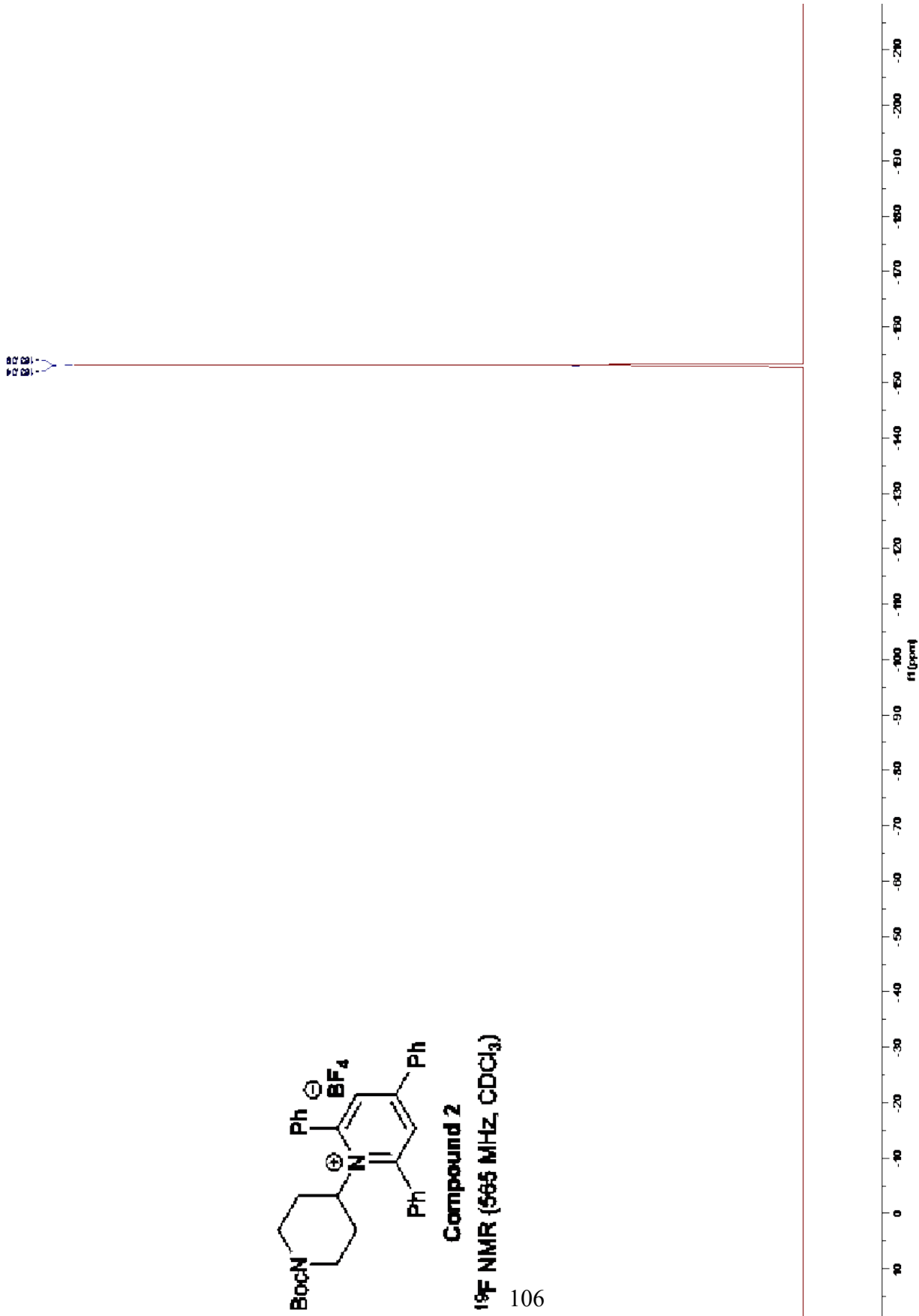




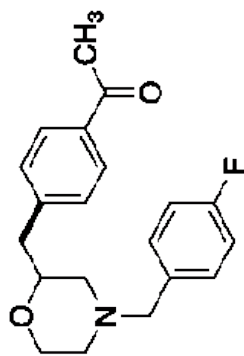
Compound 2

¹⁹F NMR (565 MHz, CDCl₃)

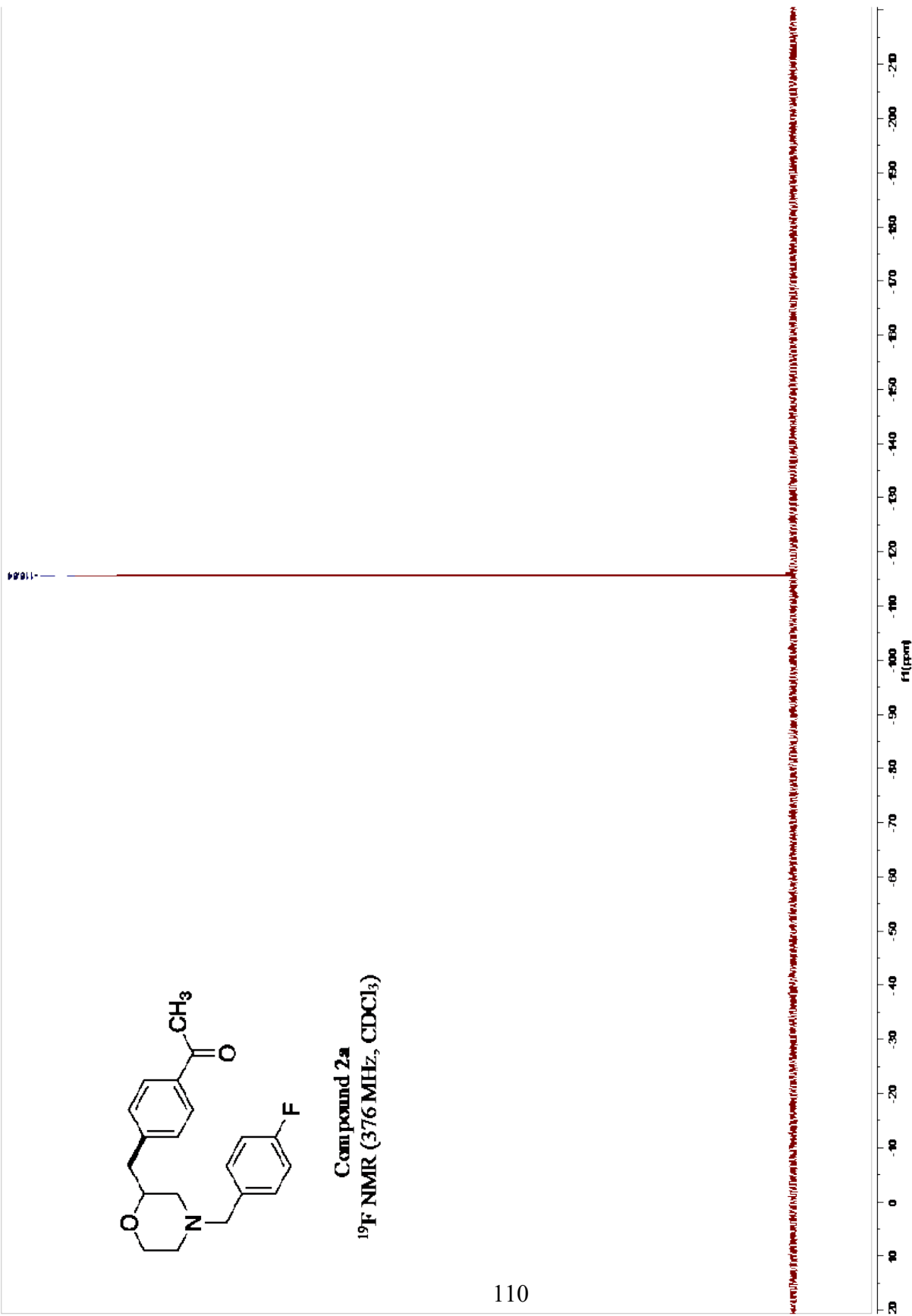
106



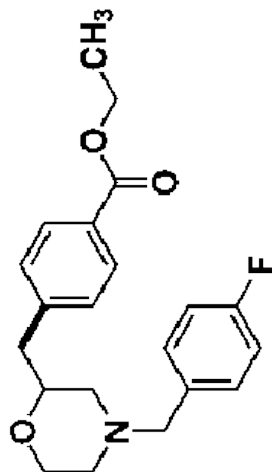
Appendix D
SPECTRAL DATA FOR CHAPTER 2



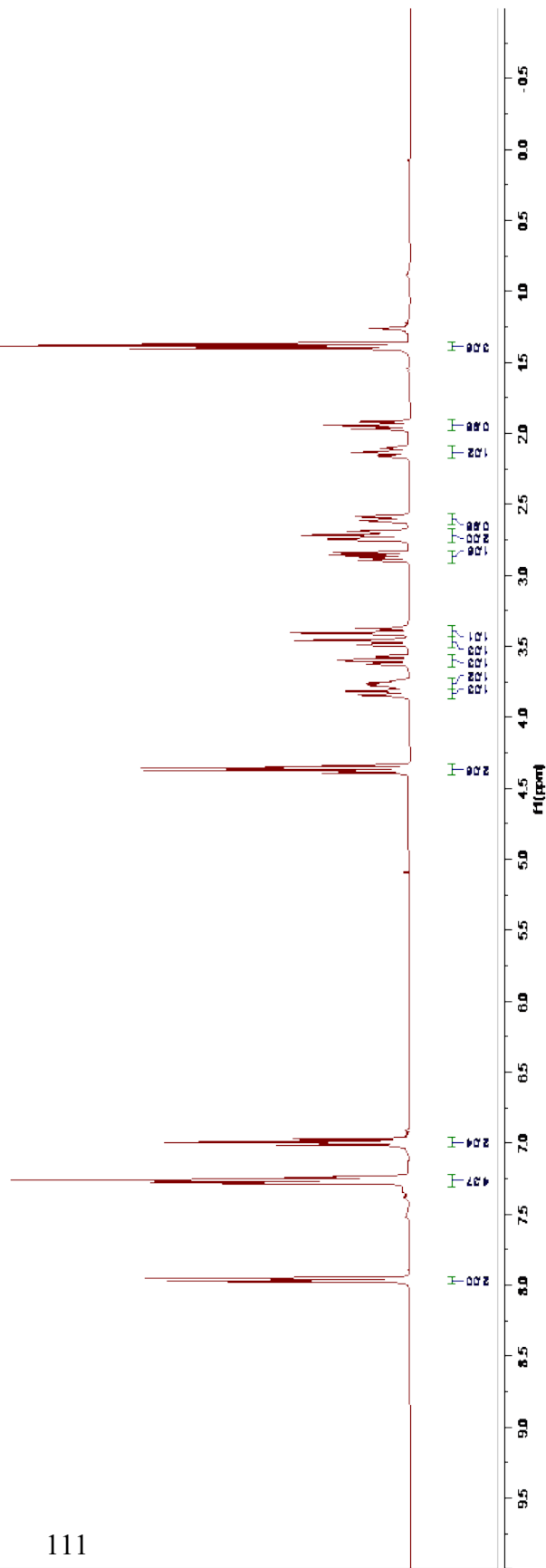
Compound 2a
¹⁹F NMR (376 MHz, CDCl₃)

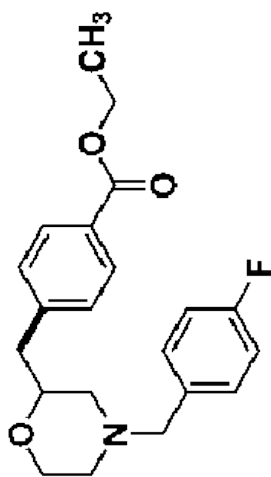


7.28 CDCl₃

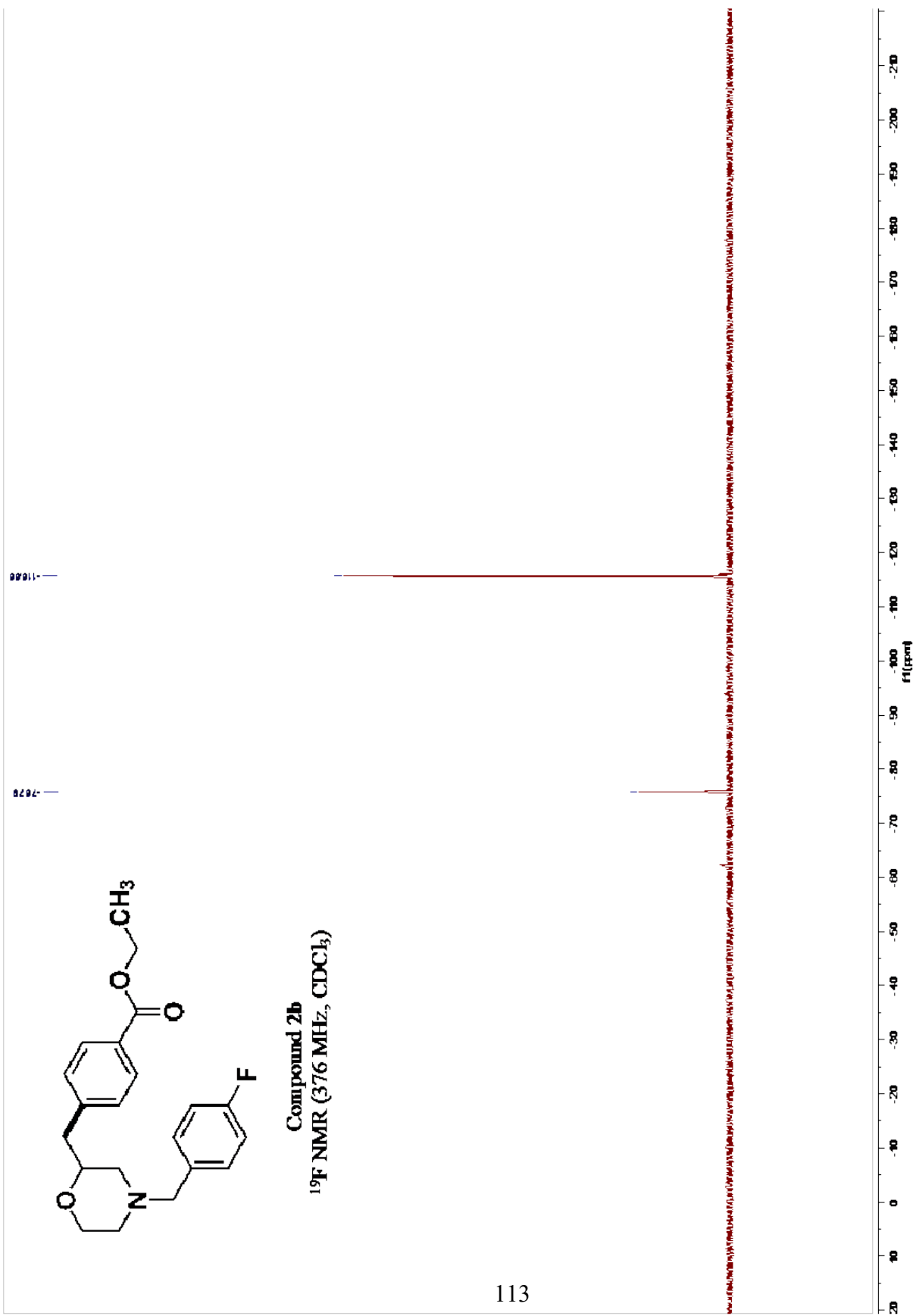


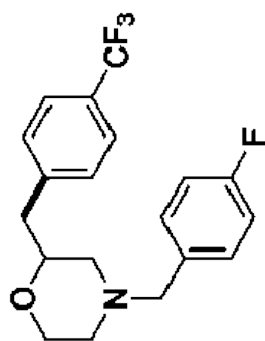
Compound 2b
¹H NMR (400 MHz, CDCl₃)



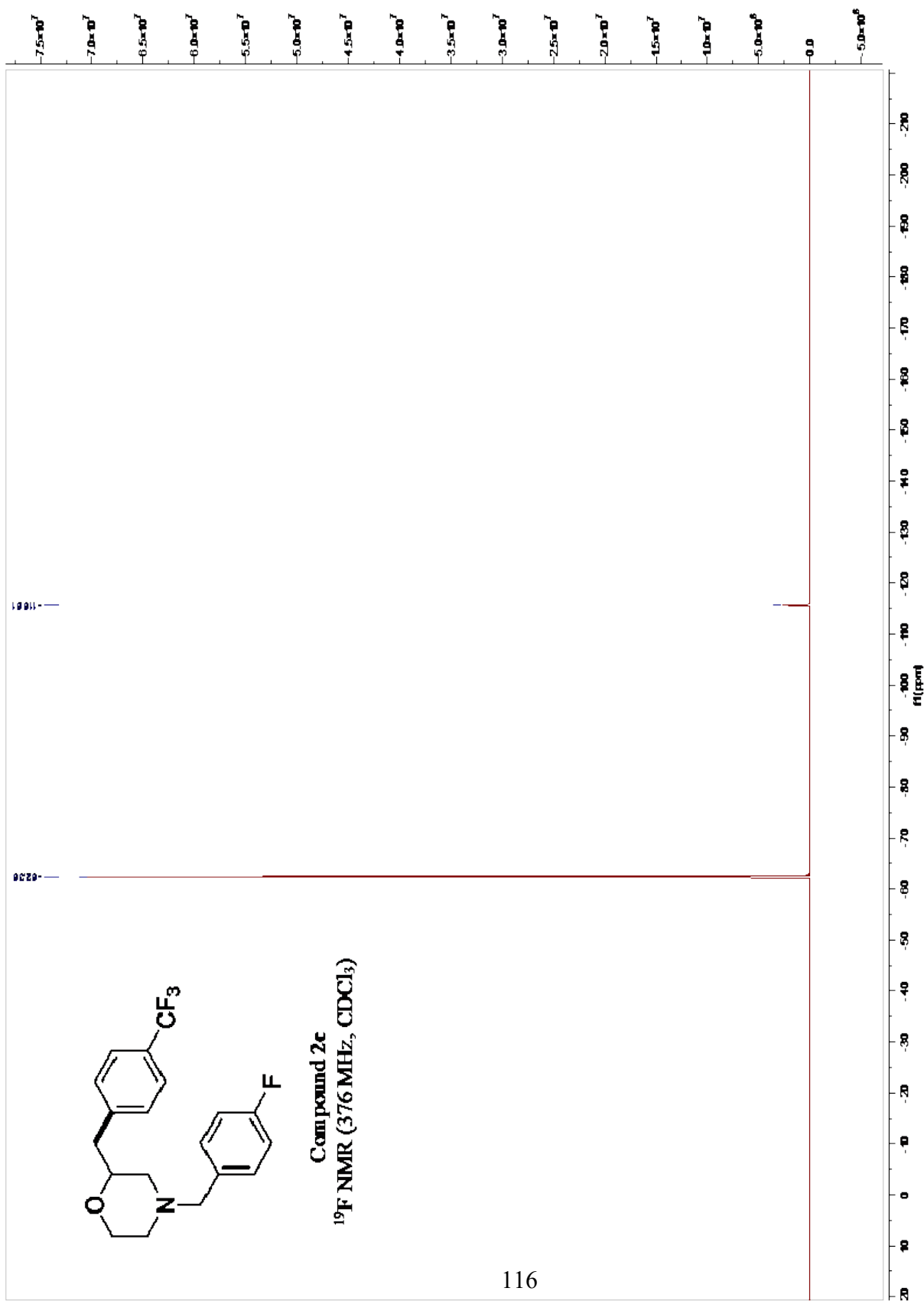


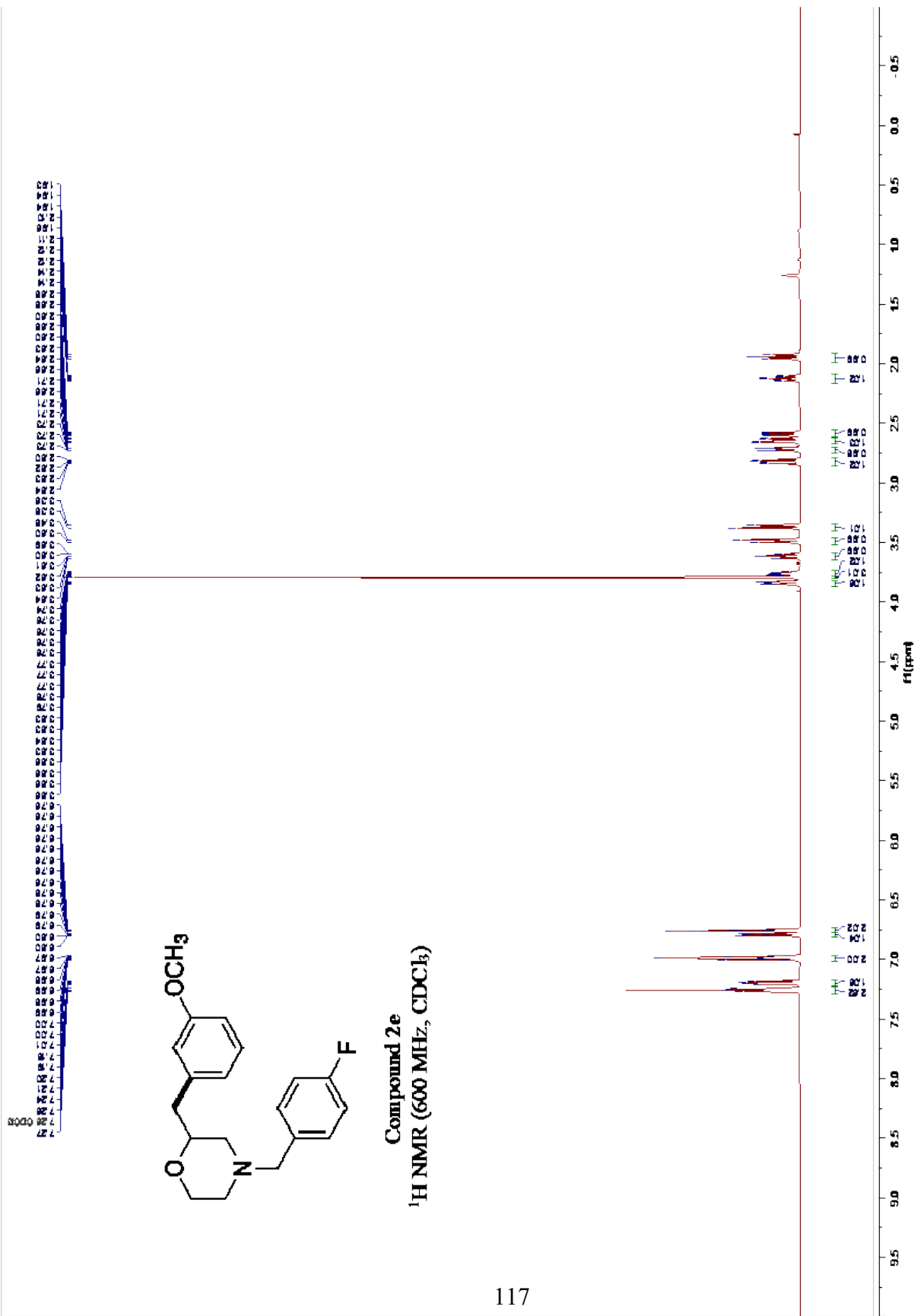
Compound 2b
¹⁹F NMR (376 MHz, CDCl₃)

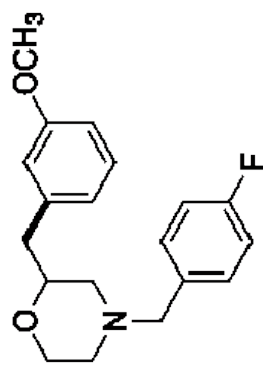




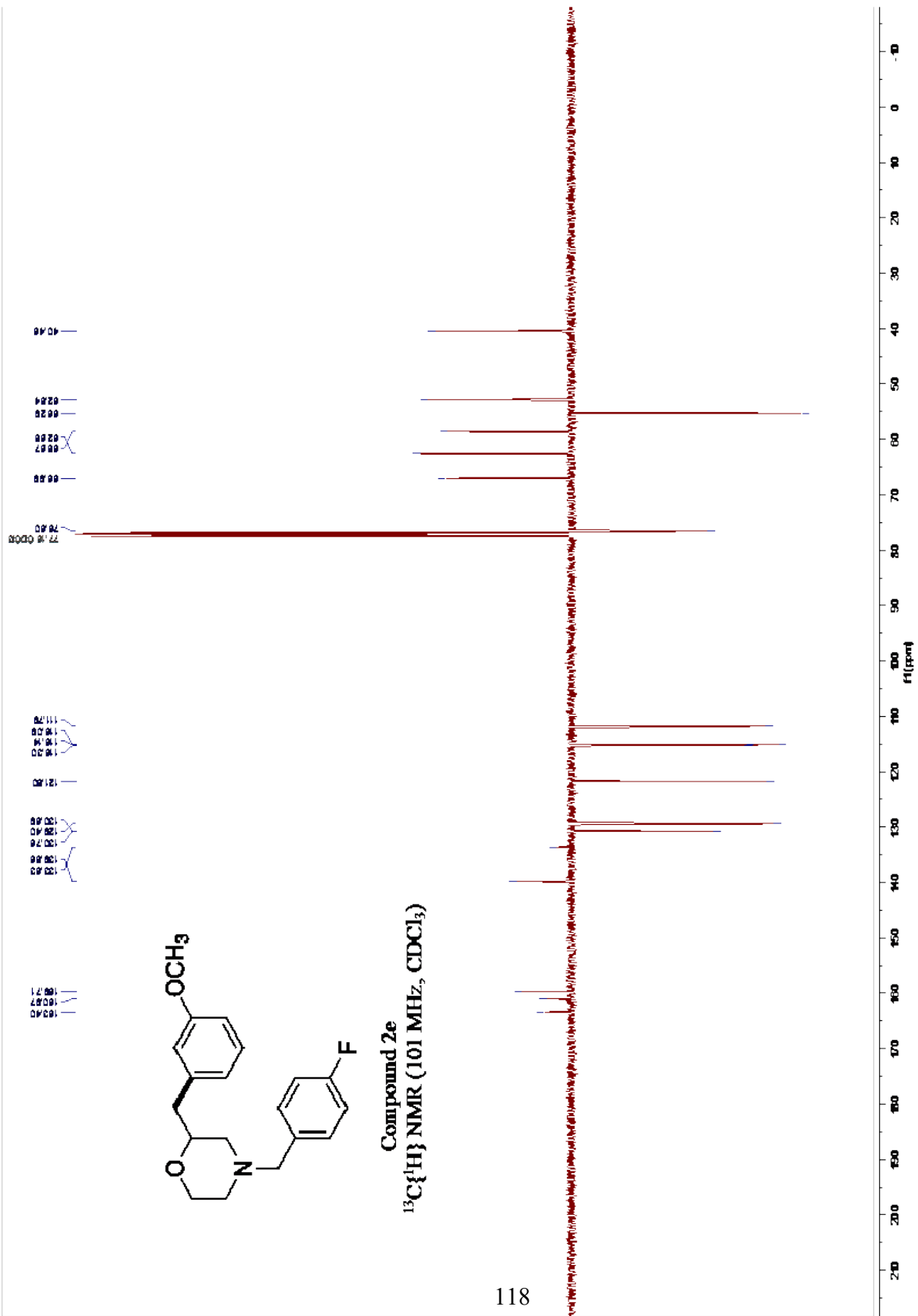
Compound 2c
¹⁹F NMR (376 MHz, CDCl₃)

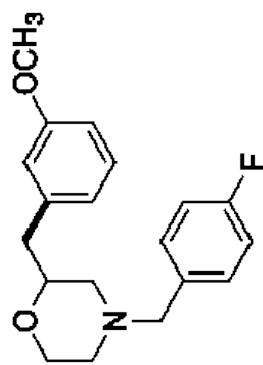




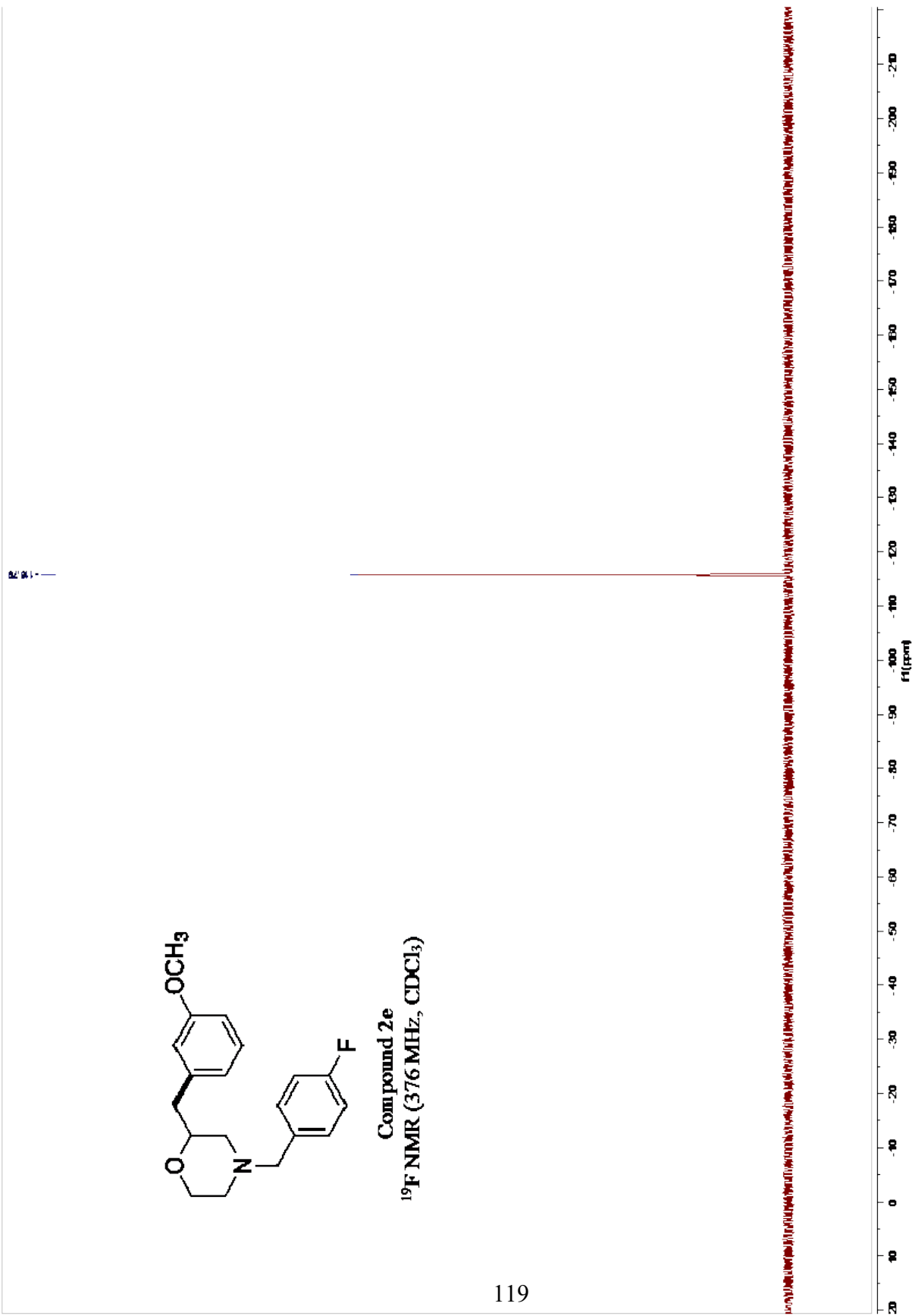


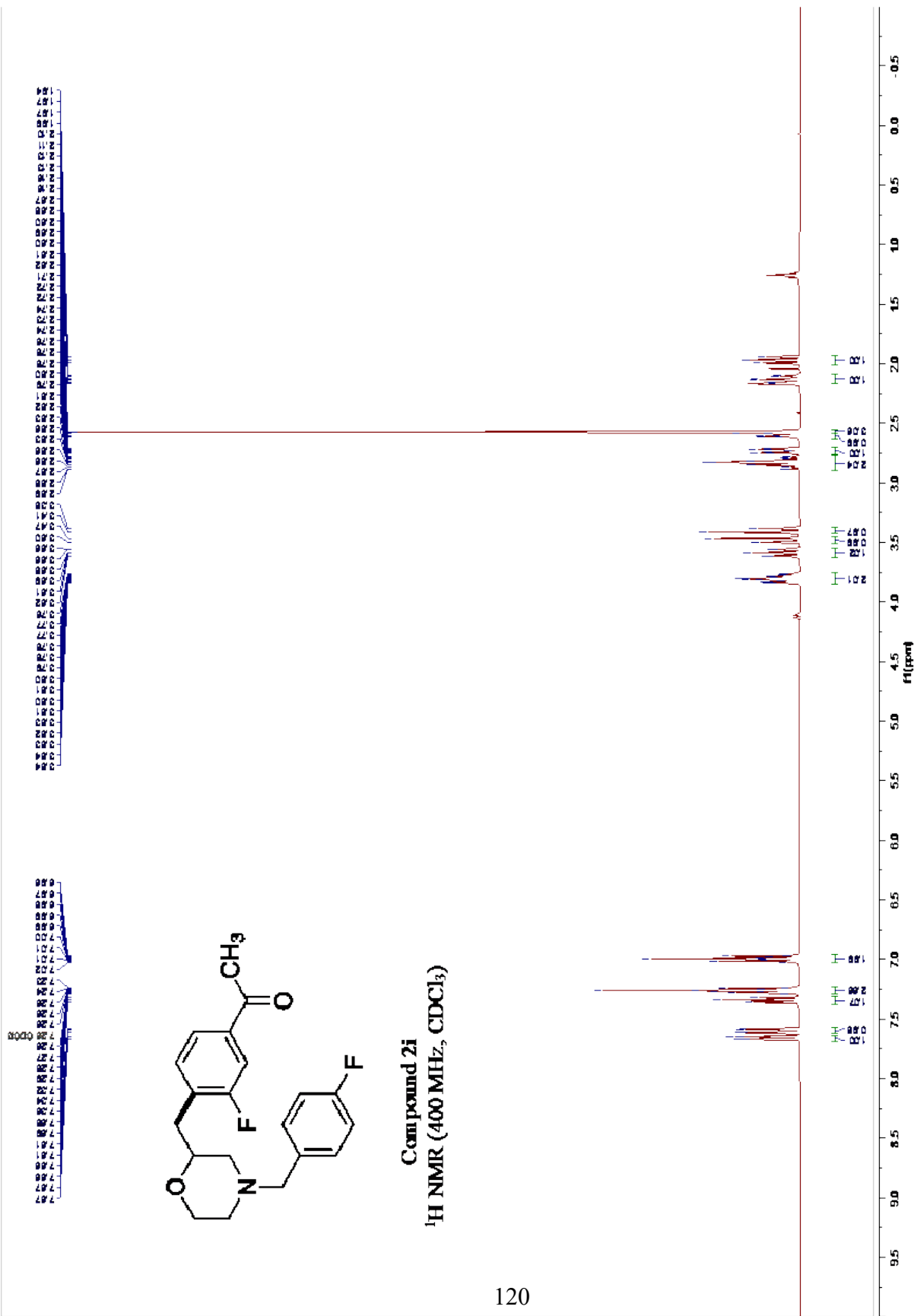
Compound 2e
 $^{13}\text{C}\{^1\text{H}\}$ NMR (101 MHz, CDCl_3)

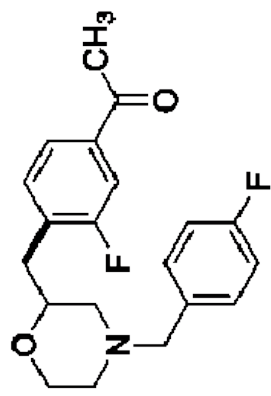




Compound 2e
 ^{19}F NMR (376 MHz, CDCl_3)

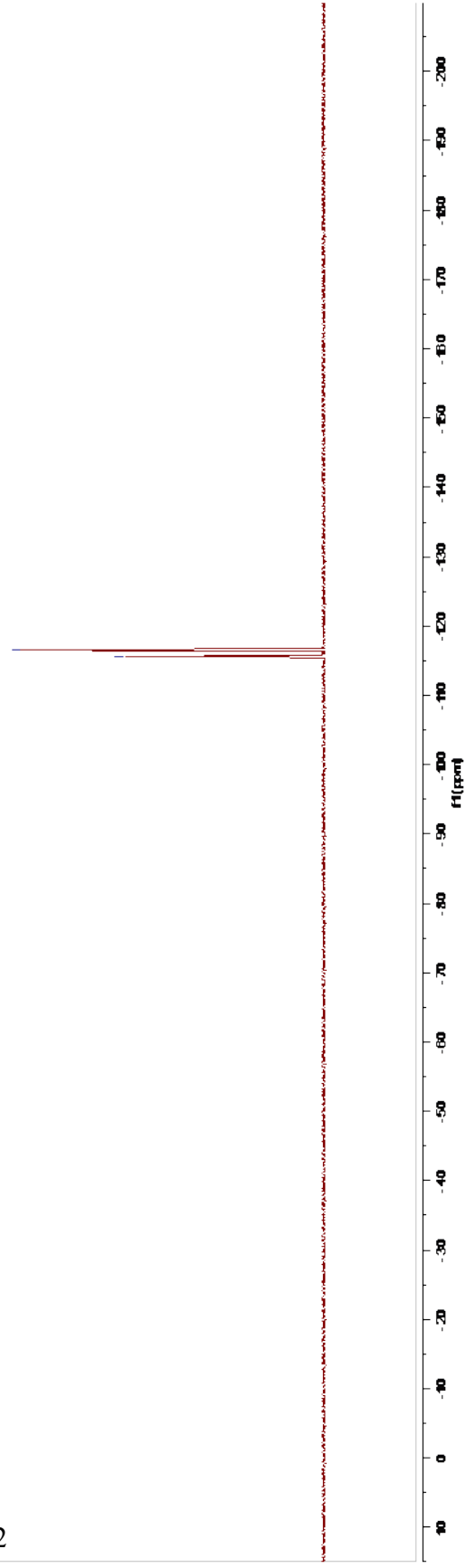


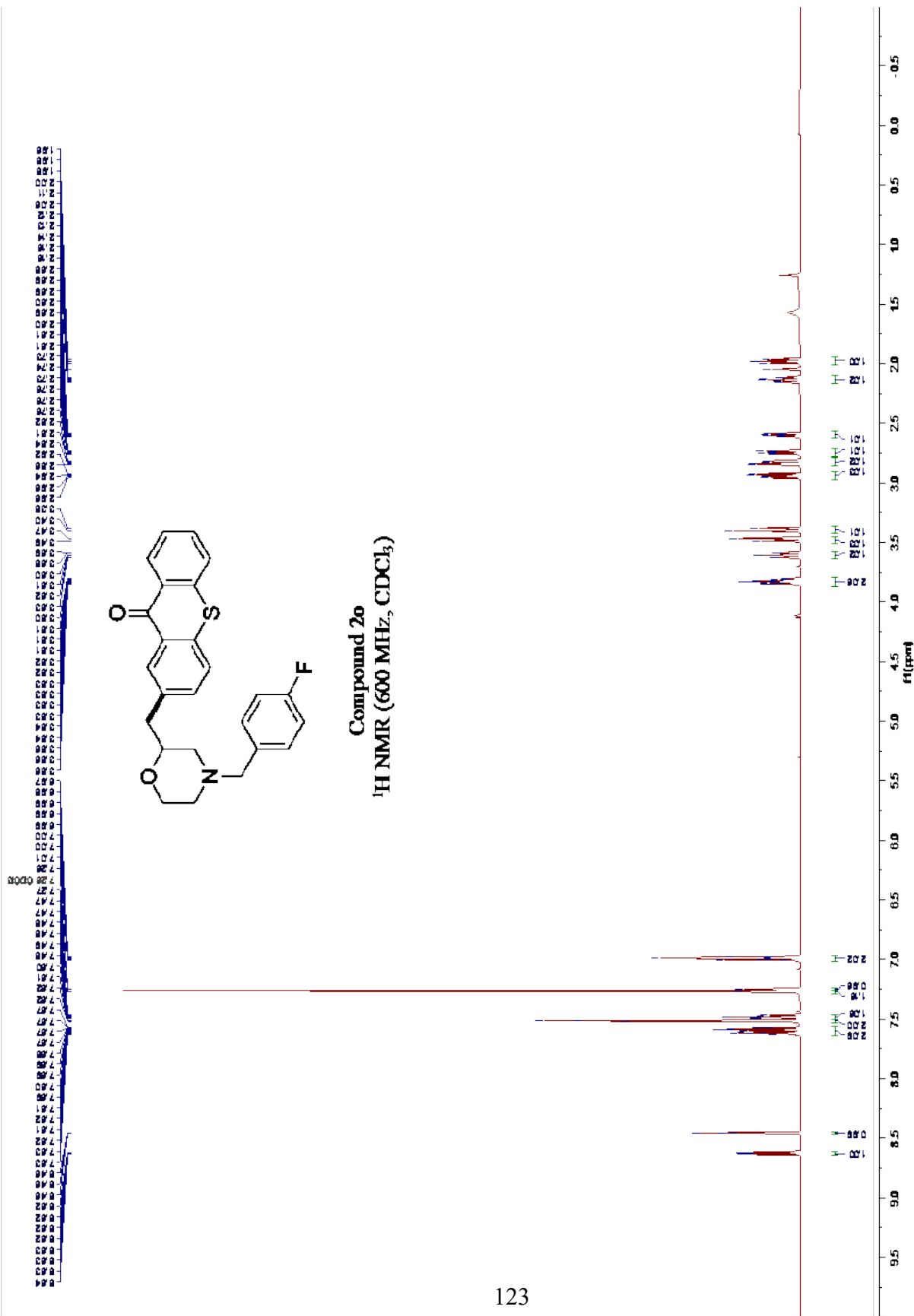


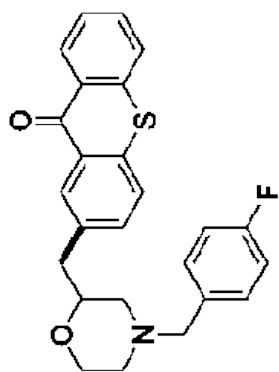


Compound 2i
¹⁹F NMR (376 MHz, CDCl₃)

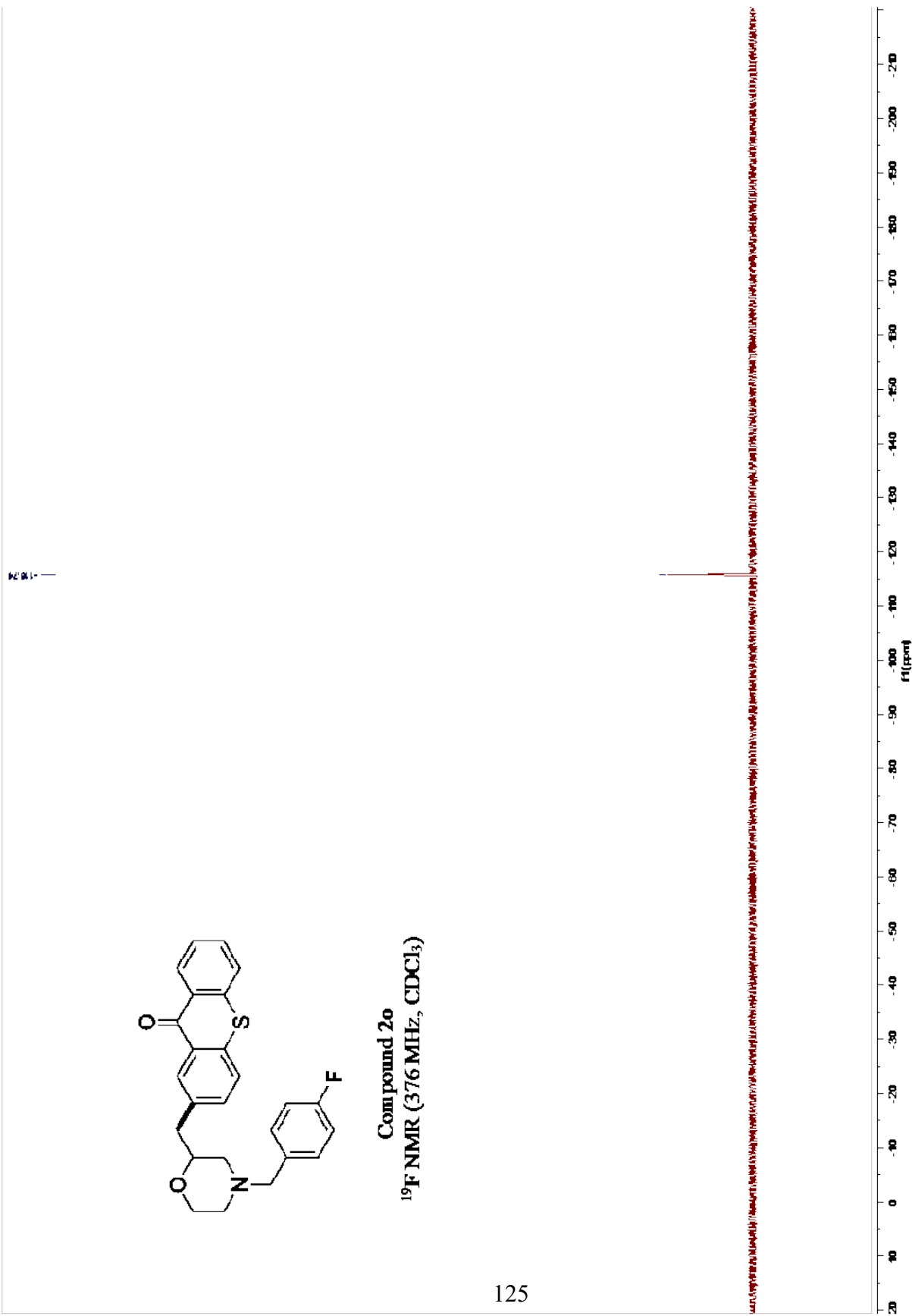
118.68
118.62

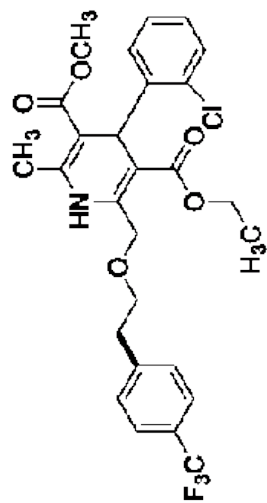






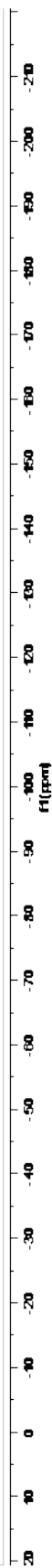
Compound 2o
 ^{19}F NMR (376 MHz, CDCl_3)

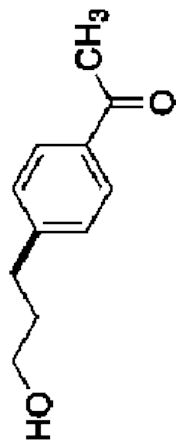




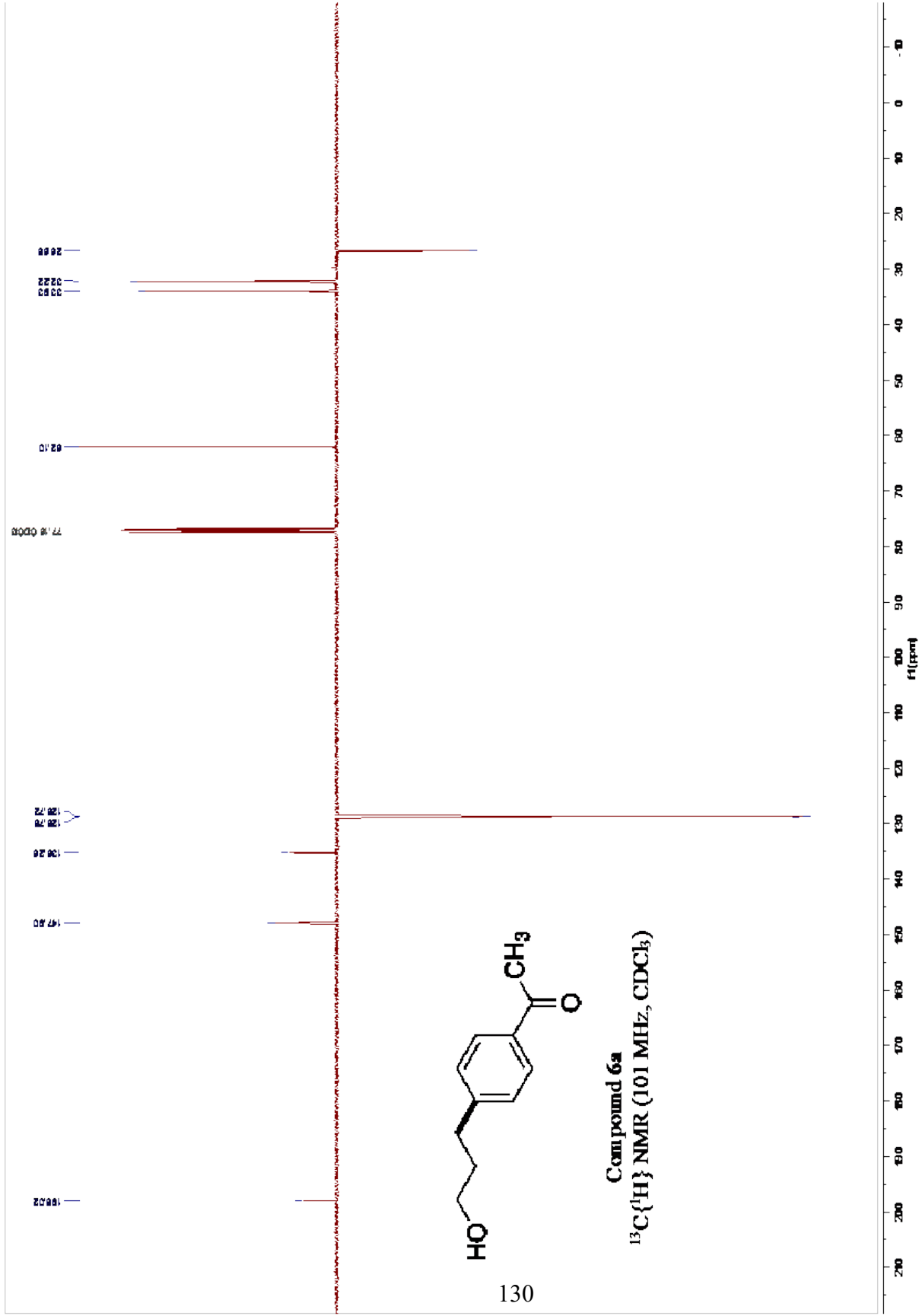
Compound 4a
¹⁹F NMR (376 MHz, CDCl₃)

-42.71

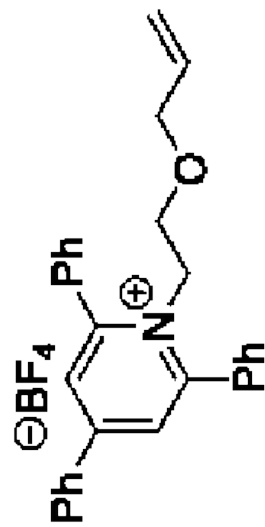




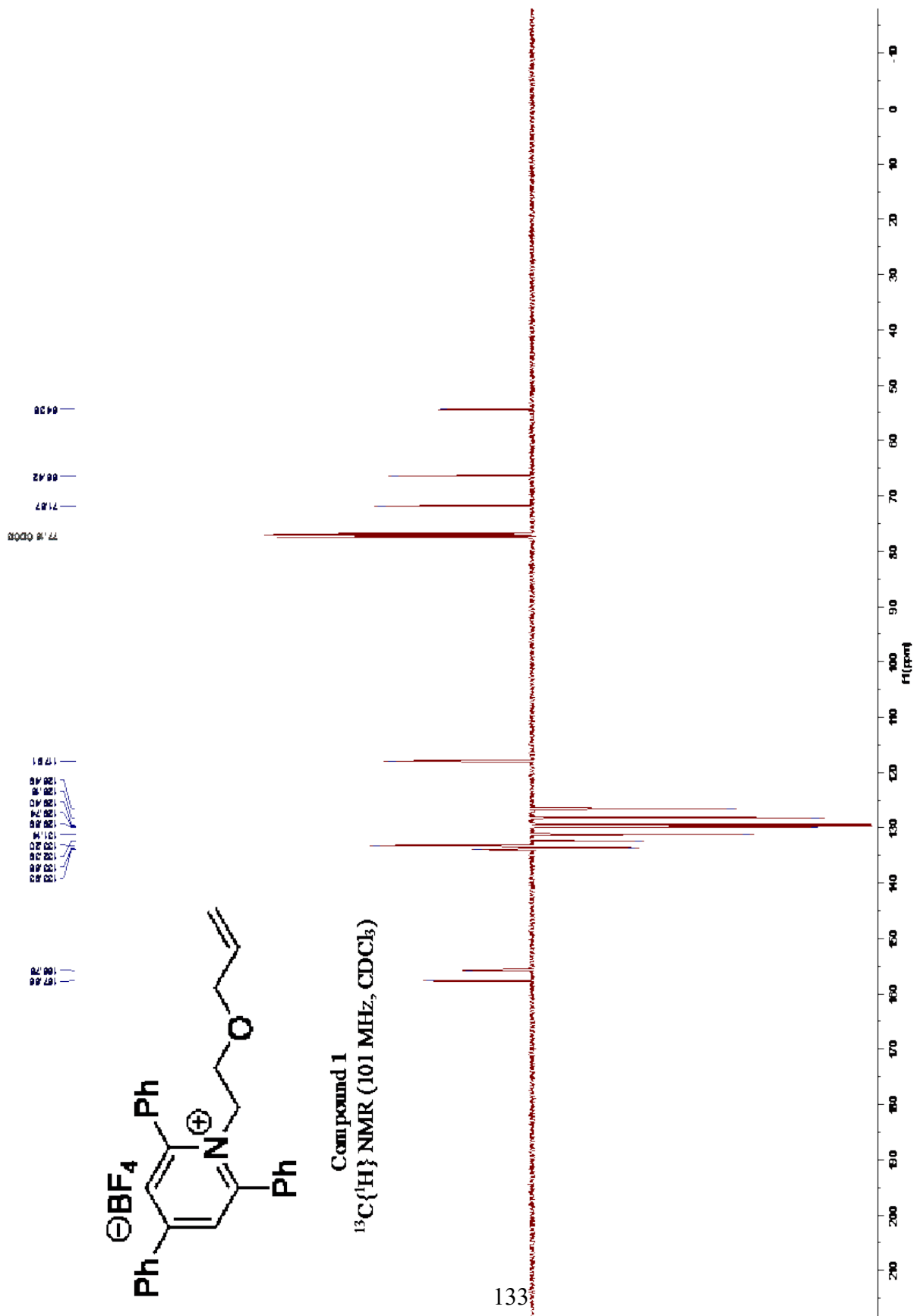
Compound 6a
 $^{13}\text{C}\{^1\text{H}\}$ NMR (101 MHz, CDCl_3)

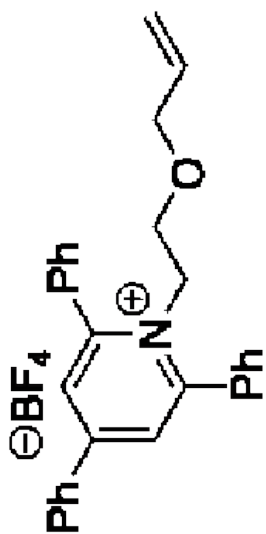


Appendix E
SPECTRAL DATA FOR CHAPTER 3



Compound 1
 $^{13}\text{C}\{^1\text{H}\}$ NMR (101 MHz, CDCl_3)

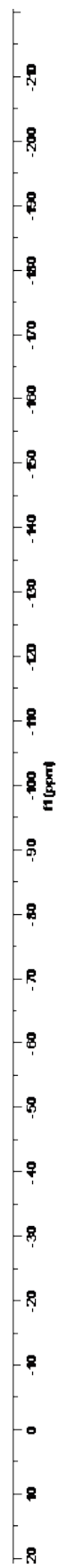


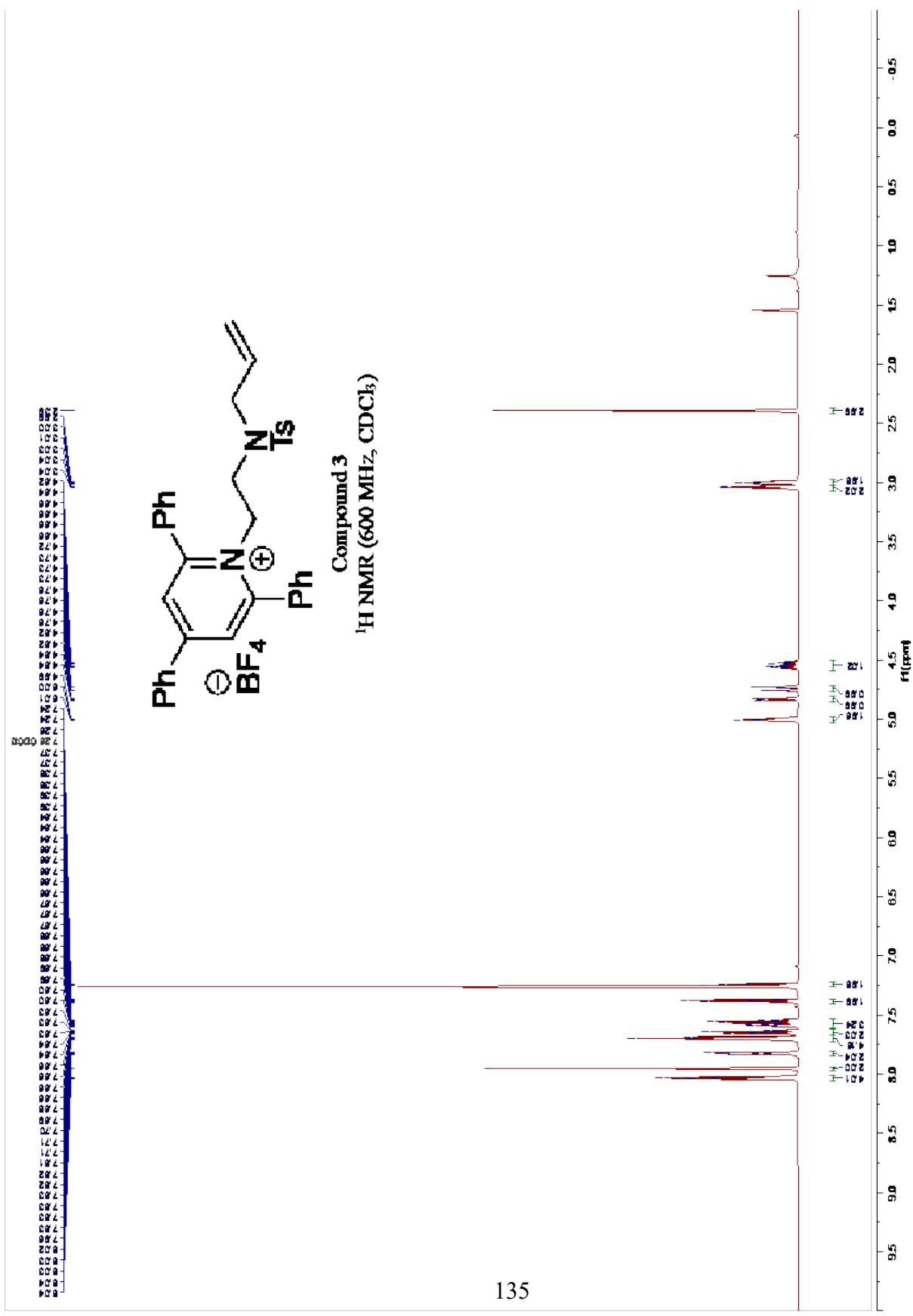


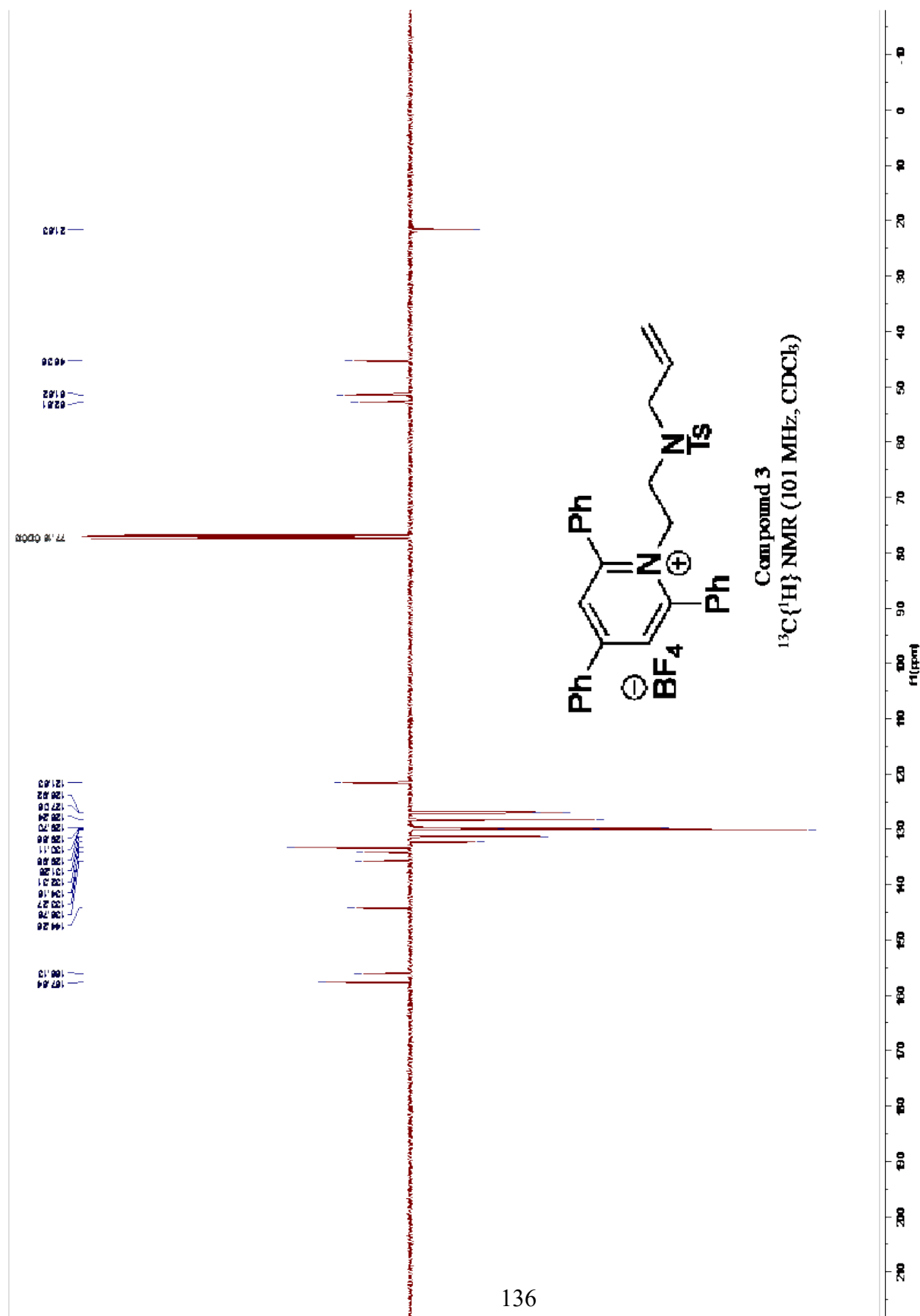
Compound 1
 ^{19}F NMR (376 MHz, CDCl_3)

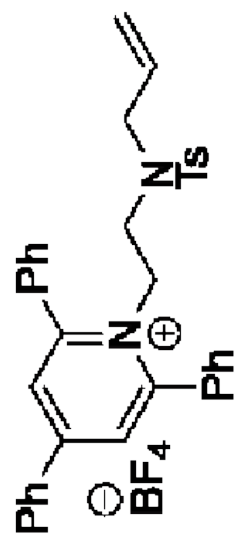
0.00
0.00

134









Compound 3
 ^{19}F NMR (376 MHz, CDCl_3)

0.00 (s, 9H)

